

HASSIBA BENBOUALI UNIVERSITY OF CHLEF
FACULTY OF SCIENCE
DEPARTMENT OF PHYSICS



A Thesis Submitted For Degree of Doctor in Physical Science

Presented By

HOURIA CHACHOU SAMET

DYNAMICS OF A TRAPPED BOSE GAS AT FINITE TEMPERATURE

Examining Committee:

Pr. Ali-Benamara Abdelkader, UHB-Chlef, Chairman

Pr. Kessal Salem, USTHB-Alger, Examiner

Pr. Bentaiba Mustapha, USD-Blida, Examiner

D. Muhammad Asad-uz-Zaman, NSU, Bangladesh, Invitee

Pr. Usama Al Khawaja, UAE university
, Co-Supervisor

Pr. Benarous Mohamed, UHB-Chlef, Supervisor

September 2014

Contents

Nomenclature	vii
Outline of the thesis	ix
<i>Resumé</i>	xi
Acknowledgments	xiii
1 General Introduction	1
1.1 Basic features of Bose-Einstein condensation	2
1.1.1 Length and energy scales	2
1.1.2 BEC of composite bosons	2
1.1.3 Bose-Einstein condensation as thermal equilibrium state	3
1.1.4 Macroscopic wavefunction	3
1.1.5 Alkali atoms	3
1.2 Atom Cooling and Trapping	3
1.2.1 Doppler cooling	4
1.2.2 Atom traps.	6
1.2.3 The MOT	7
1.2.4 Evaporative cooling	7
1.3 Weak interactions versus diluteness	7
1.4 Motivations	9
I Static Properties of Trapped Bose gas at finite temperatures	11
2 Background Theory and Experiment	17
2.1 Introduction	17
2.2 History of BEC studies	17
2.3 Bose Einstein Condensation and Solitons	20
3 Field Theory for Bose Gases	23
3.1 Introduction	23
3.2 Zero Temperature Mean Field Theory	25
3.2.1 The Gross-Pitaevskii Equation	25
3.3 The Bogoliubov approximation	27
3.4 finite Temperature Mean Field Theory	29
3.4.1 Popov approximation	30

3.4.2	Hartree-Fock-Bogoliubov approximation	31
3.4.3	Problems of HFB	32
3.4.4	Other finite temperature approaches	32
4	Time Dependent Hatree-Fock-Bogoliubov Theory For Trapped Bose gases	35
4.1	Introduction	35
4.2	The Balian-Véroni variational principle and the TDHFB Equations . . .	36
4.3	The Static Solution	38
4.3.1	Results and Discussions	43
 II Solitonic Solutions of Higher-Order Nonlinear Schrödinger equations and their Special cases		49
5	Soliton theory and nonlinear Schrödinger equation	53
5.1	Solitons, a brief history of	53
5.2	different types of solitons	58
5.3	Optical Solitons	61
5.3.1	Introduction	61
5.3.2	Why temporal and spatial solitons are different?	63
5.3.3	Quantitative consideration	63
5.3.4	Modulational instability and solitons	65
5.3.5	Nonlinear Schrödinger equation and solitons	67
5.4	Solitons in Bose Einstein Condensates	70
5.4.1	Interacting Bose system	70
5.4.2	Weakly interacting Bosons: Gross-Pitaevskii equation (GPE) for the condensate order parameter	70
5.4.3	Linear excitations in GPE	71
5.4.4	Nonlinear excitations of the GPE	72
6	Darboux transformation and Lax pairs: General formalism	73
6.1	Darboux transformation and Lax pair: General formalism	73
6.1.1	Introduction	73
6.1.2	Darboux Transformation for Linear Ordinary Differential Equations	74
6.1.3	Darboux Transformation for Nonlinear Partial Differential Equations	75
7	Solitonic Solution of higher-order nonlinear Schrödinger equations	91
7.1	Introduction	91
7.2	A Systematic search approach to find the Lax pair	91
7.3	Darboux transformation	95
7.4	Special cases	96
 Conclusion		103

List of Figures

1.1	Red-detuned lasers don't affect an atom at rest (left) but will slow an atom moving toward the light source (right).	5
4.1	Solution of Eq. (4.17) vs. the dimensionless condensate density	40
4.2	Plot of the solution of Eq. (4.18) showing a typical linear behavior	41
4.3	Noncondensate density vs. the radial distance	42
4.4	Anomalous density vs. the radial distance	42
4.5	Condensate radius vs. the condensate fraction	44
4.6	Central density vs. the condensate fraction	44
4.7	Condensate density vs. the radial distance for varying condensate fraction for $N = 10^5$ and $a/a_0 = 0.5 \cdot 10^{-3}$	45
4.8	Noncondensate density vs. the radial distance for varying condensate fraction for $N = 10^5$ and $a/a_0 = 0.5 \cdot 10^{-3}$	45
4.9	Anomalous density vs. the radial distance for varying condensate fraction for $N = 10^5$ and $a/a_0 = 0.5 \cdot 10^{-3}$	46
5.1	. A soliton collision via the KdV equation; Notice how the amplitude and direction of the waves is the same before and after the collision, but phase shift	56
5.2	Do these 'animals' belong to the same soliton family? (the drawing made by Marc Haelterman in 1989).	62
5.3	Intensity and phase as functions of normalized coordinate x for bright (a), black (b) and (c) gray solitons [adapted from Tomlinson et al. (1989)] . . .	66
7.1	(Color online) (a) Solitonic solution of HNSLE with constant coefficients, $a_1 = 1$ and $a_2 = 1$. (b) The solution of Eq. (9) with constant coefficients, namely, $a_1 = 1$, $a_2 = 1$, and $a_3 = 0.05$. (c) Trigonometric time dependence for $a_1 = \cos(t)$, $a_2 = \cos(t)$ and constant third order dispersion $a_3 = 0.05$. (d) All the three coefficients are trigonometric time dependent $a_1 = \cos(t)$, $a_2 = \cos(t)$, and $a_3 = 0.05 \cos(t)$	95
7.2	Solitonic solution of NLSE with constant coefficients, $a_1 = 2$, $a_2 = 1$	97
7.3	Solitonic solution of HE with constant coefficients, $a_1 = 1$, $a_2 = 1$ and $a_3 = 2$	99
7.4	Solitonic solution of SSE with constant coefficients, $a_3 = 1$, $a_5 = 1$, $\lambda_3 = 5$, $c_1 = c_2 = c_3 = 1$	101

Nomenclature

BEC: Bose Einstein Condensation.
TDHFB: Time Dependent Hertree-Fock-Bogoliubov.
BV: Balian Vénéroni variational principle.
TF: Thomas Fermi.
 μ : the chemical potential.
 V : the volume.
 N : the particle number.
 $\lambda(T)$: the thermal de Broglie wavelength.
 d : the average separation between particles.
 a : the s-wave scattering length.
 $\hat{\Psi}$: the Bose field operator.
 $\tilde{\Psi}$: the field operators for the non-condensed atoms.
GPE : Gross-Pitaevskii Equation.
 E : the energy.
 E_{kin} : the kinetic energy of the condensate.
 E_p : the trapping energy.
 E_{int} : the interaction energy.
HFB: Hartree-Fock-Bogoliubov .
 ϵ_k : the energy spectrum.
 ZNG : Zaremba-Nikoni and Griffin.
 n_c : the condensate density.
 \tilde{n} : the non-condensed density.
 \tilde{m} : the anomalous density.
HF: Hartree-Fock.
 $D(t)$: the gaussian density operator.
 I : the Heisenberg parameter.
 g : is the coupling constant.
 $V_{ext}(\mathbf{r})$: the trapping potential.
KdV: Korteweg-de-Vries equation.
BT: Bäcklund transform.
SG: Sine-Gordon.
NLS: nonlinear Schrödinger equation.
RI : refractive index.
GSs: gap solitons.
SPM: self-phase modulation.
GVD: group-velocity-dispersion.
cw: continuous wave.
DS: dark soliton.
DNLSE: derivative nonlinear Schrödinger equation.

HE: Hirota equation.

SSE: Sasa-Satsuma equation.

HNLSE: higher-order nonlinear Schrödinger equation.

Constants

$\xi(\frac{3}{2}) \simeq 2.612$.

Outline of the thesis

- In the first part we rely on a variational approach to derive a set of equations governing the dynamics of trapped self-interacting Bose gas at finite temperature. We analyze the static situation both at zero and finite temperature in the Thomas-Fermi limit. We derive simple analytic expressions for the condensate properties at finite temperature. The noncondensate and anomalous density profiles are also analyzed in terms of the condensate fraction. The results are quite encouraging owing to the simplicity of the formalism.
- In the second part we derive the solitonic solution of nonlinear Schrödinger equation with cubic nonlinearity, complex potentials, and time-dependent coefficients using the Darboux transformation and the Lax Pair. We establish the integrability condition for the most general nonlinear Schrödinger equation with cubic nonlinearity and discuss the effect of the coefficients of the higher order terms in the solitonic solution. We find that the third-order dispersion term can be used to control the soliton motion without the need for an external potential. We discuss the integrability conditions and find the solitonic solution of some of the well known nonlinear Schrödinger equations as special cases .

Resumé

- Dans la *première* partie nous nous appuyons sur une approche variationnelle pour driver un ensemble *d'équations* rgissant la dynamique des gaz de Bose *piégé température finie*. Nous analysons la situation statique la fois *zéro* et *température finie* dans la limite Thomas Fermi. Nous obtenons des expressions analytiques pour les propriés du condensat *température finie*. Non condensat et la *densité* anormale sont *également analysés* en termes de la fraction du condensat. Les rsultats sont assez encourageants en raison de la *simplicité* du formalisme.
- Dans la *deuxième* partie, nous avons *trouvé* la solution solitonique de *l'équation* de Schrödinger non linéaire avec non-linéarité cubique, potentiels complexes et des coefficients *dépendant* du temps en utilisant la transformation de Darboux et Lax Paire.
- Nous *établissons* aussi les conditions de *l'intégrabilité* pour *l'équation* de Schrödinger non *linéaire* la plus *générale* avec non – *linéarité* cubique et discuter l'effet du coefficients des termes d'ordre *supérieur* aux solution solitonique. Nous constatons que le terme de dispersion de *troisième* ordre peut tre *utilisé* pour contrler le mouvement du soliton sans la *nécessite* d'un potentiel *extérieur*.
- Nous discutons aussi les conditions de *l'intégrabilité* et trouver la solution solitonique de certains *équations* non *linéaire* comme cas particuliers de *l'équation* de Schrödinger

Acknowledgments

Praise to Allah the most gracious, the most merciful for whom has granted us existence and whom is the source of every success.

There are many people who deserve my gratitude for their role in the completion of my thesis, and it would be impossible to mention them all in a few short paragraphs.

I am grateful to my family particularly to my husband Madjid and to my children Abdelmadjid and Firas who have given me the force to carry on this thesis. Thank you for supporting me and believing in me.

I express my sincere gratitude to my Supervisors Mr. Mohamed Benarous professor at UHBC of Chlef, for his great patience, help and discussions. He was always willing to help and answer to any question. I really appreciated his competence and availability.

I owe a special thanks to the Professor Usama Al Khawaja for his generous invitation and hosting me on scientific visits in UAEU. This visit has been incredibly beneficial to me and has highlighted my career as a young scientist. I should also thank him for his efforts to train me as Co-Supervisor.

My special thanks also to Doctor M. Asad-uz-zaman my first meeting with him in the Arab Emirates University when I visited Professor Usama Alkhawadja. The opportunity to work with Asad has been both an honour and a privilege. The fruitful collaboration with Usama and Asad on the solitons and soliton molecules were really a big plus in my career and I hope to have the opportunity to do so again in the future.

All gratitude to Professor Abdelkader Ali Benamara who has accepted to chair the jury of my thesis. I also thank the members of the jury, Professor Kessel Salem and Professor Bentaiba Mustapha to accept the responsibility to report this thesis. I am especially grateful for the attention with which they read this manuscript, and for their suggestions to improve it.

I also have great appreciation to Professor Maamar Benkraouda and all the members of the physics department of United Arab Emirates University for their support and hospitality. The many professors who introduced me to physics at Universities of Chlef, Blida are responsible for instilling in me the desire to scrutinize the inner workings of the physics, for giving me the knowledge and confidence necessary to pursue a graduate degree in physics.

My thanks go to all the members of the LPTPM (Laboratory for Theoretical Physics and Material Physics) I name Malika, Saida, Hocine, Nabil, Madani.

My gratitude goes to all my colleagues of the physics department and the faculty of sciences at university of Chlef.

I especially want to thank my Parents. They gave me an education that I am proud and I defend, that made me who I am and that I will carry throughout my life whether in science, in education and in private life. I admire them very much because they are people of integrity and honesty, which I have always been taught to be sincere and honest, to move on its own without overwriting other and never forget where we come from. I

thank them for everything they gave me and given the value of which has no equivalent material but a great human value. They gave me a peaceful and happy room to study in, were also a great, although long distance, support during my graduate formation. And my brothers sisters, have always been ready to lend a listening ear or a helping hand. My thanks also to the family of my husband especially his Parents.

Chapter 1

General Introduction

The experimental realization in 1995 of Bose-Einstein condensation in dilute atomic gases marked the beginning of a very rapid development in the study of quantum gases. The initial experiments were performed on vapours of rubidium [121], sodium [122], and lithium [123]. have been demonstrated to undergo Bose-Einstein condensation. In related developments, atomic Fermi gases have been cooled to well below the degeneracy temperature, and a superfluid state with correlated pairs of fermions has been observed. Also molecules consisting of pairs of fermionic atoms such as $6Li$ or $40K$ have been observed to undergo Bose Einstein condensation. Atoms have been put into optical lattices, thereby allowing the study of many-body systems that are realizations of models used in condensed matter physics. Although the gases are very dilute, the atoms can be made to interact strongly, thus providing new challenges for the description of strongly correlated many-body systems. In a period of less than ten years the study of dilute quantum gases has changed from an esoteric topic to an integral part of contemporary physics, with strong ties to molecular, atomic, subatomic and condensed matter physics. The dilute quantum gases differ from ordinary gases, liquids and solids in a number of ways, as we shall now illustrate by giving values of physical quantities. The particle density at the centre of a Bose-Einstein condensed atomic cloud is typically $10^{13} - 10^{15} cm^{-3}$. By contrast, the density of molecules in air at room temperature and atmospheric pressure is about $10^{19} cm^{-3}$. In liquids and solids the density of atoms is of order $10^{22} cm^{-3}$, while the density of nucleons in atomic nuclei is about $10^{38} cm^{-3}$. To observe quantum phenomena in such low-density systems, the temperature must be of order $10^{-5} K$ or less. This may be contrasted with the temperatures at which quantum phenomena occur in solids and liquids. In solids, quantum effects become strong for electrons in metals below the Fermi temperature, which is typically $10^4 - 10^5 K$, and for phonons below the Debye temperature, which is typically of order $10 K$. For the helium liquids, the temperatures required for observing quantum phenomena are of order $1 K$. Due to the much higher particle density in atomic nuclei, the corresponding degeneracy temperature is about $10^{11} K$. The path that led in 1995 to the first realization of Bose-Einstein condensation in dilute gases exploited the powerful methods developed since the mid 1970s for cooling alkali metal atoms by using lasers. Since laser cooling alone did not produce sufficiently high densities and low temperatures for condensation, it was followed by an evaporative cooling stage, in which the more energetic atoms were removed from the trap, thereby cooling the remaining atoms. Cold gas clouds have many advantages for investigations of quantum phenomena. In a weakly interacting BoseEinstein condensate, essentially all atoms occupy the same quantum state, and the condensate may be described in terms of a mean

field theory similar to the HartreeFock theory for atoms. +

1.1 Basic features of Bose-Einstein condensation

BEC in an ideal gas, described in various textbooks(e.g.[124]), is a paradigm of quantum statistical mechanics which offers profound insight into macroscopic quantum phenomena. We want to focus here on selected aspects of BEC pertaining to experiments in trapped Bose gases.

1.1.1 Length and energy scales

BEC is based on the indistinguishability and wave nature of particles, both of which are at the heart of quantum mechanics. In a simplified picture, atoms in a gas may be regarded as quantum-mechanical wavepackets which have an extent on the order of a thermal de Broglie wavelength $\lambda_{dB} = \sqrt{\frac{2\pi\hbar^2}{mk_B T}}$ where T is the temperature and m the mass of the atom. λ_{dB} can be regarded as the position uncertainty associated with the thermal momentum distribution. The lower the temperature, the longer λ_{dB} . When atoms are cooled to the point where λ_{dB} is comparable to the interatomic separation, the atomic wavepackets overlap and the indistinguishability of particles becomes important. At this temperature, bosons undergo a phase transition and form a Bose-Einstein condensate, a coherent cloud of atoms all occupying the same quantum mechanical state. The transition temperature and the peak atomic density n are related as $n\lambda_{dB}^3 = \xi(\frac{3}{2}) \simeq 2.612$. Bose-Einstein condensation in gases allows for a first-principles theoretical description because there is a clear hierarchy of length and energy scales. In a gas, the separation between atoms $n^{-\frac{1}{3}}$ is much larger than the size of the atoms (characterized by the s-wave scattering length a), i.e. the quantity $na^3 \ll 1$. In a Bose condensed gas, the separation between atoms is equal to or smaller than the thermal de Broglie wavelength. The largest length scale is the confinement, either characterized by the size of the box potential or by the oscillator length $a_{H_0} = \sqrt{\frac{\hbar}{m\omega}}$ which is the size of the ground state wavefunction in a harmonic oscillator potential with frequency ω .

With each length scale l there is an associated energy scale which is the kinetic energy of a particle with a de Broglie wavelength l . The energy scale associated with the scattering length is the temperature below which s-wave scattering predominates. The energy scale associated with the separation between atoms, $n^{-\frac{1}{3}}$, is the BEC transition temperature. The energy associated with the size of the confining potential is the energy spacing between the lowest levels. Atom-atom interactions are described by a mean field energy $g = \frac{4\pi\hbar^2 a}{m}$. The length scale associated with this energy is the healing length $\xi = (8\pi n a)^{-\frac{1}{2}}$. In most experiments, $k_B T > g$, but the opposite case has also been realized [125, 126]. In comparison, superfluid helium is a strongly interacting quantum liquid, the size of the atom, the healing length, the thermal de Broglie wavelength and the separation between the atoms are all comparable, creating a complex and rich situation.

1.1.2 BEC of composite bosons

Atoms are bosonic if they have integer spin, or equivalently, if the total number of electrons, protons, and neutrons they contain is even [127, 128]. However, in the context of BEC, we regard these composite particles as pointlike particles obeying Bose-Einstein

statistics. Under what conditions will this assumption break down and the composite nature of the particles affect the properties of the system?

The composite nature manifests itself in internal excitations. If the energy necessary for an internal excitation is much larger than $k_B T$, then the internal degree of freedom is frozen out and inconsequential for describing thermodynamics at that temperature. For molecules of mass m and size a , the lowest rotational levels are spaced by $\frac{\hbar^2}{m a^2}$. The first electronically excited state is at $\frac{\hbar^2}{m_e a^2}$ where m_e is the electron mass. In any case, the condition of diluteness $na^3 \ll 1$ guarantees that $k_B T_c$ is much smaller than the internal excitation energy. Therefore, the composite nature of particles cannot affect the properties of a dilute Bose condensate.

1.1.3 Bose-Einstein condensation as thermal equilibrium state

Bose-Einstein condensation occurs in thermal equilibrium when entropy is maximized by putting a macroscopic population of atoms into the ground state of the system. It might appear counter-intuitive that an apparently highly ordered state as the Bose condensate maximizes entropy. However, only the particles in excited states contribute to the entropy. Their contribution is maximized at a given total energy by forming a Bose condensate in the ground state and distributing the remaining atoms among higher energy states.

1.1.4 Macroscopic wavefunction

In an ideal gas, Bose condensed atoms all occupy the same singleparticle ground-state wavefunction. The many-body ground-state wavefunction is then the product of N identical single-particle ground-state wavefunctions. This single-particle wavefunction is therefore called the condensate wavefunction or macroscopic wavefunction. This picture retains validity even when we include weak interactions. The ground-state many-body wavefunction is still, to a very good approximation, a product of N single-particle wavefunctions which are now obtained from the solution of a non-linear Schrödinger equation.

1.1.5 Alkali atoms

One might ask why alkali gases are good systems for studying BEC. Experimentally, this is so, because they can be laser-cooled to temperatures in the nK region. This is based on sub-Doppler cooling methods (Castin et al. 1995) that rely on the ground state hyperfine structure and provide the starting point for evaporative cooling (Ketterle et van Druten 1996) that is used to cool the gas to even lower temperatures. When the temperature decreases to about a few hundred nK , BEC occurs in sufficiently dilute samples, which allow a clear observation of the quantum statistical effects. This is, of course, very appealing to theoreticians, as it means we can use simple weakly-interacting Bose-gas theory and make direct predictions for the experiments.

1.2 Atom Cooling and Trapping

The discovery that laser light can cool atoms to less than a millionth of a degree above absolute zero opened a new world of quantum physics. Previously, the speeds of atoms due to their thermal energy were always so high that their de Broglie wavelengths were much smaller than the atoms themselves. This is the reason why gases often behave like

classical particles rather than systems of quantum objects. At ultra-low temperatures, however, the de Broglie wavelength can actually exceed the distance between the atoms. In such a situation, the gas can abruptly undergo a quantum transformation to a state of matter called a Bose-Einstein condensate. This section, we describe some of the techniques for cooling and trapping atoms that have opened up a new world of ultracold physics. The atom-cooling techniques enabled so much new science that the 1997 Nobel Prize was awarded to three of the pioneers: Steven Chu, Claude Cohen-Tannoudji, and William D. Phillips.

1.2.1 Doppler cooling

An atom that absorbs a photon recoils from the momentum kick, just as you experience recoil when you catch a ball. Laser cooling manages the momentum transfer so that it constantly slows the atom's motion, slowing it down. In absorbing a photon, the atom makes a transition from its ground state to a higher energy state. This requires that the photon has just the right energy. Fortunately, lasers can be tuned to precisely match the difference between energy levels in an atom. After absorbing a photon, an atom does not remain in the excited state but returns to the ground state by a process called spontaneous emission, emitting a photon in the process. At optical wavelengths, the process is quick, typically taking a few tens of nanoseconds. The atom recoils as it emits the photon, but this recoil, which is opposite to the direction of photon emission, can be in any direction. As the atom undergoes many cycles of absorbing photons from one direction followed by spontaneously emitting photons in random directions, the momentum absorbed from the laser beam accumulates while the momentum from spontaneous emission averages to zero. The process of photon absorption followed by spontaneous emission can heat the atoms just as easily as cool them. Cooling is made possible by a simple trick: Tune the laser so that its wavelength is slightly too long for the atoms to absorb. In this case, atoms at rest cannot absorb the light. However, for an atom moving toward the laser, against the direction of the laser beam, the wavelength appears to be slightly shortened due to the Doppler effect. The wavelength shift can be enough to permit the atom to absorb the light. The recoil slows the atom's motion. To slow motion in the opposite direction, away from the light source, one merely needs to employ a second laser beam, opposite to the first. These two beams slow atoms moving along a single axis. To slow atoms in three dimensions, six beams are needed (Figure 1.1). This is not as complicated as it may sound: All that is required is a single laser and mirrors. Laser light is so intense that an atom can be excited just as soon as it gets to the ground state. The resulting acceleration is enormous, about 10,000 times the acceleration of gravity. An atom moving with a typical speed in a room temperature gas, thousands of meters per second, can be brought to rest in a few milliseconds. With six laser beams shining on them, the atoms experience a strong resistive force no matter which way they move, as if they were moving in a sticky fluid. Such a situation is known as optical molasses. As one might expect, laser cooling cannot bring atoms to absolute zero. The limit of Doppler cooling is actually set by the uncertainty principle, which tells us that the finite lifetime of the excited state due to spontaneous emission causes an uncertainty in its energy. This blurring of the energy level causes a spread in the frequency of the optical transition called the natural linewidth. When an atom moves so slowly that its Doppler shift is less than the natural linewidth, cooling comes to a halt. The temperature at which this occurs is known as the Doppler cooling limit. The theoretical predictions for this temperature are in the low millikelvin

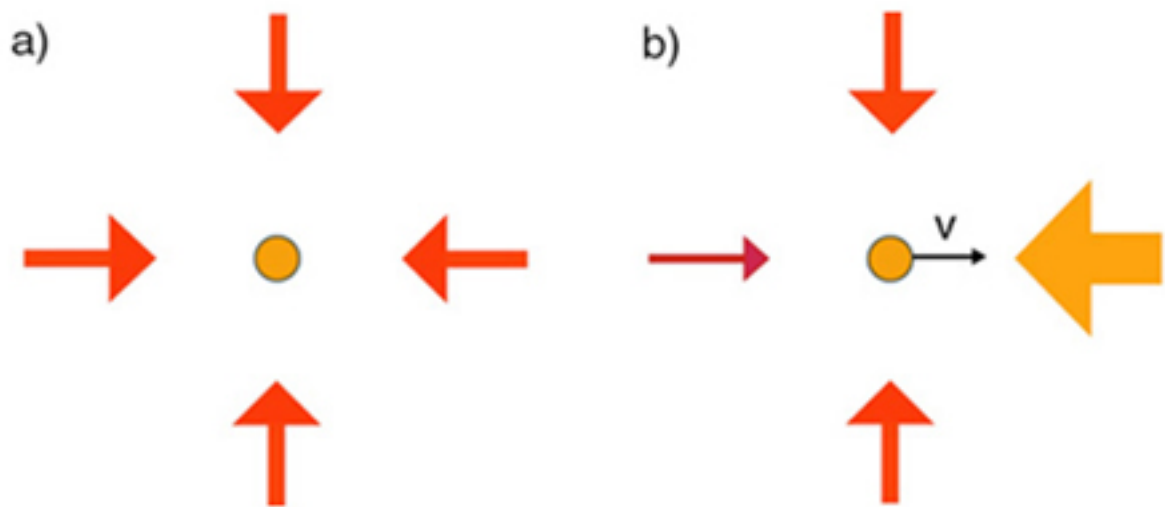


Figure 1.1: Red-detuned lasers don't affect an atom at rest (left) but will slow an atom moving toward the light source (right).

regime. However, by great good luck, it turned out that the actual temperature limit was lower than the theoretical prediction for the Doppler cooling limit. Sub-Doppler cooling, which depends on the polarization of the laser light and the spin of the atoms, lowers the temperature of atoms down into the microkelvin regime.

spontaneous emission

An atom in an excited state can decay down to a lower state by emitting a photon with an energy equal to the difference between the initial, higher energy level and the final, lower energy level. When this process takes place naturally, rather than being initiated by disturbing the atom somehow, it is called spontaneous emission.

Doppler effect.

The Doppler shift is a shift in the wavelength of light or sound that depends on the relative motion of the source and the observer. A familiar example of a Doppler shift is the apparent change in pitch of an ambulance siren as it passes a stationary observer. When the ambulance is moving toward the observer, the observer hears a higher pitch because the wavelength of the sound waves is shortened. As the ambulance moves away from the observer, the wavelength is lengthened and the observer hears a lower pitch. Likewise, the wavelength of light emitted by an object moving toward an observer is shortened, and the observer will see a shift to blue. If the light-emitting object is moving away from the observer, the light will have a longer wavelength and the observer will see a shift to red. By observing this shift to red or blue, astronomers can determine the velocity of distant stars and galaxies relative to the Earth. Atoms moving relative to a laser also experience a Doppler shift, which must be taken into account in atomic physics

experiments that make use of laser cooling and trapping.

Optical molasses.

Optical molasses is formed when laser beams for Doppler cooling are directed along each spatial axis so that atoms are laser cooled in every direction. Atoms can reach microkelvin temperatures in optical molasses. However, the molasses is not a trap, so the atoms can still, for example, fall under the influence of gravity.

Doppler cooling.

Doppler cooling is a technique that uses laser light to slow, and thus cool, moving atoms. An atom will absorb a photon that has an energy equal to the difference between two energy levels in the atom. When the atom absorbs a photon, it also absorbs the photon's momentum and gets a push in the direction that the photon was traveling. If the photon and atoms were traveling in opposite directions, the atom slows down. However, when the atom is moving relative to the laser, the laser light is Doppler shifted in the atom's reference frame. To cool moving atoms, the laser must be tuned slightly to the red to account for the Doppler shift of atoms moving toward the light source.

Natural linewidth.

The natural linewidth of an atomic energy level is the intrinsic uncertainty in its energy due to the uncertainty principle.

Polarization.

The polarization of a wave is the direction in which it is oscillating. The simplest type of polarization is linear, transverse polarization. Linear means that the wave oscillation is confined along a single axis, and transverse means that the wave is oscillating in a direction perpendicular to its direction of travel. Laser light is most commonly a wave with linear, transverse polarization. If the laser beam travels along the x-axis, its electric field will oscillate either in the y-direction or in the z-direction. Gravitational waves also have transverse polarization, but have a more complicated oscillation pattern than laser light.

1.2.2 Atom traps.

Like all matter, ultracold atoms fall in a gravitational field. Even optical molasses falls, though slowly. To make atoms useful for experiments, a strategy is needed to support and confine them. Devices for confining and supporting isolated atoms are called "atom traps." Ultracold atoms cannot be confined by material walls because the lowest temperature walls might just as well be red hot compared to the temperature of the atoms. Instead, the atoms are trapped by force fields. Magnetic fields are commonly used, but optical fields are also employed.

Magnetic traps depend on the intrinsic magnetism that many atoms have. If an atom has a magnetic moment, meaning that it acts as a tiny magnet, its energy is altered when it is put in a magnetic field. The change in energy was first discovered by examining the spectra of atoms in magnetic fields and is called the Zeeman effect after its discoverer, the Dutch physicist Pieter Zeeman.

Because of the Zeeman effect, the ground state of alkali metal atoms, the most common atoms for ultracold atom research, is split into two states by a magnetic field. The energy of one state increases with the field, and the energy of the other decreases. Systems tend toward the configuration with the lowest accessible energy. Consequently, atoms in one state are repelled by a magnetic field, and atoms in the other state are attracted. These energy shifts can be used to confine the atoms in space.

Zeeman effect.

Each atomic energy level in which an atom has a non-zero spin splits into two or more separate levels when the atom is placed in an external magnetic field. The splitting grows with the strength of the external field. This effect is named the Zeeman effect after the experimentalist who first studied it in the laboratory, Pieter Zeeman. He received the 1902 Nobel Prize for this work, along with Hendrik Lorentz, the theorist who explained the effect.

1.2.3 The MOT .

The magneto-optical trap, or MOT, is the workhorse trap for cold atom research. In the MOT, a pair of coils with currents in opposite direction creates a magnetic field that vanishes at the center. The field points inward along the z-axis but outward along the x- and y-axes. Atoms in a vapor are cooled by laser beams in the same configuration as optical molasses, centered on the midpoint of the system. The arrangement by itself could not trap atoms because, if they were pushed inward along one axis, they would be pushed outward along another. However, by employing a trick with the laser polarization, it turns out that the atoms can be kept in a state that is pushed inward from every direction. Atoms that drift into the MOT are rapidly cooled and trapped, forming a small cloud near the center.

1.2.4 Evaporative cooling

Gaseous Bose-Einstein condensates have so far only been obtained by evaporative cooling. Evaporative cooling is done by continuously removing the high-energy tail of the thermal distribution from the trap. The evaporated atoms carry away more than the average energy, which means that the temperature of the remaining atoms decreases. The high energy tail must be constantly repopulated by collisions, thus maintaining thermal equilibrium and sustaining the cooling process. The essential condition for evaporative cooling is a long lifetime of the atomic sample compared to the collisional thermalization time. Trapped atom clouds are extremely dilute (about ten orders of magnitude less dense than a solid or a liquid) and collisional thermalization can take seconds. A major step was taken in May 1994 when the MIT and JILA groups combined laser cooling with evaporative cooling, extending the applicability of evaporative cooling to alkali atoms [135, 136]. Evaporative cooling reduces the temperature of the atoms to nanokelvin.

1.3 Weak interactions versus diluteness

The condensation of conserved particles that obey the same statistics as photons was predicted by Einstein in 1924 even before the concept of Fermi statistics was intro-

duced(1926). Einsteins prediction was preceded by an ingenious conjecture of Bose, who realized that black body radiation can be treated as a gas of indistinguishable photons. Einstein generalized ideas of Bose to material particles and published two famous papers, in which he developed what we now call Bose-Einstein statistics[167, 168]. The ideal gas of Bose particles is remarkably the only example of a non-interacting system in condensed matter physics that undergoes a phase transition upon decreasing the temperature. However, experimental realization of ideal Bose-Einstein condensates is extraordinarily difficult, since realistic systems always involve interactions. Largely for this reason Einsteins ideas did not receive a wide recognition in the scientific community for many years as being devoid of any practical significance. The condensation phenomenon did not even appear in the textbooks, until in 1938 F. London recognized the analogy between superfluidity of liquid $4He$, discovered by Kapitza [169](, and Allen and Misener [170]and an ideal Bose gas and emphasized that Einsteins statement was erroneously discredited[171]. In support of Londons phenomenological ideas, the first microscopic theory of superfluidity in a system of weakly-interacting Bose particles was introduced in a brilliant paper by Bogoliubov [172]. Subsequent discussion about the connection between superfluidity and Bose Einstein condensation led Penrose and Onsager [173] to formulate the generalized criterion for BE condensation. This line of research culminated in a paper of C. N. Yang, who in 1962 extended this criterion to superfluidity and superconductivity and proposed the concept of off-diagonal long-range order (ODLRO)[174]. The condensed phase is characterized then by a non-vanishing asymptotic of a one-body density matrix at large distances. During the decades which followed the work of Bogoliubov,successful field-theoretical approaches were developed and many important predictions about the thermodynamics of the interacting Bose system were made. However, apart from the successful observation of superfluidity in liquid Helium systems, the quest to create Bose-Einstein condensates (BEC) proved unrewarding for several decades. Finally, in 1995 Bose-Einstein condensates were realized in a fascinating series of experiments on rubidium and sodium vapours [175, 176]. The importance of this experimental achievement was recognized in the 2001 Nobel Prize for Physics, shared by E. A. Cornell, W. Ketterle, and E. Wieman. The experimental realization of BEC has offered a unique opportunity to probe and control many interesting phenomena, not accessible or unstudied in the field of superfluidity, such as dimensional transitions, the crossover from Bose Einstein condensation to BCS pair condensation, interference effects, and disorder effects. Exotic links to cosmology [177], quantum optics [178] (two-state atomic quantum dots within a condensate), and even wetting phenomena [179] have been recently proposed. The growing interest in Bose systems has resulted in more than 600 studies per year. The actual observation of condensation was hindered by enormous technical difficulties, so that even 15 years ago researchers dared not to believe that nature would ever provide them with the right system. The main problem to overcome is the condensation of most systems into a solid or liquid upon cooling to low temperatures, which by-passes the BEC transition. In particular, the formation of clusters or molecules is driven by three body collisions. The hard task for an experimentalist was therefore the creation of a gaseous system, in which three body collisions occur much less frequently than two-body interactions. The gas in which the two-body interactions prevail is called dilute. Diluteness implies a very low density of the gas, so that the characteristic range a of the potential between the Bose particles is small compared to the mean particle distance, proportional to $n^{-\frac{1}{3}}$ in three dimensions ($n = N/V$ being the density of the gas). The diluteness condition is therefore equivalent to the requirement that the gas parameter $n^{\frac{1}{3}}a$ be small $n^{\frac{1}{3}}a \ll 1$.

Ultra low density of the system leads to extremely low condensation temperatures (in the nanokelvin range), realization of which was another technical obstacle for the experimentalists. At low temperature the thermal velocity of the particles ($v = \frac{\hbar}{m\lambda_{dB}} \sim 1mm/sec$) and at temperatures of the order of a few nK all the particles jump into a coherent ground state. Sufficient diluteness of the gas is therefore one of the crucial conditions for BEC to be observed in the experiment. In order to reach the required regime of temperature and density, various cooling and trapping techniques have been developed [176]. Before being cooled atoms are confined in an external potential created by an applied magnetic field. The finite extent of the condensate cloud and its inherent inhomogeneity introduce a number of important differences between BEC in a trap and uniform gas. For example, a trapped gas of Bose atoms exhibits a BEC transition not only in momentum space, but in coordinate space as well [180]. In practice however, condensates are so small that the literal observation of their size and shape is limited by the resolution of existing experimental equipment. Nevertheless real space Bose condensates provide a novel resource for exploring many interesting phenomena, such as quantum interference effects and frequency dependent collective excitations.

1.4 Motivations

Indistinguishable particles with integer (bosons) and half-integer (fermions) spin differ in how they occupy quantum states. While no more than one fermion can occupy each state (known as the Pauli exclusion principle), the number of bosons in a state is unrestricted. The difference becomes most apparent when one cools down a gas to low temperatures, where the de Broglie wavelength, becomes the same order or larger than the distance between particles. The system then enters a quantum degenerate regime. The most spectacular manifestation of this occurs for bosons, which below a critical temperature T_c undergo a phase transition, or Bose Einstein Condensation (BEC), where particles tend to macroscopically occupy a single quantum state (the condensate). Thus, at all temperatures below T_c a Bose-Einstein condensate co-exists with non-condensed particles, which collectively make up a thermal cloud. For temperatures very close to zero the thermal cloud can be, to some extent, neglected, leading to a relatively simple description in terms of a nonlinear Schrödinger equation, also known as the Gross-Pitaevskii Equation. Despite its evident simplicity, this equation nonetheless contains much interesting physics and provides a good description of many experiments, with much of the early theoretical work in Bose-Einstein condensation focusing on solving the Gross-Pitaevskii Equation, an effort that continues to the present day. Nevertheless, it is important to remember that experiments actually take place at finite temperatures. A thermal cloud is always present, and as one increases the temperature towards T_c the influence of this on the system behaviour will become progressively more important. In some situations the thermal cloud is absolutely central, for instance in the problem of condensate growth, or the heating of the gas under strong external perturbations. Future applications of Bose-Einstein condensation, such as precision measurements based on matter wave interferometry, would also benefit from a good understanding of the behaviour of the system at finite temperatures. A wide variety of different approaches to the theory of BEC were developed for the homogeneous case and have now been extended to trapped gases. Such as Hartree-Fock-Bogoliubov formalism, which makes the assumption that most of the atoms are in the same (ground) state and that these atoms may be represented classically in the form of a complex-valued wave-function (the condensate wave-function), and treats the remainder

as excitations of the ground state by means of a fluctuation operator. The assumption is then made that these excited atoms (non-condensate) may be represented as collective excitations in the form of non-interacting quasi-particles. To do this, one assumes that such a quasi-particle basis exists, and makes a canonical transformation, known as the Bogoliubov transformation. The condensate wave-function then obeys a wave equation similar to the Gross-Pitaevskii equation, but with the effects of the non-condensate now included. The transformation amplitudes for the quasi-particle creation and annihilation operators satisfy the Bogoliubov-de Gennes equations. These equations are collectively known as the Hartree-Fock-Bogoliubov equations. The problem with this approach is that in assuming the presence of a condensate, the symmetry is broken. This implies by the Hugenholtz-Pines theorem, that there must exist a zero-energy quasi-particle. This is known as the Goldstone mode, and implies that the energy spectrum must be gapless. Unfortunately in the above decomposition of the Bose field into a classical field, and a fluctuation operator which itself is represented in terms of a non-interacting quasi-particle basis, and in taking quantum expectation values (the mean-field approximation), the condensate and non-condensate are treated inconsistently, resulting in a non-zero lowest energy excitation, and hence a gap in the excitation energy spectrum. Since there is no zero-energy excitation, this implies there is no Goldstone mode, and therefore the Hugenholtz-Pines theorem is violated. However, since this theory is also a variational theory, and hence a conserving theory, all the physical conservation laws, for example number, both linear and angular, and energy conservation, are satisfied. The energy gap problem may be corrected in one of several ways by making a further approximation. In the so-called Popov approximation, the anomalous density is ignored. This is justified along the lines that two-body collisions are double-counted when one takes into account the 2-body T-matrix. The result of this approximation is that the energy spectrum is now gapless, however the number, both angular and linear momentum, and energy conservation laws are violated in the time-dependent case. We stay in the same context and we focus in the first part of our thesis to understand the static properties of BEC at zero and finite temperature by using the time-dependent variational principle of Balian and Vénéroni together with the trial Gaussian ansatz we got a set of equations governing the dynamics of a trapped Bose gas at finite temperature namely time Dependent Hatree Fock Bogoliubov Equations (TDHFB)). We show that this dynamics generalizes the Gross-Pitaevskii equations in that it introduces a consistent dynamical coupling between the evolution of the condensate density, the thermal cloud and the anomalous density. We have to mention at this point that the equations that we have derived in our thesis are quite general and fully consistent as they do not require any simplifying assumption on the noncondensed or the anomalous densities. As shown by recent theoretical studies at zero temperature, a weakly interacting BEC obeys a nonlinear wave equation that supports solitons, this wave equation is known as the Gross-Pitaevskii equation so instead to continue work on the dynamics properties of our system we prefer in the second part of our thesis to understanding more the dynamics of this equation at zero temperature in mathematical viewpoint. We use the Darboux transformation and Lax pair and we found solitonic solutions for the higher-order nonlinear Schrödinger equation (HNLSE) and some of the most well-known equation namely, Gross-Pitaevskii , Hirota, Sasa-Satsuma Equations. These equations are considered to be special cases of the general HNLSE .

Part I

Static Properties of Trapped Bose gas at finite temperatures

Introduction

Bose-Einstein condensation (BEC) [167] was observed in 1995 in a remarkable series of experiment on vapors of rubidium [141] and sodium [142] in which the atoms were confined in magnetic traps and cooled down to extremely low temperature, of the order of fractions of microkelvins. The first evidence for condensation emerged from time of flight measurements. The atoms were left to expand by switching off the confining trap and then imaged with optical methods. A sharp peak in the velocity distribution was then observed below a certain critical temperature, providing a clear signature for BEC. In the same year, first signatures of the occurrence of BEC in vapors of lithium were also reported [143].

Through the experiment of 1995 on the alkalis should be considered a milestone in the history of BEC, the experimental and the theoretical research on this unique phenomenon predicted by quantum statistical mechanics is much older and has involved different areas of physics. In particular, from the very beginning, superfluidity in helium was considered by London (1938) as a possible manifestation of BEC. Evidences for BEC in helium have later emerged from the analysis of the momentum distribution of the atoms measured in neutron scattering experiment. In recent years, BEC has been also investigated in the gas of paraexcitons in semiconductors but an unambiguous signature for BEC in this system has proven difficult to find.

Efforts to Bose condense atomic gases began with hydrogen more than 15 years ago. In a series of experiments hydrogen atoms were first cooled in a dilution refrigerator, then trapped by a magnetic field and further cooled by evaporation. This approach has come very close to observing BEC, but is still limited by recombination of individual atoms to form molecules [144]. The first observations of BEC in spin polarized hydrogen have been reported. In the 80s laser-based techniques, such as laser cooling and magneto-optical trapping, were developed to cool and trap neutral atoms [145]. Alkali atoms are well suited to laser-based methods because their optical transitions can be excited by available lasers and because they have a favorable internal energy-level structure for cooling to very low temperatures. Once they are trapped, their temperature can be lowered further by evaporative cooling [146]. By combining laser and evaporative cooling for alkali atoms, experimentalists eventually succeeded in reaching the temperatures and densities required to observe BEC.

It is worth noticing that, in these conditions, the equilibrium configuration of the system would be the solid phase. Thus, in order to observe BEC, one has to preserve the system in a metastable gas phase for a sufficiently long time. This is possible because three-body collisions are rare events in dilute and cold gases, whose lifetime is hence long enough to carry out experiments. So far BEC has been realized in ^{87}Rb [121], in ^{23}Na [122] and in ^7Li [123]. The number of experiments on BEC in vapors of rubidium and sodium is now growing fast. Meanwhile, intense experimental research is currently carried out also on vapors of Caesium, Potassium and metastable Helium.

One of the most relevant features of these trapped Bose gases is that they are inhomogeneous and finite-sized systems, the number of atoms ranging typically from a few thousands to several millions. In most cases, the confining traps are well approximated by harmonic potentials. The trapping frequency, ω_0 , provides also a characteristic length scale for the system, $a_0 = \sqrt{\frac{\hbar}{m\omega_0}}$, of the order of a few microns in the available samples. Density variations occur on this scale. This is a major difference with respect to other systems, like for instance superfluid helium, where the effects of inhomogeneity take place on a microscopic scale fixed by the interatomic distance. In the case of 87 Rb and 23 Na, the size of the system is enlarged as an effect of repulsive two-body forces and the trapped gases can become almost macroscopic objects, directly measurable with optical methods. A sequence of in situ images of an oscillating condensate of sodium atoms was taken at the Massachusetts Institute of Technology (MIT), where the mean axial extent is of the order of 0.3 mm.

The fact that these gases are highly inhomogeneous has several important consequences. First BEC shows up not only in momentum space, as happens in superfluid helium, but also in co-ordinate space. This double possibility of investigating the effects of condensation is very interesting from both the theoretical and experimental points of view and provides novel methods of investigation for relevant quantities, like the temperature dependence of the condensate, energy and density distributions, interference phenomena, frequencies of collective excitations, and so on. Another important consequence of the inhomogeneity of these systems is the role played by two-body interactions. The main point is that, despite the very dilute nature of these gases (typically the average distance between atoms is more than ten times the range of interatomic forces), the combination of BEC and harmonic trapping greatly enhances the effects of the atom-atom interactions on important measurable quantities. For instance, the central density of the interacting gas at very low temperature can be easily one or two orders of magnitude smaller than the density predicted for an ideal gas in the same trap. Despite the inhomogeneity of these systems, which makes the solution of the many-body problem nontrivial, the dilute nature of the gas allows one to describe the effects of the interaction in a rather fundamental way. In practice a single physical parameter, the s-wave scattering length, is sufficient to obtain an accurate description. The recent experimental achievements of BEC in alkali vapors have renewed a great interest in the theoretical studies of Bose gases. A rather massive amount of work has been done in the last couple of years, both to interpret the initial observations and to predict new phenomena. In the presence of harmonic confinement, the many-body theory of interacting Bose gases gives rise to several unexpected features. This opens new theoretical perspectives in this interdisciplinary field, where useful concepts coming from different areas of physics (atomic physics, quantum optics, statistical mechanics and condensed matter physics) are now merging together. The natural starting point for studying the behavior of these systems is the theory of weakly interacting bosons which, for inhomogeneous systems, is described by the Gross-Pitaevskii approximation. This is a mean field approach for the order parameter associated with the condensate. It provides closed and relatively simple equations for describing the relevant phenomena associated with BEC. In particular, it reproduces typical properties exhibited by superfluid systems, like the propagation of collective excitations and the interference effects originating from the phase of the order parameter. The theory is well suited to describing most of the effects of two-body interactions in these dilute gases at zero temperature and can be extended to explore also thermal effects. In the following, we outline the remaining chapters of this part

- We will begin this part by general notions about the ultracold Bose gases, where we give a short history and background of the domain. This includes a discussion of the early experiments. We also discuss the relation between BEC and Solitons.
- In chapter 3, we present the second-quantized description of a quantum many body system of interacting bosons and systematically derive the set of mean-field equations that describe the condensate field and the quantum fluctuations of the dilute, interacting Bose gas at zero-temperature.
- Chapter 4 is devoted to review the main steps used to derive the Time dependent Hartree-Fock-Bogoliubov (TDHFB) equations from the Balian-Véroni variational principle. The TDHFB equations are applied to a system of self-interacting trapped bosons to derive a coupled dynamics of the condensate, the non condensate and the anomalous densities. Then, we present the static solutions of the system and discuss their properties at zero temperature. At finite temperature, the equations are much more involved and require a careful analysis. In the TF limit, we present a simple method which allows for a self-consistent determination of the various density profiles as well as some other static properties of the condensate such as the chemical potential and the condensate radius. Indeed, the TF approximation obviously provides simple enough analytical expressions since it amounts to neglecting the second order derivatives thus yielding algebraic equations instead of partial differential equations. This is the main advantage of our method which yields the most important qualitative features without having to handle highly non-linear self-consistent equations.

We present the results of our calculations. We plot first the condensate radius and the central density as functions of the condensate fraction and note in particular the compression effect of the condensate due to the thermal cloud. Moreover, we discuss the TF profile obtained for the condensate density even at low condensate fraction. The noncondensate density profile is also plotted for a wide range of condensate fraction and shows a good qualitative agreement with experiments. Finally, the anomalous density, although not yet measured experimentally, is shown to behave in a quite intuitive way.

- Some concluding remarks and improvements of our method are given in the conclusion.

Chapter 2

Background Theory and Experiment

2.1 Introduction

. One of fundamental results of the quantum theory was the prediction of the Bose Einstein statistics in a gas of boson particles at zero temperature. Such a state of matter in the form of the Bose Einstein condensate (BEC) remained a theoretical concept during seventy years after it had been predicted. A breakthrough, which has turned out to be, arguably, the greatest achievement in the field of fundamental physics in the course of the past fifteen years, was the creation of BEC in ultracold gases of alkali metals, which was reported in 1995 by Anderson et al. (in the gas of atoms of $87Rb$), Bradley et al. (in $23Na$), and Davis et al. (in $7Li$). In these celebrated experiments, the gas composed of several thousands of atoms was chilled, by means of a combination of the laser cooling and evaporation techniques, to temperatures on the order of fractions of nano Kelvin. One of milestones in the subsequent experimental work on BEC was the creation of effectively one dimensional bright(i.e., localized) matter-wave solitons in the condensate of $7Li$ atoms trapped in "cigar-shaped" configurations [166]. In particular, multi-soliton trains have been created in the former work, in addition to single soliton modes. Later, similar solitons were also created in a post collapse state of the $85Rb$ condensate by Cornish, Thompson, and Wieman, 2006 (the collapse was caused by the switch of the interaction from repulsive to attractive by means of the FR). A fundamental theoretical model of the matter-wave dynamics in BEC, including the description of solitons, is provided, with a very good accuracy, by the Gross-Pitaevskii equation(GPE), which is based on the mean field approximation, and a more review of nonlinear aspects of the matter-wave dynamics and solitons [138]. Various aspects of the matter wave dynamics, both theoretical and experimental, have been thoroughly reviewed in a recent collection of articles edited by Kevrekidis, Frantzeskakis, and Carretero-Gonzalez, 2008 [139].

2.2 History of BEC studies

It is useful to first give a brief history of BEC studies, starting with the initial prediction of Einstein in 1925 [167] for the case of a non-interacting gas of Bose atoms. Atoms with an even number of neutrons satisfy Bose statistics, which accounts for about 70 of the atoms in the periodic table[168].

The momentum distribution of an ideal uniform Bose gas is given by

$$f_B(\epsilon_k) = \frac{1}{e^{\beta(\epsilon_k - \mu)} - 1}, \quad (2.1)$$

where $\epsilon_k = \frac{k^2 \hbar^2}{2m}$, $\beta = \frac{1}{k_B T}$ and μ is the chemical potential determined by the condition that the sum over all possible states equals the total number of particles N . In a system of macroscopic size, the sum can be converted into an integral

$$N = \sum_k f_B(\epsilon_k) = \int D(\epsilon) f_B(\epsilon) d\epsilon, \quad (2.2)$$

where the density of states $D(\epsilon)$ goes as $\sim \sqrt{\epsilon}$ in $3D$. If the volume V and the particle number N are fixed, the (negative) chemical potential μ increases as the temperature T decreases. At a certain temperature T_c , μ reaches zero, the maximum value it can reach in an ideal Bose gas, and thus the integral in Eq. (2.2) gives

$$N = 2.612V\lambda^3(T_c), \quad (2.3)$$

where the thermal de Broglie wavelength $\lambda(T)$ is

$$\lambda(T) \equiv \left(\frac{2\pi\hbar^2}{mk_B T}\right)^{\frac{1}{2}}, \quad (2.4)$$

One may view T_c defined by Eq. (2.3) as equivalent to the condition that the thermal de Broglie wave length $\lambda(T)$ becomes comparable to the average separation d between particles ($d \sim n^{-\frac{1}{3}}$). In this case, the quantum mechanical wave nature of the particles leads to all atoms becoming increasingly correlated. This is the essential physics behind BEC in an ideal Bose gas. As T goes lower than T_c , μ is pinned at zero, and the right-hand side of Eq. (2.3) becomes smaller than N . As Einstein [167] first pointed out, the additional particles enter the ground state to form what is now called the Bose-Einstein condensate. The number of particles in this lowest state is given by

$$N_0 = N - 2.612V\lambda^3(T) > 0 \text{ if } T < T_c, \quad (2.5)$$

From Eq. (2.3) and Eq. (2.5), one obtains the temperature-dependent condensate fraction

$$\frac{N_0(T)}{N} = 1 - \left(\frac{T}{T_c}\right)^{\frac{3}{2}}, \quad (2.6)$$

It is immediately seen that $N_0 = N$ at $T = 0$, that is, all the atoms are in the lowest single-particle state ($k = 0$). Bose-Einstein statistics described by Eq. (2.1) predicts that at a finite temperature given by Eq. (2.3), the lowest state becomes macroscopically occupied and a transition occurs to a new phase of matter characterized by the condensate fraction. It is the only phase transition in condensed matter physics that can occur in the absence of interactions being entirely due to quantum mechanical effects related to Bose statistics.

At the time of Einstein's prediction, the nature of second-order phase transitions was not yet understood, and Uhlenbeck (a graduate student of Paul Ehrenfest) criticized Einstein's analysis in his thesis in 1927. In his article he explained that mathematically the condensation could not occur in the fundamental mode because the process gas saturation was not valid; simply varying the temperature to change the particle density and vice versa. Uhlenbeck criticism was generally accepted.

It was only in 1937 that Uhlenbeck's objections to a phase transition in an ideal Bose gas was shown to be incorrect. Around the same time, superfluidity had been just discovered in liquid He below $2.17K$. Fritz London[169] immediately made the bold conjecture that this superfluidity was related to a form of Bose-Einstein condensation, suitably generalized to a liquid. The basis of London's argument was that He was a Bose atom ($S = 0$) and moreover if liquid He was treated as an ideal gas, with the density $2.20 \times 10^{22} \frac{\text{atoms}}{\text{cm}^3}$, its BEC transition temperature given by Eq. (2.3) would be $3.15K$. This is remarkably close to the observed superfluid transition temperature. Essentially, London and Tiza argued that the superfluid characteristics were related to the motion of the Bose condensate, moving as a whole. The development and conformation of these ideas about superfluid He took many years. They remain controversial since the successful work of Landau[170] of the low-temperatures properties of superfluid He. Indeed based on a phenomenological model of a weakly interacting gas of phonon-roton excitations, it made no explicit reference to any role of the Bose statistics, let alone a Bose condensate. In view of the difficulties in dealing with a strongly interacting, dense system like superfluid He, it is not surprising that since 1960s, there has been an increasing experimental effort to achieve BEC in a dilute Bose gas. At the low temperature needed for BEC, most system will form condensed phase (liquid or solid) due to the attractive inter-atomic interaction. Thus, one requires conditions that allow Bose condensation to occur rapidly, relative to the longer time scales needed for the competing phase change.

In 1957 a theory proposed by John Bardeen, Leon Neil Cooper, and John Robert Schrieffer called BCS theory in which pairs of electrons form composite bosons in superconductors, linking superconductivity to phenomena very similar to Bose-Einstein condensation[171].

Beliaev in 1958 [173] presented an approach forming the basis of the systematic application of the quantum field theory methods to Bose systems with condensate, including anomalous propagators representing two particles going into or out of the condensate. In 1959, this approach was developed further by Hugenholtz and Pines [174, 175], and was thoroughly reexamined in 1963 by Gavoret and Nozières[176, 177]. They showed that the singular character of the interactions in a Bose system with condensate remarked by Bogoliubov manifests itself in divergences of perturbation theory at small momenta (infrared divergences). Gavoret and Nozières scrutinized this question inspired by the higher-order calculations by Beliaev [173] and Hugenholtz-Pines [173, 174]. They showed that infrared divergences cancel out in all physical quantities; the energy gap in elementary excitation spectrum vanishes to all order of perturbation theory. For further developments see [178, 179].

A key development relevant to trapped gases was due to Pitaevskii. Many of us now are very familiar with the famous Gross-Pitaevskii equation[180, 181]. However, Pitaevskii's real contribution was not this particular equation rather it lies more in introducing the whole idea of a macroscopic wavefunction which could depend on both position and time. Pitaevskii's work, of course, was inspired by the use of a similar wavefunction by Ginzburg and Landau in their pioneering theory of spatially inhomogeneous superconductors[182]. In 1963, the Hugenholtz-Pines-Gavoret-Nozières theorem was discovered by Bogoliubov under the name $2/1$ k theorem. Instead of perturbation theory, Bogoliubov's proof of this theorem is based on local gauge transformations. He showed [183, 184] that the appearance of a gap in some models is a consequence of the lack of local gauge invariance.

In 1965, Popov [185, 186] proposed a generalization of the Bogoliubov theory for $T \neq 0$

in which the density of thermal component can be taken into account. This theory gives the elementary excitation spectrum similar to that for $T = 0$, but now with temperature-dependent condensate. This leads to the collapse of the low phonon-spectrum to free particles as $T \rightarrow T_c$. A craze for low dimensions started at this period by M. Girardeau in 1960 [187] in his study on the impenetrable one dimensional Bose gas. Furthermore, Lieb and Liniger [188] solved exactly the zero-temperature interacting Bose gas with repulsive delta function potential and showed that the derived ground state properties agree with Bogoliubov's perturbation theory only in the limit of very weak coupling constant. The time-dependent thermodynamic behavior for the Lieb-Liniger model was presented by Yang and Yang [189] through the use of the Bethe ansatz. Regarding the case of a gas without interactions, all began with H. Casimir in 1968 [190] who studied the Bose-Einstein condensation of an ideal gas Bose in anisotropic boxes.

2.3 Bose Einstein Condensation and Solitons

The term soliton, i.e., a stable solitary wave propagating in a nonlinear medium, was coined by Zabusky and Kruskal about 50 years ago. These authors were not the first to notice the remarkable properties of solitary waves, whose first known description in the scientific literature, in the form of "a large solitary elevation, a rounded, smooth and well defined heap of water", goes back to the historical observation made in a canal near Edinburgh by John Scott Russell in the 1830s. In the course of the nearly five decades that have elapsed since the publication of the paper by Zabusky and Kruskal (1965), the theoretical and experimental studies of solitary waves have seen an astonishing proliferation and penetration into many branches of science, from applied mathematics and physics to chemistry and biology. Several celebrated equations, in both their canonical and extended forms, emerge as universal models of solitons. These include Korteweg de Vries and modified Korteweg de Vries, nonlinear Schrödinger (with two opposite signs of the nonlinearity), sine-Gordon, Landau-Lifshitz, Kadomtsev-Petviashvili and several other classical equations. The specific features of the evolution and interactions of solitons in these models are intimately related to the integrability of the above-mentioned equations. Diverse factors that in practice often break the integrability should be taken into regards, which naturally leads to the perturbation theory for solitons in nearly integrable system [191]. A very significant contribution to the experimental and theoretical studies of solitons was the identification of various forms of robust solitary waves in nonlinear optics. Optical solitons may be naturally subdivided into three broad categories temporal, spatial, and spatiotemporal ones. They may exist in the form of one-dimensional (1D) or multi-dimensional objects. One-dimensional temporal solitons in optical fibers with a cubic (Kerr) nonlinearity were predicted by Hasegawa and Tappert (1973), and observed experimentally by Mollenauer, Stolen, and Gordon (1980), while stable self-trapping of light in the spatial domain was first observed in planar waveguides by Maneuf, Desailly, and Froehly (1988). Spatial two-dimensional (2D) solitary waves were first observed in photorefractive crystals, which feature a saturable nonlinearity [192], and in optical media with a quadratic nonlinearity [193]. Effectively two-dimensional spatio-temporal self-trapping of light into quasi-soliton objects was observed by Liu, Qian, and Wise (1999) also in quadratic nonlinear media. Stable fully three-dimensional (3D) solitons, or light bullets (LBs) in quadratic media were predicted almost three decades ago [194]. However, to date, experimental generation of such long-lived 3D solitons remains elusive. In

a landmark observation, the signature of 3D soliton formation was achieved recently by Minardi et al. (submitted) in an artificial optical material with cubic nonlinearity. Another species of robust solitary waves in optics occurs in the form of gap solitons (GSs), that are supported by the interplay of an appropriate lattice structure (alias grating), embedded into an optical medium, and nonlinearity. The observation of the first optical GSs in fiber Bragg gratings was reported by Eggleton et al. (1996).

A milestone achievement of modern physics, the creation of Bose-Einstein condensates (BECs) in ultracold vapors of alkali metals [195, 196, 197], was shortly followed by the creation of dark solitons of matter waves in BEC with repulsion between atoms [198] and, eventually, by the creation of bright 1D matter-wave solitons in BEC with attractive interatomic interactions [199, 200]. This was followed by the generation of one-dimensional GSs in condensates with repulsive interactions between atoms loaded into a periodic potential induced by an optical lattice (OL), i.e., the pattern created by the interference of counter-propagating coherent laser beams illuminating the condensate [201].

Chapter 3

Field Theory for Bose Gases

3.1 Introduction

When describing a many-particle system, like the dilute Bose gas in a trap, it is impossible in practice to take the motion of every single particle into account. A characteristic of the phenomenon of Bose-Einstein condensation is the occurrence of a macroscopically occupied state that can be described by a classical wave function. At temperatures well below the critical temperature, where the phase transition to Bose-Einstein condensation occurs, this is an excellent description of the condensed state. Even at higher temperatures one can treat the thermal atoms as fluctuations of this classical field to a very good approximation. Important properties of the condensate, like its shape and its momentum distribution, can be described by a non-linear Schrödinger equation. The interactions between the atoms are accounted for by a term proportional to the condensate density $|\Phi|^2$. Let us consider a system of trapped bosons interacting via a two-body potential. The grand canonical Hamiltonian may be written in the form

$$H = \int d\vec{r} \hat{\Psi}^\dagger(\vec{r}, t) h^{sp} \hat{\Psi}(\vec{r}, t) + \frac{1}{2} \int \int d\vec{r} d\vec{r}' \hat{\Psi}^\dagger(\vec{r}', t) \hat{\Psi}^\dagger(\vec{r}, t) V(\vec{r}, \vec{r}') \hat{\Psi}(\vec{r}', t) \hat{\Psi}(\vec{r}, t). \quad (3.1)$$

Where $h^{sp} = -\frac{\hbar^2}{2m} \Delta + V_{ext}(\vec{r})$ is the single particle Hamiltonian, $V(\vec{r}, \vec{r}')$ is the two-body interaction potential, and $V_{ext}(\vec{r})$ the external confining field. $\hat{\Psi}(\vec{r})$ and $\hat{\Psi}^\dagger(\vec{r})$ are the creation and annihilation operators satisfying the usual commutation relations.

$$[\hat{\Psi}(\vec{r}), \hat{\Psi}^\dagger(\vec{r}', t)] = \delta(\vec{r}, \vec{r}'). \quad (3.2)$$

$$[\hat{\Psi}^\dagger(\vec{r}), \hat{\Psi}^\dagger(\vec{r}')] = [\hat{\Psi}(\vec{r}), \hat{\Psi}(\vec{r}')]. \quad (3.3)$$

This Hamiltonian is the starting point for all theoretical treatments of dilute Bose gases, and includes both thermal and quantum fluctuations. All theories appearing in the literature arise from distinct approximations for this Hamiltonian. For dilute gases at very low temperature, the usual procedure is to make a contact interaction approximation

$$V(\vec{r}, \vec{r}') = g \delta(\vec{r}, \vec{r}'). \quad (3.4)$$

The potential Eq. (3.4)) means that the two atoms undergo perfectly elastic local collisions, like two billiard balls. The strength of the interaction is given by $g = \frac{4\pi\hbar^2 a}{m}$, where a is the s-wave scattering length for a particular atomic species, which can be determined from experiments. This is a somewhat idealized scenario, which can nonetheless be put on firm ground by a more careful treatment - the origin and validity of this approximation will be discussed later. Substitution into the Hamiltonian Eq. (3.1)) then gives:

$$H = \int d\vec{r} \hat{\Psi}^\dagger(\vec{r}, t) h^{sp} \hat{\Psi}(\vec{r}, t) + \frac{g}{2} \int d\vec{r} \hat{\Psi}^\dagger(\vec{r}, t) \hat{\Psi}^\dagger(\vec{r}, t) \hat{\Psi}(\vec{r}, t) \hat{\Psi}(\vec{r}, t). \quad (3.5)$$

The starting point for the dynamics of ultracold gases is to consider the equation[218] governing the evolution of the bosonic field operator $|\hat{\Psi}(\vec{r}, t)|$, i.e. the so-called equation of motion. The second-quantized form of the appropriate equation can be analyzed in one of three distinct pictures, known as the Schrödinger, Heisenberg and the interaction pictures, depending on whether the state-vectors, the operators corresponding to system observables, or both are time-dependent [295, 296]. In the Schrödinger picture, the state vectors are time-dependent and the operators are time-independent; in this picture, the solution of the Schrödinger equation at time t , given the initial solution at t_0 , is given by unitary transformation $|\Psi_S(t)\rangle = \exp \frac{-i\hat{H}(t-t_0)}{\hbar} |\Psi_0(t)\rangle$ where \hat{H} does not contain any explicit time-dependence, and the subscript S has been introduced to denote the Schrödinger picture. In the interaction picture, both operators and state vectors depend on time. Finally, in the Heisenberg picture the state vectors, which can be constructed from the corresponding Schrödinger picture state vectors via $|\Psi_H(t)\rangle = \exp \frac{i\hat{H}t}{\hbar} |\Psi_S(t)\rangle$, are time-independent and all time dependence is contained in the operators. While all three pictures can be used interchangeably, most subsequent discussion will be given in the Heisenberg picture in which the equation of motion of a general operator \hat{O}_H obeys

$$i\hbar \frac{d\hat{O}_H}{dt} = [\hat{O}_H, \hat{H}]. \quad (3.6)$$

In studying the system dynamics, we will actually be concerned with the equations of motion of the Bose field operator $\hat{\Psi}$. For the Hamiltonian of Eq. (3.6)), this evolves according to the Heisenberg equation of motion

$$i\hbar \frac{d\hat{\Psi}(\vec{r}, t)}{dt} = [\hat{\Psi}(\vec{r}, t), \hat{H}] = h^{sp} \hat{\Psi}(\vec{r}, t) + g \hat{\Psi}^\dagger(\vec{r}, t) \hat{\Psi}(\vec{r}, t) \hat{\Psi}(\vec{r}, t). \quad (3.7)$$

In order to extract information from this equation, it is convenient to separate the condensate contribution, which corresponds to the macroscopic occupation of a single quantum state, from the remaining part of the Bose field operator. Hence the Bose field operator is divided into two parts [297, 298]

$$\hat{\Psi}(\vec{r}, t) = \Phi(\vec{r}, t) + \tilde{\Psi}(\vec{r}, t). \quad (3.8)$$

corresponding respectively to a field operator for the condensate, Φ and one for the non-condensed atoms, $\tilde{\Psi}$. These could either correspond to thermally-excited atoms, quantum-mechanical fluctuations, or atoms promoted into higher energy states due to interactions. It is important to notice at this level that the condensate is described by a classical function and not by a field operator. This approximation is well justified since the ground state is macroscopically occupied [299]. Then we break down the full system Hamiltonian

into various contributions based on the number of condensate and non-condensate factors contained in each of them. In particular, substitution of Eq. (3.8) into the system Hamiltonian Eq. (3.5) leads to

$$H = H_0 + H_1 + H_2 + H_3 + H_4. \quad (3.9)$$

Where

$$\begin{aligned} H_0 &= \int d\vec{r} [\Phi^* \hat{h}^{sp} \Phi + \frac{g}{2} |\Phi|^4], \\ H_1 &= \int d\vec{r} [\hat{\Psi}^+ (\hat{h}^{sp} + g |\Phi^2|) \Phi + \Phi^* (\hat{h}^{sp} + g |\Phi^2|) \hat{\Psi}], \\ H_2 &= \int d\vec{r} [\hat{\Psi}^+ (\hat{h}^{sp} + 2g |\Phi^2|) \hat{\Psi} + \frac{g}{2} (\Phi^{*2} \hat{\Psi} \hat{\Psi} + \Phi^2 \hat{\Psi}^+ \hat{\Psi}^+)], \\ H_3 &= g \int d\vec{r} [\Phi \hat{\Psi}^+ \hat{\Psi}^+ \hat{\Psi} + \Phi^* \hat{\Psi}^+ \hat{\Psi} \hat{\Psi}], \\ H_4 &= \frac{1}{2} \int d\vec{r} \hat{\Psi}^+ \hat{\Psi}^+ \hat{\Psi} \hat{\Psi} \end{aligned} \quad (3.10)$$

H_0 has no 'hat' as there are no operators within it (it is a purely classical quantity represented by a complex function).

3.2 Zero Temperature Mean Field Theory

we focus in this section on the simplest possible mean field theory. This is based on the approximation $H \approx H_0$, in which the non-condensate field operator is neglected completely. This gives rise to the well-known Gross-Pitaevskii equation, which is valid at $T = 0$ and in the limit of negligible quantum fluctuations. By linearization we then derive equations for the collective modes around the ground state. These are shown to be identical to the modes of Bogoliubov quasiparticles found by diagonalization of the first three terms of the Hamiltonian, i.e. $H \approx (H_0 + H_1 + H_2)$. We start by the zero temperature formalism to understand well the finite temperature.

3.2.1 The Gross-Pitaevskii Equation

In the $T = 0$ limit, all of the particles are in the condensate, so that $N = N_0$ and the non condensate operator can be neglected ($\hat{\Psi} = \hat{\Psi}^+ = 0$); in other words, we set $\hat{\Psi}(\vec{r}, t) \rightarrow \Phi(\vec{r}, t)$. Hence, $\hat{\Psi}^+ \rightarrow \Phi^*(\vec{r}, t)$, so in this case we consider only H_0 . The exact Heisenberg equation of motion Eq. (3.6) reduces then to the so-called Gross-Pitaevskii Equation (GPE)[300, 301]

$$i \hbar \frac{d\Phi(\vec{r}, t)}{dt} = [\hat{h}^{sp}(\vec{r}, t) + g |\Phi(\vec{r}, t)|^2] \Phi(\vec{r}, t) = \left[\frac{-\hbar^2}{2m} \nabla^2 + V_{ext}(\vec{r}, t) + g |\Phi(\vec{r}, t)|^2 \right] \Phi(\vec{r}, t). \quad (3.11)$$

This equation is a nonlinear Schrödinger equation, corresponding to the zero temperature hydrodynamic description of Bose gases, first introduced to study vortex lines in an imperfect Bose gas. This equation is mathematically analogous to a Ginzburg-Landau-type approach [302], valid near the critical regime although the origin of the various contributions and the physical interpretation here is actually quite distinct. Remarkably, the GPE, which was first numerically implemented for dilute weakly-interacting trapped Bose gases was undertaken by Mark Edwards, Keith Burnett and collaborators[227, 228, 229],

provides a good description of the dynamics of a Bose-Einstein condensate for a wide class of problems at temperatures as high as $T \approx \frac{T_c}{2}$. The GPE can be used, at low temperature, to explore the macroscopic behavior of the system, characterized by variations of the order parameter over distances larger than the mean distance between atoms.

One can find static solutions by eliminating the time-dependence via the transformation:

$$\Phi(\vec{r}, t) = \Phi(\vec{r}) \exp \frac{-i \mu t}{\hbar}. \quad (3.12)$$

where μ is the chemical potential (which is equal to the energy per particle only for non-interacting particles). Substituting Eq. (3.12) into Eq. (3.11) yields the time-independent GPE:

$$\mu \Phi(\vec{r}) = \left[\frac{-\hbar^2}{2m} \nabla^2 + V_{ext}(\vec{r}, t) + g |\Phi(\vec{r}, t)|^2 \right] \Phi(\vec{r}, t). \quad (3.13)$$

In the form given above, the wavefunction is normalized to the total number of particle, i.e $\int |\Phi(\vec{r}, t)|^2 d\vec{r} = N$. Alternatively, the Gross-Pitaevskii equation Eq. (3.11) can also be obtained using a variational procedure:

$$i \hbar \frac{d\Phi}{dt} = \frac{\delta E}{\delta \phi^*}. \quad (3.14)$$

where the energy functional E is given by

$$E[\Phi] = \int dr \left[-\frac{\hbar^2}{2m} |\nabla \Phi|^2 + V_{ext}(r) |\Phi|^2 + \frac{g}{2} |\Phi|^4 \right] = E_{kin} + E_p + E_{int}. \quad (3.15)$$

The first term in the integral Eq. (3.15) is the kinetic energy of the condensate E_{kin} , the second is the trapping energy E_p , while the last one is the mean field interaction energy E_{int} . In the case of nonnegative and finite-range interatomic potentials, rigorous bounds for this term have been obtained by Dyson [230], and Lieb and Yngvason [231].

Ground state Solution of GPE in Thomas-Fermi limit :

In the case of atoms with repulsive interaction ($a > 0$) the limit $\frac{Na}{a_{H_0}} \gg 1$ is particularly interesting, since this condition is well satisfied by the parameters N, a and a_{H_0} used in most of current experiments. Moreover, in this limit the predictions of mean-field theory take a rather simple analytic form (Edwards and Burnett [232]; Baym and Pethick [233]). As regards the ground state, the atoms are pushed outwards, the central density becomes rather flat, and the radius grows. As a consequence, the kinetic term in the Gross-Pitaevskii takes a significant contribution only near the boundary and becomes less and less important with respect to the interaction energy. If one neglects completely the kinetic term in Eq. (3.13), one gets the density profile in the form

$$n(r) = \frac{\mu - V_{ext}(r)}{g}. \quad (3.16)$$

Note that chemical potential $\frac{\partial E}{\partial N}$ turns out to be $\frac{E}{N} = \left(\frac{5}{7}\right)\mu$ in the region where $\mu > V_{ext}(r)$. This is often referred to as Thomas Fermi (TF) approximation. The normalization condition on $n(r)$ provides the relation between chemical potential and number of particles:

$$\mu = \frac{\hbar \omega}{2} \left(\frac{15 N a}{a_{H_0}} \right)^{\frac{2}{5}}. \quad (3.17)$$

This energy is the sum of the interaction and oscillator energies, since the kinetic energy gives a vanishing contribution for large N . The density profile Eq. (3.16) has the form of an inverted parabola, which vanishes at the classical turning point R defined by the condition $\mu = V_{ext}(R)$. For a spherical trap, this implies $\mu = \frac{m\omega^2 R^2}{2}$ and, using the result Eq. (3.17) for μ , one finds the following expression for the radius of the condensate

$$R_{TF} = a_{Ho} \left(\frac{15 N a}{a_{Ho}} \right)^{\frac{1}{5}} \quad (3.18)$$

which grows with N . It is interesting to note at this stage that the application of the TF approximation to the trapped Bose gases was pioneered by the earlier work of Goldman, Silvera and Leggett [234], by Oliva [235] and by Chou, Yang, and Yu [236], by Timmermans, Tommasini and K. Huang [237] and P. Schuck et al [238]. It is worth mentioning that a finite temperature version of the Thomas-Fermi approximation was also investigated by using the Time dependent Hartree-Fock-Bogoliubov equations [243], where in particular extended analytic expressions for the condensate, the non condensate and anomalous densities are derived. The exploration of these equations at finite temperature leads to the fact that all the thermodynamics quantities deviate from the standard values in the TF regime. The results are quite encouraging owing to the simplicity of the formalism [244].

3.3 The Bogoliubov approximation

The Hamiltonian of Eq. (3.1) thus represents, in the occupation number representation of second quantization the basic system Hamiltonian corresponding to the original position representation. For a uniform gas occupying a volume, the field operator $\hat{\Psi}(\vec{r})$ can be expanded by plane waves:

$$\begin{aligned} \hat{\Psi}(\vec{r}) &= \sum_{\vec{k}} \frac{1}{V} \exp(i\vec{k}\vec{r}) \hat{a}_{\vec{k}}, \\ \hat{\Psi}^+(\vec{r}) &= \sum_{\vec{k}} \frac{1}{V} \exp(-i\vec{k}\vec{r}) \hat{a}_{\vec{k}}^+ \end{aligned} \quad (3.19)$$

which are summed over the complete set of single-particle quantum numbers. Upon plugging Eq. (3.18) in Eq. (3.1), we get

$$\hat{H} = \sum_{\vec{k}} \frac{\hbar^2 k^2}{2m} \hat{a}_{\vec{k}}^+ \hat{a}_{\vec{k}} + \frac{1}{2V} \sum_{\vec{k}} \tilde{V}(\vec{q}) \hat{a}_{\vec{k}+\vec{q}}^+ \hat{a}_{\vec{k}-\vec{q}}^+ \hat{a}_{\vec{k}} \hat{a}_{\vec{k}}. \quad (3.20)$$

Here $\tilde{V}(\vec{q}) = \int V(\vec{r}) \exp(-i\vec{q}\vec{r}) d\vec{r}$ is the Fourier transform of the two body scattering potential.

In real systems $V(\vec{r})$ always contains a short-range term, which makes it difficult to solve the Schrödinger equation at the microscopic level. However, by virtue of the above assumptions on dilute and cold gases, one can conclude that the actual form of $V(\vec{r})$ is not important for describing the macroscopic properties of the gas, as far as the assumed fictitious potential $V_{eff}(\vec{r})$ gives the correct value for the low momentum value of its Fourier transform. It is therefore convenient to replace the actual potential $V(\vec{r})$ with an effective, smooth potential. Since the macroscopic properties of the system depend on $\tilde{V}(q=0) = g$, this procedure will provide the correct answer to this complicated many-body problem as far as the system is dilute and cold.

Replacing $\tilde{V}(q=0) = g$ in Eq. (3.20), yields a new simpler Hamiltonian

$$\hat{H} = \sum_{\vec{k}} \frac{\hbar^2 k^2}{2m} \hat{a}_{\vec{k}}^+ \hat{a}_{\vec{k}} + \frac{g}{2V} \sum_{\vec{k}} \hat{a}_{\vec{k}+q}^+ \hat{a}_{\vec{k}-q}^+ \hat{a}_{\vec{k}} \hat{a}_{\vec{k}}. \quad (3.21)$$

Since the lowest energy state is macroscopically occupied, one can neglect the quantum fluctuation of this state and replace the operator a_0 by a c-number: $a_0 \simeq a_0^+ \simeq \sqrt{N}$. The Hamiltonian Eq. (3.21) separates into eight distinct parts

$$\begin{aligned} E_0 &= \frac{1}{2} V n^2 \tilde{V}(0), \\ V_1 &= \frac{1}{2} n \sum_{\vec{k}} \tilde{V}(q) \hat{a}_{\vec{k}} \hat{a}_{-\vec{k}}, \\ V_2 &= \frac{1}{2} n \sum_{\vec{k}} \tilde{V}(q) \hat{a}_{\vec{k}}^+ \hat{a}_{-\vec{k}}, \\ V_3 &= \frac{1}{2} n \sum_{\vec{k}} \tilde{V}(q) \hat{a}_{\vec{k}}^+ \hat{a}_{\vec{k}}, \\ V_4 &= \frac{1}{2} n \sum_{\vec{k}} \tilde{V}(0) \hat{a}_{\vec{k}}^+ \hat{a}_{\vec{k}}, \\ V_5 &= \frac{n}{V} n \sum_{\vec{k}} \tilde{V}(q) \hat{a}_{\vec{k}+q}^+ \hat{a}_{\vec{k}} \hat{a}_{\vec{q}}, \\ V_6 &= \frac{n}{V} \sum_{\vec{k}, \vec{q}} \tilde{V}(q) \hat{a}_{\vec{k}}^+ \hat{a}_{\vec{q}} \hat{a}_{\vec{k}+\vec{q}}, \\ V_7 &= \frac{1}{2V} n \sum_{\vec{k}, \vec{k}', \vec{q}} \tilde{V}(q) \hat{a}_{\vec{k}+\vec{q}}^+ \hat{a}_{\vec{k}'-\vec{q}}^+ \hat{a}_{\vec{k}} \hat{a}_{\vec{k}} \end{aligned} \quad (3.22)$$

We note that in \hat{H} there is no term containing a single because these would violate momentum conservation. By using the normalization relation,

$$\begin{aligned} \hat{a}_0^+ \hat{a}_0 &= \hat{N}_c = N - \sum_{\vec{k} \neq 0} \hat{a}_{\vec{k}}^+ \hat{a}_{\vec{k}} \\ (\hat{a}_0^+ \hat{a}_0)^2 &= (N - \sum_{\vec{k} \neq 0} \hat{a}_{\vec{k}}^+ \hat{a}_{\vec{k}})^2 \approx N^2 - 2N \sum_{\vec{k} \neq 0} \hat{a}_{\vec{k}}^+ \hat{a}_{\vec{k}}, \end{aligned} \quad (3.23)$$

Substitution of Eq. (3.22) and Eq. (3.23) into Eq. (3.21) yields the following expression for the Hamiltonian:

$$\hat{H} = \frac{1}{2} g n N + \sum_{\vec{r}} \frac{\hbar^2 k^2}{2m} \hat{a}_{\vec{r}}^+ \hat{a}_{\vec{k}} + \frac{1}{2} g n \sum_{\vec{k} \neq 0} [2\hat{a}_{\vec{k}}^+ \hat{a}_{\vec{k}} + \hat{a}_{-\vec{k}}^+ \hat{a}_{\vec{k}}^+ + \hat{a}_{\vec{k}} \hat{a}_{-\vec{k}}] \quad (3.24)$$

The third term of this Hamiltonian represents the self-energy of the excited state due to the interaction, simultaneous creation of the excited states of momenta and simultaneous annihilation of the excited states, respectively. Eq. (3.24) can be diagonalized by the following linear transformation

$$\begin{aligned} \hat{a}_{\vec{k}} &= u_{\vec{k}} \hat{b}_{\vec{k}} - v_{\vec{k}} \hat{b}_{-\vec{k}}^+ \\ \hat{a}_{-\vec{k}}^+ &= u_{\vec{k}} \hat{b}_{-\vec{k}}^+ - v_{\vec{k}} \hat{b}_{\vec{k}}, \end{aligned} \quad (3.25)$$

which is known as the Bogoliubov transformation. The two parameters, $u_{\vec{k}}$ and $v_{\vec{k}}$, are determined uniquely by the following requirements. The quasi particles, described by the new operators $\hat{b}_{\vec{k}}$ and $\hat{b}_{\vec{k}}^+$ are sometimes called bogolons. They are assumed to obey the same bosonic commutation relation as the real particle operators

$$[\hat{b}_{\vec{k}}, \hat{b}_{\vec{k}'}] = \delta_{\vec{k}, \vec{k}'} \quad (3.26)$$

This commutation relation imposes the following constraint for the two parameters $u_{\vec{k}}$ and $v_{\vec{k}}$:

$$u_k^2 - v_k^2 = 1, \quad (3.27)$$

or equivalently $u_k = \cosh \theta_k$ and $v_k = \sinh \theta_k$. Then the Hamiltonian Eq. (3.24) writes

$$\begin{aligned} \hat{H} = \frac{1}{2} g n N + \sum_{\vec{k} \neq 0} \left[\frac{\hbar^2 k^2}{2m} v_k^2 + g n (v_k^2 - u_k v_k) \right] + \sum_{\vec{k} \neq 0} \left[\frac{\hbar^2 k^2}{2m} (v_k^2 + u_k^2) + g n (v_k^2 + u_k^2 - 2u_k v_k) \right] \hat{b}_{\vec{k}}^+ \hat{b}_{\vec{k}} \\ + \sum_{\vec{k} \neq 0} \left[\frac{\hbar^2 k^2}{2m} u_k v_k + \frac{1}{2} (v_k^2 + u_k^2 - 2u_k v_k) \right] (\hat{b}_{-\vec{k}}^+ \hat{b}_{\vec{k}} + \hat{b}_{\vec{k}} \hat{b}_{-\vec{k}}) \end{aligned} \quad (3.28)$$

The value of θ_k must be chosen in order to make the coefficients of the non-diagonal terms $\hat{b}_{\vec{k}}^+$ and $\hat{b}_{\vec{k}}$ in Eq. (3.28) vanish. This condition is rewritten as

$$u_k, v_k = \frac{1}{2} \left(\sqrt{\frac{E_k}{\epsilon_k}} \pm \sqrt{\frac{\epsilon_k}{E_k}} \right), \quad (3.29)$$

where the Bogoliubov spectrum is

$$\epsilon_k = \sqrt{E_k^2 + 2gnE_k}, \quad (3.30)$$

and $E_k = \frac{\hbar^2 k^2}{2m}$ is the free particle energy. Eq. (3.30) is the famous Bogoliubov excitation spectrum. Substituting Eq. (3.30) and Eq. (3.29) into Eq. (3.28), the resulting diagonal Hamiltonian is

$$H = E_0 + \sum_{\vec{k} \neq \vec{0}} \epsilon_k \hat{b}_{\vec{k}}^+ \hat{b}_{\vec{k}}, \quad (3.31)$$

where the ground state energy is

$$E_0 = \frac{1}{2} g n N + \sum_{\vec{k} \neq \vec{0}} (\epsilon_k - g n + E_k), \quad (3.32)$$

3.4 finite Temperature Mean Field Theory

We now extend the formalism to finite temperatures, by explicitly retaining the non-condensate operator $\tilde{\Psi}(\vec{r}, t)$ in Eq. (3.8). We proceed via the technique of Hamiltonian diagonalization already discussed in this section. In order to go beyond the zero temperature discussion, we must additionally include the remaining contributions $H_3 + H_4$ of equation Eq. (3.9) to the system Hamiltonian. This Section discusses their approximate mean field inclusion, which amounts to a static thermal cloud approximation. In order to reduce the full Hamiltonian of Eq. (3.9) to a desired quadratic form, one may use Wick's theorem for the non-condensate operators in \hat{H}_4 [239, 240], which states that at

equilibrium, an average over multiple operators can be approximated by sums of averages of pairwise contracted operators, i.e.

$$\langle \hat{\Psi}^+ \hat{\Psi}^+ \hat{\Psi} \hat{\Psi} \rangle = \langle \hat{\Psi}^+ \hat{\Psi}^+ \rangle \langle \hat{\Psi} \hat{\Psi} \rangle + 2 \langle \hat{\Psi}^+ \hat{\Psi} \rangle \langle \hat{\Psi}^+ \hat{\Psi} \rangle \quad (3.33)$$

The above approximation maintains correlations of non-condensate operators only to quadratic order. One may thus also wish to approximate products of three noncondensate operators appearing in \hat{H}_3 by their corresponding quadratic form,

$$\begin{aligned} \hat{\Psi}^+ \hat{\Psi} \hat{\Psi} &= 2 \langle \hat{\Psi}^+ \hat{\Psi} \rangle \hat{\Psi} + \langle \hat{\Psi} \hat{\Psi} \rangle \hat{\Psi}^+, \\ \hat{\Psi}^+ \hat{\Psi}^+ \hat{\Psi} &= \langle \hat{\Psi}^+ \hat{\Psi}^+ \rangle \hat{\Psi} + 2 \hat{\Psi}^+ \langle \hat{\Psi}^+ \hat{\Psi} \rangle, \end{aligned} \quad (3.34)$$

Since by construction $\langle \hat{\Psi} \rangle = \langle \hat{\Psi}^+ \rangle = 0$ the approximation of Eq. (3.34) implies that $\langle \hat{\Psi}^+ \hat{\Psi}^+ \hat{\Psi} \rangle = 0$. We have already seen that the system may be split into two sub-components, namely the condensate contribution, $n_c = |\phi|^2$ and the thermal cloud $\tilde{n} = \langle \hat{\Psi}^+ \hat{\Psi} \rangle$ satisfying: $n = n_c + \tilde{n}$. Similarly, the approximations of Eq. (3.33), Eq. (3.34) motivate the definition of an additional mean field contribution $\tilde{m} = \langle \hat{\Psi} \hat{\Psi} \rangle$. This is often referred to as the pair anomalous average.

3.4.1 Popov approximation

In this crude approximation one often neglects the anomalous average $\tilde{m} = \langle \hat{\Psi} \hat{\Psi} \rangle$ [241, 242]. The condensate wavefunction is coupled only to the noncondensed density

$$\mu \phi = \left[-\frac{\hbar^2}{2m} \Delta + V_{ext}(\vec{r}) + g(n_c + 2\tilde{n}) \right] \Phi, \quad (3.35)$$

The usual Bogoliubov transformation $\tilde{\Psi} = \sum_k [u_k(\vec{r}) \hat{b}_k - v_k(\vec{r}) \hat{b}_k^+]$ leads to the coupled Bogoliubov-de Gennes equation

$$\begin{pmatrix} \hat{L}(r) & \hat{M}(r) \\ -\hat{M}^*(r) & -\hat{L}^*(r) \end{pmatrix} \begin{pmatrix} u_k(r) \\ v_k(r) \end{pmatrix} = \epsilon_k \begin{pmatrix} u_k(r) \\ v_k(r) \end{pmatrix} \quad (3.36)$$

where $\hat{L} = -\frac{\hbar^2}{2m} \Delta + V_{ext}(\vec{r}) - \mu$, $\hat{M} = g \Phi^2$ and $n = n_c + \tilde{n}$ is the total density. The equilibrium thermal cloud density is given by

$$\tilde{n} = \frac{1}{2} \sum_k \left[\frac{E_k + gn_c}{\epsilon_k} \coth\left(\frac{\epsilon_k}{2T}\right) - 1 \right] \quad (3.37)$$

The Popov approximation is a finite temperature approximation, since it endows condensate interactions with both condensate and thermal atoms. The set of equations Eq. (3.32) predicts excitations at finite temperatures with no gap in the energy spectrum for uniform gas. We use the term gapless theory. The advantage is that they are in agreement with Goldstones theorem.

3.4.2 Hartree-Fock-Bogoliubov approximation

The Bogoliubov approximation [245, 246] is valid for low temperatures and weak interactions. A more general approximation, that would be valid for all temperatures and any interaction strength, is the Hartree-Fock-Bogoliubov (HFB) approximation. Early works employing this approximation, confronted the inconsistency problem, which will be discussed in the next section, because of an unphysical gap in the particle spectrum. In the frame of HFB formalism, the condensate wave function is defined within the generalized Gross-Pitaevskii equation. In this approximation, the condensate wavefunction is coupled to the noncondensed density via the generalized Gross-Pitaevskii equation

$$\mu \phi = \left[-\frac{\hbar^2}{2m} \Delta + V_{ext}(\vec{r}) + g(n_c + 2\tilde{n}) \right] \Phi + g \tilde{m} \Phi^*, \quad (3.38)$$

Using the above Bogoliubov transformation, we get the generalized coupled Bogoliubov-de Gennes equations

$$\begin{pmatrix} \hat{L}(r) & \hat{M}(r) \\ -\hat{M}^*(r) & -\hat{L}^*(r) \end{pmatrix} \begin{pmatrix} u_k(r) \\ v_k(r) \end{pmatrix} = \epsilon_{\mathbf{k}} \begin{pmatrix} u_k(r) \\ v_k(r) \end{pmatrix} \quad (3.39)$$

where $\hat{L} = -\frac{\hbar^2}{2m} \Delta + V_{ext}(\vec{r}) - \mu$, $\hat{M} = g \Phi^2$, $\hat{M} = g(\Phi^2 + \hat{m})$ and $n = n_c + \tilde{n}$ is the total density. These equations define the Bogoliubov energy spectrum ϵ_k and the quasiparticle amplitudes u_k and v_k . Once these quantities have been determined, the noncondensed and the anomalous densities for a homogeneous Bose gas are obtained from the following expressions

$$\tilde{n} = \frac{1}{2} \sum_k \left[\frac{E_k + g(n_c + \tilde{m})}{\epsilon_k} \coth\left(\frac{\epsilon_k}{2T}\right) - 1 \right] \quad (3.40)$$

$$\tilde{m} = - \sum_k \left[\frac{g(n_c + \tilde{m})}{\epsilon_k} \coth\left(\frac{\epsilon_k}{2T}\right) \right] \quad (3.41)$$

Where

$$\epsilon_k = [(E_k + 2gn - \mu)^2 - g^2(n_c + \tilde{m})^2]^{\frac{1}{2}} \quad (3.42)$$

Making use of the HFB chemical potential μ given by Equation Eq. (3.38)

$$\mu = g(n + \tilde{n} + \tilde{m}) \quad (3.43)$$

one sees that there is a finite energy gap at $k = 0$.

$$\epsilon_k = 2g \sqrt{|\tilde{m} n_c|} \quad (3.44)$$

Clearly the HFB does not satisfy the Hugenholtz-Pines theorem. The spectrum Eq. (3.42) be not gapless in the long wavelength limit. To correct this inconsistency ad hoc procedure [247] for the chemical potential was proposed.

$$\mu = g(n + \tilde{n} - \tilde{m}) \quad (3.45)$$

3.4.3 Problems of HFB

The difficulties of the generalized HFB theory are summarized in the following:

1. The anomalous pair average is ultraviolet divergent. Physically this comes from the approximate parameterization of collisions through a hard sphere interaction potential, which treats collisions of different momenta with the same probability. In reality, however, collisions with high energies are much more unlikely in the Bose condensed system and this unequal treatment leads to the divergence in the anomalous average.
2. The HFB theory is not gapless. The excitation spectrum contains a finite energy gap ($\varepsilon_k = 2g\sqrt{\tilde{n}n_c}$), which is a relic of divergences in the homogeneous case at low momenta.

3.4.4 Other finite temperature approaches

In order to circumvent the well-known HFB problems, many approaches were proposed in these two last decades. Among them we can cite, the so-called selfconsistent, coupled Gross-Pitaevskii-Boltzmann approach, which is often referred as the Zaremba-Nikuni and Griffin (ZNG) theory [250, 251]. In such approach, the thermal cloud itself is described by a quantum Boltzmann equation self-consistently coupled to the condensate [251]. This method reproduces the two-fluid hydrodynamics in the collisional and hydrodynamic regime [252, 253], and has been tested successfully against experiment for collective modes [253, 254, 255, 256] and macroscopic excitations [257, 258]. Despite their elegant formulation, kinetic theories based on mean field potentials have the drawback in lower dimensions of not fully capturing the large phase fluctuations in the quasi-condensate. In addition, so called anomalous averages (or pair correlations) in the thermal cloud, typically omitted in such approaches, are expected to become particularly relevant at lower dimensions. It is not entirely clear, however, how to obtain a gapless excitation spectrum for the system in the homogeneous limit, as required by the Hugenholtz-Pines theorem [259].

Classical field methods have been developed to simulate numerically those modes of the system that feature a macroscopic occupation. These methods rely upon the observation that for highly occupied modes, the field operator can be replaced by a classical complex field which evolves in time according to the GPE [260, 261]. This description extends the $T = 0$ GPE, by adding stochastic elements that describe fluctuations of the condensate modes; these may be further coupled to the thermal cloud where the mean occupation numbers are small. (In fact, too small to be treated in the classical field approximation and more appropriately described by quantum Boltzmann equations [262].) Within the class of classical field techniques, we mention the projected GPE [263, 264], the truncated Wigner method [265, 266] the stochastic Gross-Pitaevskii equation [267, 268, 269, 271], when implemented in the classical limit and closely related to classical field methods. Hybrid simulation techniques were also recently developed that attempt to go beyond the classical limit.

In the stochastic approaches, the relation between them and other kinetic theories and their respective applications have been reviewed in Refs [271, 272, 273]. A key appeal is that they provide an approximation to the full distribution function of the ultracold gas and give access to physics beyond the mean field. They have been used, e.g., to probe the large critical fluctuations near the phase transition [274, 275], to study dynamical

effects of fluctuations on condensate growth and macroscopic excitations[276, 277, 278]. Another quantity of interest is the counting statistics of the condensate mode [279, 280], which is analogous to the photon number distribution in quantum laser theory [281, 282]. Another kind of finite temperature approximation was proposed by Yukalov. Such approach based on the general notion of representative statistical ensembles [283] which is formulated for arbitrary statistical systems, equilibrium or not. The main idea of this notion is the necessity of taking into account all imposed conditions that uniquely define the given statistical system. Employing such a representative ensemble for Bose condensed systems removes all paradoxes, yielding both conserving and gapless in any approximation. This theory has been used to study the static and the dynamics spectrum behavior of the normal and anomalous densities [283]. System of Bose-Einstein condensed gases in random potentials is also investigated in the context of this theory [284]. In addition, this theory has been used to analyze the behavior of the Bose-Einstein condensates in optical lattices[284].

Chapter 4

Time Dependent Hartree-Fock-Bogoliubov Theory For Trapped Bose gases

4.1 Introduction

Much work has been devoted to the properties of condensed gases at very low temperatures (much smaller than the critical temperature T_c) where the non-condensed fraction is negligible. In the so called Thomas-Fermi (TF) regime, the dynamic behavior of the condensate is essentially determined by the interplay between the trapping potential and the atomic interactions. At higher temperatures, less than but comparable to T_c , a significant thermal component is also present, having its own dynamics and typically much more dilute than the condensate. Therefore one can not consider this non condensed phase as a static bath where the condensate lives. For reasons, one recalls the successful two fluid approach of Khalafnikov et al., where the two phases are treated as two fluids moving in a common field. In this situation, the kinetic energy per thermal atom is larger than the mean-field energy, and deviations from ideal gas behavior are small.

Static as well as dynamic properties of Bose-Einstein Condensate (BEC) are now intensively studied, both experimentally and theoretically, in order to apprehend the way the BEC forms, develops and vanishes. Various theoretical techniques have been used successfully, predicting correctly a great number of experimental results. Among these techniques, some are widely used, such as the Bogoliubov [285], the Beliaev [286, 287] and the Hartree-Fock-Bogoliubov [288, 289, 290] approximations. Some other methods, such as Monte-Carlo simulations [291] are rising interest since they tend to solve the exact quantum many-body problem. Although being extremely precise in the static situations, the approximations mentioned above all adopt ad-hoc assumptions about the various quantities such as the order parameter Φ (or the condensate density n_c), the non-condensed density or thermal cloud \tilde{n} or the anomalous density \tilde{m} . We will rely on a different approach, based on the time-dependent variational principle of Balian and Venéroni (BV) [292, 293]. Not only does this method retain the essential features of the physics behind the previous approximations, but it also allows one to bypass some (if not all) of the ad-hoc assumptions. Indeed, being variational, the formalism generates a consistent dynamics for the quantities Φ , n_c , \tilde{n} and \tilde{m} by choosing a certain class of trial spaces. This well-known advantage of this (and any) variational principle faces however a major difficulty related to the choice of the trial spaces. A (difficult) compromise must

be found between a correct description of the physics on one hand, and the tractability of the calculations on the other. In this order of ideas, the BV variational principle requires to specify two objects: a density-like operator and a measured observable. Our choice for the variational spaces consists of a gaussian time-dependent density-like operator and a single-particle operator for the observable. This last quantity turns out to be of no interest in our particular case but it may play a major role in other situations especially when one intends to calculate correlation functions[294, 295]. The machinery we are discussing has in fact already been used elsewhere[293], where we have recognized that the variational dynamical equations derived there are a generalization of the Gross-Pitaevskii equations[296], that takes into account the coupling between the order parameter and the various densities. We called this approach the Time-Dependent Hartree-Fock-Bogoliubov (TDHFB) approximation. The point is that the usual image of a collection of condensed atoms in a bath of thermal particles is not totally true, since the bath has its own dynamics which is sensible to the condensate dynamics. We use the time-dependent variational principle of Balian and Vénéroni to derive a set of equations governing the dynamics of a trapped Bose gas at finite temperature. We show that this dynamics generalizes the Gross-Pitaevskii equations in that it introduces a consistent dynamical coupling between the evolution of the condensate density, the thermal cloud and the anomalous density.

4.2 The Balian-Vénéroni variational principle and the TDHFB Equations

The General TDHFB equations were derived in[293] using the BV variational principle. For technical reasons, they were written in terms of the creation and annihilation operators a^+ and a . They may however easily be translated in a more appropriate notation for the BEC problem using the boson field operator $\hat{\Psi}(r)$ in the Schrödinger picture. Let us first recall some of our notations. We introduced the gaussian density operator $D(t)$ (with variational parameters $N(t)$, $\lambda(t)$ and $S(t)$):

$$D(t) = N(t) \exp(\lambda(t)\tau\alpha) \exp\left(\frac{1}{2}\alpha\tau S(t)\alpha\right), \quad (4.1)$$

where $\alpha = (\psi^+, \psi)$ and τ is a symplectic constant matrix. Then, we defined the one-boson expectation value $\langle\alpha\rangle$ and the single-particle density matrix ρ by:

$$\langle\alpha\rangle = \begin{pmatrix} \langle\psi\rangle \\ \langle\psi^+\rangle \end{pmatrix}, \quad (4.2)$$

$$1 + 2\rho = \begin{pmatrix} \langle\psi\psi^+ + \psi^+\psi\rangle & -2\langle\psi\psi\rangle \\ 2\langle\bar{\psi}^+\bar{\psi}^+\rangle & -\langle\bar{\psi}\bar{\psi}^+ + \bar{\psi}^+\bar{\psi}\rangle \end{pmatrix}, \quad (4.3)$$

which are directly related to $\lambda(t)$ and $S(t)$ respectively (see Eq. A.6 of ref.[295]). Operators such as $\bar{\psi}$ are simply the centered operators $\psi - \langle\psi\rangle$. The expectation values are to be taken with respect to the density operator Eq. (4.1). Introducing the ansatz in the BV variational action-like leads, beside the conservation of the partition function $Z = TrD(t)$, what we called the TDHFB equations:

$$\begin{aligned} i\hbar\frac{d\langle\alpha\rangle}{dt} &= \tau\frac{\partial\langle H\rangle}{\partial\langle\alpha\rangle}, \\ i\hbar\frac{d\rho}{dt} &= -2\left[\rho, \frac{\partial\langle H\rangle}{\partial\rho}\right], \end{aligned} \quad (4.4)$$

in which $\langle H \rangle$ is the energy. Some interesting properties are discussed in [293, 295]. In order to make connection with the BEC phenomenon, we introduce the Grand Canonical Hamiltonian for trapped bosons [4]:

$$H = \int_{\mathbf{r}} \psi^+(\mathbf{r}) \left[-\frac{\hbar^2}{2m} \Delta + V_{\text{ext}}(\mathbf{r}) - \mu \right] \psi(\mathbf{r}) + \frac{g}{2} \int_{\mathbf{r}} \psi^+(\mathbf{r}) \psi^+(\mathbf{r}) \psi(\mathbf{r}) \psi(\mathbf{r}). \quad (4.5)$$

The quantity $V_{\text{ext}}(\mathbf{r})$ is the trapping potential, μ is the chemical potential and g is the coupling constant. The energy $\xi = \langle H \rangle$ is easily computed yielding.

$$\begin{aligned} \xi = \int_{\mathbf{r}} \left[-\frac{\hbar^2}{2m} \Phi^* \Delta \Phi - \frac{\hbar^2}{2m} \Phi \Delta \Phi^* + (V_{\text{ext}}(\mathbf{r}) - \mu + 2g\tilde{n}) |\Phi|^2 + \frac{g}{2} |\Phi|^4 - \frac{\hbar^2}{2m} \tilde{n} \Delta \right. \\ \left. + V_{\text{ext}}(\mathbf{r}) - \mu) \tilde{n} + g\tilde{n}^2 + \frac{g}{2} (|\tilde{m}^2| + \tilde{m}^* + \tilde{m}(\Phi^*)^2) \right] \end{aligned} \quad (4.6)$$

where the condensate density $n_c = |\Phi|^2$, the non-condensed density \tilde{n} and the anomalous density \tilde{m} are identified respectively with $|\langle \phi \rangle|^2$, $\langle \bar{\psi}^+ \bar{\psi} \rangle$ and $\langle \bar{\psi} \bar{\psi} \rangle$. The Eq. (4.4) now take the form

$$\begin{aligned} i\hbar \dot{\Phi} &= \frac{\partial \zeta}{\partial \Phi^*}, \\ i\hbar \dot{\tilde{n}} &= 2 \left(\tilde{m}^* \frac{\partial \zeta}{\partial \tilde{m}^*} - \tilde{m} \frac{\partial \zeta}{\partial \tilde{m}} \right), \\ i\hbar \dot{\tilde{m}} &= 4 \left(\tilde{n} + \frac{1}{2} \right) \frac{\partial \zeta}{\partial \tilde{m}^*} + 4 \frac{\partial \zeta}{\partial \tilde{n}} \tilde{m}, \end{aligned} \quad (4.7)$$

which constitutes a closed self-consistent system. The coupling between the order parameter Φ , the non-condensed density and the anomalous density occurs via the derivatives of ζ which still contain \tilde{n} and \tilde{m} .

Beside the conservation of the energy, the equations Eq. (4.7) exhibit the unitary evolution of the density matrix (already visible in Eq. (4.4)) by means of the conservation of the Heisenberg parameter I defined as $\rho(\rho + 1) = \frac{I-1}{4}$ or equivalently

$$I = (2\tilde{n} + 1)^2 - 4|\tilde{m}|^2. \quad (4.8)$$

We recall the reader that $I = \coth^2(\frac{E}{kT})$ for a thermal distribution at energy E .

The expression Eq. (4.6) for the energy allows us to write down the Eq. (4.7) more explicitly. They indeed read

$$\begin{aligned} i\hbar \dot{\Phi} &= \left(-\frac{\hbar^2}{2m} \Delta + V_{\text{ext}} - \mu + gn_c + 2g\tilde{n} \right) \Phi + g\tilde{m}\Phi^*, \\ i\hbar \dot{\tilde{n}} &= g \left(\tilde{m}^* \Phi^2 - \tilde{m} \Phi^{*2} \right), \\ i\hbar \dot{\tilde{m}} &= \frac{g}{V} (2V\tilde{n} + 1) \Phi^2 + 4 \left(-\frac{\hbar^2}{2m} \Delta + V_{\text{ext}} - \mu + 2gn + \frac{g}{4V} (2V\tilde{n} + 1) \right) \tilde{m}, \end{aligned} \quad (4.9)$$

where we introduce the volume V of the system.

The equation governing Φ has been obtained elsewhere [297, 298, 299, 300, 301] as an extension of the Gross-Pitaevskii equation. Moreover, one can show that our equations (4.9) are more general than the standard HFB-BdG approach [9, 10]. To this end, it is in

fact sufficient to linearize the first equation in (4.9) (while keeping \tilde{n} and \tilde{m} constants) around a static solution. This yields:

$$i\hbar\delta\dot{\Phi} = (h^{sp} + 2gn)\delta\Phi + g(\tilde{m} + \Phi^2)\delta\Phi^*, \quad (4.10)$$

where $h^{sp} = -\frac{\hbar^2}{2m}\Delta + V_{\text{ext}} - \mu$ is the single-particle hamiltonian. In order to analyze the excitation spectrum, one expands $\delta\Phi$ as follows: $\delta\Phi = \sum_i (u_i e^{-i\hbar\omega_i t} - v_i e^{+i\hbar\omega_i t})$ (where u_i and v_i are real space functions) and gets

$$\begin{aligned} \hbar\omega_i u_i &= (h^{sp} + 2gn)u_i - g(n_c + \tilde{m})v_i, \\ -\hbar\omega_i v_i &= (h^{sp} + 2gn)v_i - g(n_c + \tilde{m})u_i, \end{aligned} \quad (4.11)$$

which are just the time dependent Bogoliubov-De Gennes equations. Hence, the standard HFB-BdG approach consists in using the generalized GP equation coupled to the equations (4.11). We note in particular that our two remaining equations in (4.9) have no analogue in this approach.

The TDHFB equations couple in a consistent and closed way the three densities. They should in principle yield the general time, space and temperature dependence of the various densities. They are not only energy and number conserving, but also satisfy the Hugenholtz-Pines theorem (see below) which leads to a gapless excitation spectrum in the uniform limit. It is to be mentioned that the TDHFB equations have also been derived by other groups using different variational formulations[20, 21]. For instance, the authors of the first reference have used a gaussian trial wave functional and have obtained a set of equations very similar to ours. In fact, we can show that our two last equations in (4.9) are just the diagonal parts (in space representation) of a more general set involving the dynamics of the two-point correlation functions $\tilde{n}(\mathbf{r}, \mathbf{r}')$ and $\tilde{m}(\mathbf{r}, \mathbf{r}')$. When one sets $\mathbf{r} = \mathbf{r}'$, the non-diagonal and diagonal parts decouple, the latter being Eqs.(4.9) with $\tilde{n}(\mathbf{r}, \mathbf{r}) = \tilde{n}(\mathbf{r})$ and $\tilde{m}(\mathbf{r}, \mathbf{r}) = \tilde{m}(\mathbf{r})$.

4.3 The Static Solution

In order to show that our equations do indeed yield conclusive results even in their simpler form, we will focus in this section on the static solution both at zero and finite temperature in the Thomas-Fermi (TF) limit. The interest is evident, since there remain many unanswered questions such as the general dependence of the density profiles on the temperature and on the interaction strength and the effect of the interactions on the critical temperature. More particularly, recent experiments are raising challenging questions about the precise determination of the thermal cloud and its back effects on the condensate[18]. Indeed, due to the difficulties inherent to these experiments, there is no clear image on the way the condensed and non condensed phases mix up. Hence, in these preliminary calculations, we intend to provide some simple answers. We do not of course pretend to reproduce exactly the experimental data, neither do we pretend reproducing the full Monte-Carlo calculations. All that we intend to do here is to show that the simplifications that we are actually using (Static Mean field + Thomas-Fermi) are controllable and retain also the most important qualitative features without destroying the underlying physics. As we will see, they will in fact imitate in many respects the full HFB self-consistent calculations[10]. This provides a simple enough tool which can be considered as a starting point for a more elaborate treatment.

The static solutions, are obtained by setting to zero the right hand sides of (4.9). At zero temperature, the standard TF limit[22] amounts to neglecting the kinetic (or Δ) term in the Gross-Pitaevskii equation. This is particularly satisfied for strong interacting regimes or large atom numbers. At finite temperature and below the transition, since there are two phases (condensed and non condensed) which coexist, one has to provide a complementary recipe for what we shall call the finite temperature TF limit. First, neglecting the kinetic energy of the condensate remains a justifiable approximation since the atoms are slowed down in order to obtain condensation. On the other hand, \tilde{m} is believed to be an extremely small and slowly varying function whatever the temperature is (recall that it describes the correlations between the condensed and non-condensed phases). Hence, one may in a first approximation safely neglect $\Delta\tilde{m}$. Heuristically, one may argue that, since the equations for n_c and \tilde{m} contain almost comparable operators, h and $h + g(n_c + \tilde{n}/2)$, where h is the self-consistent mean field hamiltonian $h = V_{\text{ext}}(r) - \mu + gn_c + 2g\tilde{n}$, the TF condition $h \gg T$ (T being the kinetic operator), if fulfilled for n_c should also be satisfied for \tilde{m} . For this approximation to be consistent, n_c and \tilde{m} should vary on the same characteristic length, which is indeed the case as we will show later.

Before proceeding further, it is important to notice at this point that a kinetic-like term of the thermal cloud does not appear explicitly in the equations but is rather hidden in the third equation of (4.9). Indeed, the kinetic term of the thermal cloud is related to the second derivative of the anomalous density. Differentiating equation $I = (1 + 2V\tilde{n})^2 - (2V|\tilde{m}|)^2$ yields a relation of the form: Before proceeding further, it is important to notice at this point that a kinetic-like term of the thermal cloud does not appear explicitly in the equations but is rather hidden in the third equation of (4.9). Indeed, the kinetic term of the thermal cloud is related to the second derivative of the anomalous density. Differentiating the equation $I = (1 + 2V\tilde{n})^2 - (2V|\tilde{m}|)^2$ yields a relation of the form:

$$\Delta\tilde{n} \sim (\nabla|\tilde{m}|)^2 - (\nabla|\tilde{n}|)^2 + |\tilde{m}|\Delta|\tilde{m}|, \quad (4.12)$$

which shows in particular that neglecting $\Delta\tilde{m}$ does not necessarily mean neglecting $\Delta\tilde{n}$. That is precisely the recipe that we shall adopt below. With this finite temperature prescription, the static equations corresponding to (4.9) now write

$$\begin{aligned} (V_{\text{ext}}(r) - \mu + gn_c + 2g\tilde{n})\Phi + g\tilde{m}\Phi^* &= 0, \\ \tilde{m}^*\Phi^2 - \tilde{m}\Phi^{*2} &= 0, \\ (V_{\text{ext}}(r) - \mu + 2gn + \frac{g}{4V}(2V\tilde{n} + 1))\tilde{m} + \frac{g}{4V}(2V\tilde{n} + 1)\Phi^2 &= 0, \end{aligned} \quad (4.13)$$

These equations are naturally gapless and satisfy the Hugenholtz-Pines theorem[9]. Indeed, owing to the second equation in (4.13), one can easily show that at zero momentum, the relation $\mu = g(n + \tilde{n} - |\tilde{m}|)$ is clearly satisfied without adding further assumptions, as is usually performed[9]. In order to solve these equations, we may distinguish two rather different situations. The first one is for $T = 0$. When all the atoms are condensed, $\tilde{n} = \tilde{m} = 0$, and n_c equals the total density n of the gas. Omitting the trivial solution with $n_c = 0$, one may take into account just the first equation in (4.13), since we consider a gas without a quantum cloud. Indeed, within the present set of equations, it is an approximation (although justifiable) to ignore the quantum depletion at $T = 0$. The last two equations in (4.13) become therefore meaningless, and we are left with a simple expression for the condensate density

$$n_c(r) = -\xi(r) = \frac{1}{g}(\mu - V_{\text{ext}}(r)). \quad (4.14)$$

Upon defining the oscillator length $a_0 = (\hbar/m\omega_0)^{1/2}$ and the s-wave scattering length $a = mg/4\pi\hbar^2$, we obtain for a spherical trapping potential $V_{\text{ext}}(r) = \frac{1}{2}m\omega_0^2 r^2$, the condensate radius R and the reduced chemical potential $\nu_0 = \mu/\frac{1}{2}\hbar\omega_0$ for a gas of N bosons as

$$\frac{R}{a_0} = \left(15N\frac{a}{a_0}\right)^{1/5}, \quad (4.15)$$

$$\nu_0 = \left(15N\frac{a}{a_0}\right)^{2/5}. \quad (4.16)$$

The preceding expressions show that the spreading of the condensate depends essentially on the balance between the self-interactions and the trapping potential. These results have also been obtained by many other authors, see e.g. [8, 12, 13].

When $0 \leq T < T_{\text{BEC}}$, we have of course $n_c \neq 0$ and $\tilde{n} \neq 0$. Let us introduce the parametrization $2V\tilde{n} + 1 = \sqrt{I} \cosh \sigma$, $2V|\tilde{m}| = \sqrt{I} \sinh \sigma$, which automatically endows the relation $I = (1 + 2V\tilde{n})^2 - (2V|\tilde{m}|)^2$. Then, from the third equation in (4.13), one obtains a simple equation for $X = e^\sigma$:

$$3X^4 - 4X^2 + 1 + \frac{4Vn_c}{\sqrt{I}}(X^2 - 3)X = 0, \quad (4.17)$$

from which one extracts \tilde{n} and $|\tilde{m}|$ as functions of n_c . Next, one uses these expressions in the first equation (4.13) to get the condensate density

$$n_c(r) = -\xi(r) - \frac{1}{V} \left(\frac{X + 3X^{-1}}{4} \sqrt{I} - 1 \right). \quad (4.18)$$

What is remarkable is that the sole acceptable solution of equation (4.17) is a bounded function of $\eta = Vn_c/\sqrt{I}$. It is represented on figure 1.

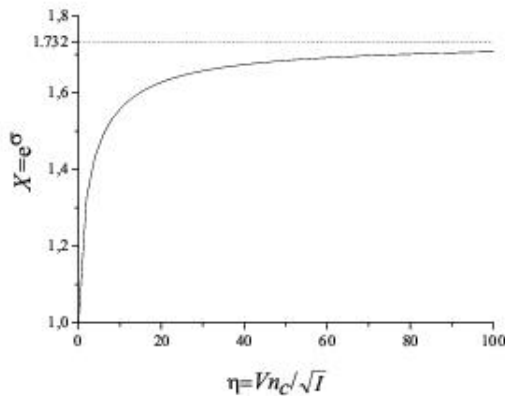


Figure 4.1: Solution of Eq. (4.17) vs. the dimensionless condensate density

Due to this behavior, one can easily show that the quantity $\frac{X+3X^{-1}}{4}$ which appears in (4.18) is almost independent of n_c and becomes rapidly close to unity. Indeed, since equation (4.18) may also be rewritten as $\eta = \frac{(1-V\xi)}{\sqrt{I}} - (X + 3X^{-1})/4$, its solution provides

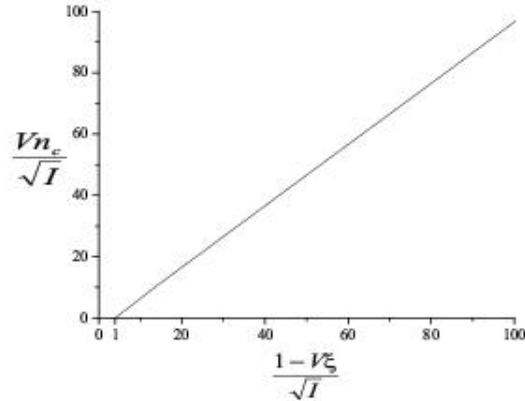


Figure 4.2: Plot of the solution of Eq. (4.18) showing a typical linear behavior

the typical linear behavior shown in figure 4.2. Hence, one may safely approximate (4.18) by

$$n_c(r) \simeq -\xi(r) - \frac{1}{V} \left(\sqrt{I} - 1 \right). \quad (4.19)$$

In fact, one can check that the relative error between the two expressions (4.18) and (4.19) is less than 1%. Finally, since \sqrt{I} does not depend on space, the result (4.19) shows that the finite temperature correction to the Thomas-Fermi profile (4.14) is simply a space-independent (but temperature dependent) shift. This shift may be absorbed in a redefinition of the chemical potential which now writes

$$\mu = V_{\text{ext}}(R) + \frac{g}{V} \left(\sqrt{I} - 1 \right), \quad (4.20)$$

where R is the condensate radius. The condensate density finally writes in the suggestive form

$$n_c(r) = \frac{V_{\text{ext}}(R) - V_{\text{ext}}(r)}{g}, \quad (4.21)$$

which is formally the zero temperature TF profile. It is then easy to show that the condensate radius takes also a simple form

$$\frac{R}{a_0} = \left(15N_c \frac{a}{a_0} \right)^{1/5}, \quad (4.22)$$

but now, it is the number of condensed atoms N_c which is involved and not the total number of atoms. The same conclusion may be drawn for the chemical potential (4.20). Hence, our finite temperature prescription for the TF approximation provides natural extensions of the zero temperature expressions, since the Thomas-Fermi parameter is now $N_c a / a_0$ instead of $N a / a_0$.

In order to apprehend better these results, let us compute the remaining unknown quantities, such as the non condensed and the anomalous densities. To this end, and in order to obtain tractable expressions, we find it more convenient to use the simple fit

$$X = \frac{\sqrt{3}\eta + 2/3}{\eta + 2/3}, \quad (4.23)$$

(instead of the full analytical solution of equation (4.17)) which reproduces correctly the solution X plotted in figure 4.1 with a residual error less than 0.1%. Upon rewriting equation (4.21) in the form $\eta = \eta_0(1 - x^2)$, with an obvious definition of η_0 , we obtain the non condensate density

$$\tilde{n}(x) = \frac{1}{2V} \left\{ \frac{\sqrt{I}}{2} \left(\frac{\sqrt{3}\eta_0(1 - x^2) + 2/3}{\eta_0(1 - x^2) + 2/3} + \frac{\eta_0(1 - x^2) + 2/3}{\sqrt{3}\eta_0(1 - x^2) + 2/3} \right) - 1 \right\}, \quad (4.24)$$

and the anomalous density

$$|\tilde{m}|(x) = \frac{1}{2V} \frac{\sqrt{I}}{2} \left(\frac{\sqrt{3}\eta_0(1 - x^2) + 2/3}{\eta_0(1 - x^2) + 2/3} - \frac{\eta_0(1 - x^2) + 2/3}{\sqrt{3}\eta_0(1 - x^2) + 2/3} \right), \quad (4.25)$$

as functions of the reduced radial distance $x = r/R$. In figures 4.3 and 4.4, we show typical density profiles (in reduced units) for $\eta_0 = 1$.

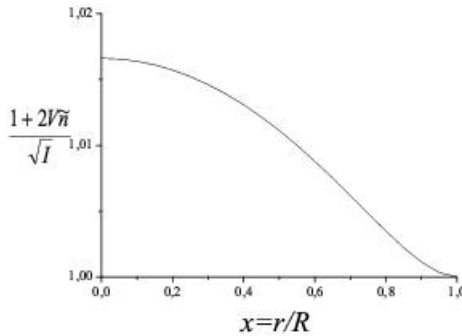


Figure 4.3: Noncondensate density vs. the radial distance

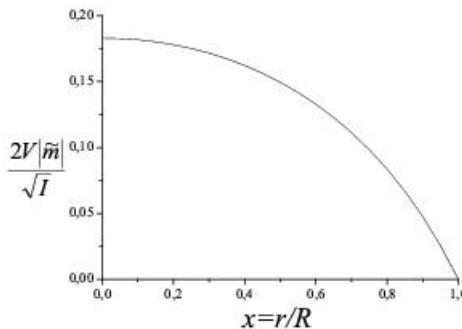


Figure 4.4: Anomalous density vs. the radial distance

It is interesting to notice that, within our TF approximation, the figure 4.3 is qualitatively consistent with the profile of the thermal cloud as depicted by Gerbier *et al*[18]. It also predicts that the thermal cloud does not vanish at the boundaries of the condensate which is also compatible with the experimental results since it is widely known that the

condensed atoms are surrounded by the thermal cloud. We will return to this point later. What is less known (even experimentally) is the anomalous density (figure 4.4). This quantity behaves quite differently from the thermal cloud and is clearly dominated by a TF-like shape. In contrast with the thermal cloud, the anomalous density vanishes at the boundaries which is also plausible since the condensate vanishes there. Furthermore, we observe that n_c , $|\tilde{m}|$ and \tilde{n} vary on the same length scale (R) which justifies *a posteriori* our previous assumption.

At this level, one should stress some discrepancies with already published HFB calculations[10]. Indeed, in the latter reference, \tilde{n} and \tilde{m} present a sharp peak at the borders of the condensate. But one must recall that these calculations are performed with a relatively small number of atoms ($N \simeq 2000$). Hence, the TF limit cannot be applied there and there is no sense to compare these calculations with ours since they apply to different regimes. Moreover, it has been observed elsewhere[23] that upon increasing the number of atoms, the peaks of \tilde{n} and \tilde{m} tend to shift toward the center of the trap (at least at low temperatures) making the profiles depicted in these figures appearing as limiting cases.

In order to obtain more quantitative results, one must determine N_c by using the normalization condition. We get easily the relation

$$1 + 2N = 2N_c + \sqrt{I}g(s), \quad (4.26)$$

where

$$g(s) = \frac{2}{\sqrt{3}} + (\sqrt{3}-1)s \left\{ 1 - \frac{3}{2}\sqrt{s+1} \operatorname{arc\,tanh} \frac{1}{\sqrt{s+1}} + \frac{1}{2}\sqrt{\frac{s}{\sqrt{3}}+1} \operatorname{arc\,tanh} \frac{1}{\sqrt{\frac{s}{\sqrt{3}}+1}} \right\}, \quad (4.27)$$

with $s = 4\sqrt{I}/15N_c$. But since the function $g(s)$ satisfies $1 \leq g(s) \leq 2/\sqrt{3}$, the equation (4.26) is approximately solved to yield, to a very good accuracy, the simple result

$$N_c \simeq N - \frac{\sqrt{I} - 1}{2}. \quad (4.28)$$

All the unknown quantities may now be determined in terms of N and \sqrt{I} alone. The corresponding results will be discussed in the next section.

4.3.1 Results and Discussions

First of all, the condensate radius (4.22) may be written as

$$R = R_{\text{TF}} \left(\frac{N_c}{N} \right)^{1/5}, \quad (4.1)$$

where R_{TF} is the zero temperature result given by equation (4.15). Figure 5 represents the condensate radius (in units of R_{TF}) as a function of the condensate fraction. We see on this figure, and also on equation (4.1), that R decreases from its zero temperature value R_{TF} when $N_c/N = 1$. Hence, when increasing T (that is decreasing the condensate fraction), the thermal component \tilde{n} grows and the condensed component collapses. This is the compression effect which is by now a well established experimental result [18] and is attributed to the thermal cloud. The same effect of compression is observed on figure

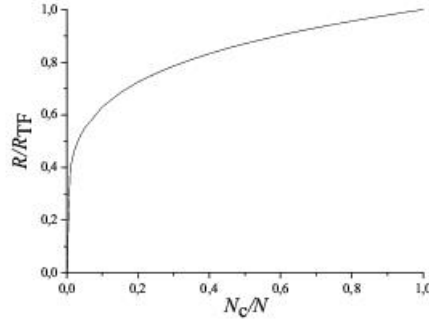


Figure 4.5: Condensate radius vs. the condensate fraction

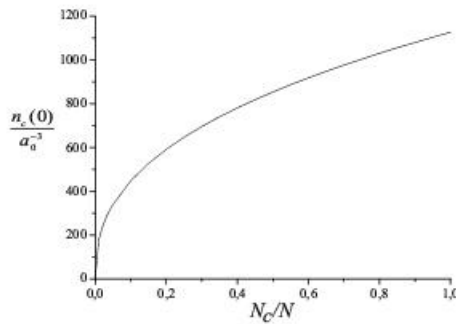


Figure 4.6: Central density vs. the condensate fraction

4.6 for the central condensate density $n_c(r = 0)$ but it is more pronounced due to the power law of $2/5$ (see 4.21) instead of $1/5$ for the condensate radius.

To be more precise, let us choose generic values for the number of atoms and the interaction strength ($N = 10^5$ and $a/a_0 = 0.5 \cdot 10^{-3}$) and plot the various densities (in units of the oscillator volume a_0^3) versus the radial distance (in units of $R_{\text{TF}} = 3.758a_0$) for a condensate fraction ranging from 5% up to 100% ($T = 0$). The figure 4.7 shows typical Thomas-Fermi profiles for the condensate density, even for low condensate fraction. This is of course what one may expect on general grounds in the TF regime. Moreover, the effect of compression of the condensate appears in this figure as a reduction of the central density and of the condensate radius with increasing temperature, which is rather due to the fact that there is less and less atoms in the condensate. Indeed, within our TF approximation, we do not expect to reproduce the "true" compression effect (that is a deformation of the condensate profile by the thermal cloud) since, as we discuss it below, the TF approximation enforces a certain uniformity of the profiles.

The noncondensate density (from which we have subtracted a constant $\tilde{n}(R)$ for clarity) is plotted on figure 4.8 with the same units as before. The information which is added here with respect to figure 4.3 is the temperature dependence which appears via the condensate fraction. We notice in particular that when increasing the condensate fraction, the thermal cloud tends to spread and flatten. This overall behavior of the thermal cloud is not however the end of the story. Indeed, as we have mentioned before, we know from

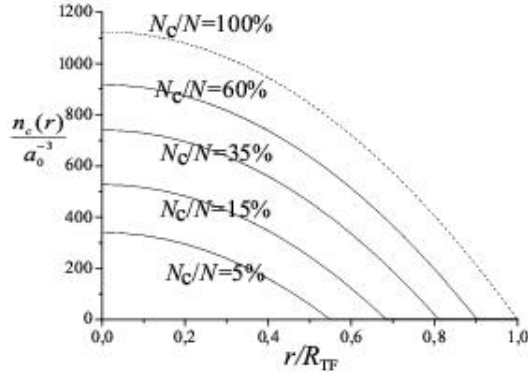


Figure 4.7: Condensate density vs. the radial distance for varying condensate fraction for $N = 10^5$ and $a/a_0 = 0.5 \cdot 10^{-3}$.

the full HFB self-consistent calculations[10] that the non-condensate density is sharply peaked at the edge of the condensate, having therefore a "hole" at the center of the trap. As it has been mentioned in the previous section, this situation would disappear with increasing N , that is when entering the TF regime [23]. Hence, our result does not only meet the HFB calculations, but is also confirmed by the experiment of Gerbier et al. In our case however, we understand heuristically that neglecting the kinetic energy entails overestimating the (effective) repulsive self-interactions which tend to make the profiles more uniform.

On the other hand, the thermal cloud takes on a (small but) finite value for $r \geq R$. Even if this behavior is less intuitive, it is not very surprising since we do know that neglecting the second order derivatives amounts to making a cut of the densities at the boundaries. It is indeed a limitation of the TF approximation at the boundaries[24]. The tail should be reproduced when one reinjects the second derivatives in the equations. In fact, it has been shown in the context of the full HFB numerical calculation[10] that this is indeed the case.

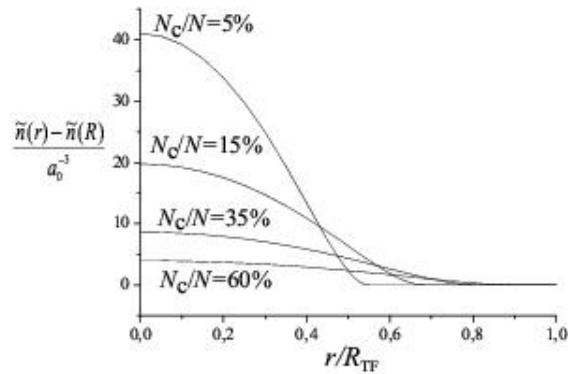


Figure 4.8: Noncondensate density vs. the radial distance for varying condensate fraction for $N = 10^5$ and $a/a_0 = 0.5 \cdot 10^{-3}$.

The figure 4.9 represents the anomalous density and depicts two phases. In a first phase, $|\tilde{m}(r)|$ grows with increasing temperature ($N_c/N = 60\%, 35\%$) while its spatial extension decreases. As we still increase the temperature, and precisely at $N_c/N \simeq 17\%$ (not represented in the figure), the anomalous density reaches a maximum and then begins to decrease ($N_c/N = 15\%, 5\%$) until the transition where it falls to zero. It is to be noted that its spatial extension is still decreasing in this second phase. Although this overall behavior meets qualitatively the self-consistent HFB calculations[10], we note however two major differences. The first one is the location of the maximum of $|\tilde{m}(r=0)|$ which is predicted by the authors of [10] to happen at $N_c/N \simeq 50\%$. Moreover, the HFB calculations yield a spatial extension of the anomalous density quite insensitive to the temperature while it is very temperature-dependent in our case. An experimental check of the way the anomalous density depends on the condensate fraction would therefore be welcome.

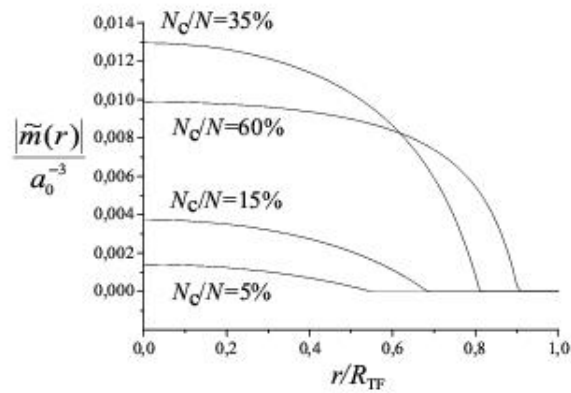


Figure 4.9: Anomalous density vs. the radial distance for varying condensate fraction for $N = 10^5$ and $a/a_0 = 0.5 \cdot 10^{-3}$.

Conclusion

We present in this part a finite temperature analysis of the static TDHFB equations in the Thomas-Fermi limit for a gas of bosons in a harmonic trap.

At zero temperature, we obtain familiar expressions for the chemical potential and the condensate radius. The standard Thomas-Fermi profile for the condensate density is also recovered.

At finite temperatures and below the transition, since there are two phases, one should provide a prescription for the TF limit. We propose such a recipe (maybe the simplest) which consists in neglecting the second order derivatives of the condensate density and the anomalous density. The underlying idea is that, although the anomalous density is necessary for the coherence of the equations, it is believed to be a very small and a very smooth quantity. We therefore obtain analytical expressions for the condensate density, the condensate radius, the chemical potential and the condensate fraction as functions of the temperature. Our expressions appear as natural extensions of the zero temperature TF limit.

Most importantly, we derive quite simple expressions for the non condensate density and for the anomalous density, which we plot as functions of the condensate fraction and draw many conclusions. First of all, the condensate profile is almost of the TF shape of which the spatial extension and the heights are controlled by N_c/N . Furthermore, the compression of the condensate by the thermal cloud with increasing temperature is clearly visible. On the other hand, the noncondensate density profile is qualitatively consistent with the temperature dependence observed in recent experiments. In particular, the non condensate density is not peaked at the edge of the condensate (as predicted by the HFB calculations) but has a broad maximum at the center of the trap. Furthermore, the thermal cloud tends to spread and flatten with increasing temperature. The calculated anomalous density, although not yet observed experimentally, shows also a very intuitive behavior; it has a broad maximum at the center of the trap and vanishes at the boundaries. Moreover, we find that the anomalous density grows with the temperature and reaches a maximum for a condensate fraction of about 17%. It decreases afterwards down to zero when the transition is reached. On the qualitative level, this behavior agrees quite well with the HFB calculations (see [10], Sect. V). However, we do observe some subtle differences such as the location of the maximum and the fact the spatial extension of the anomalous density decreases as the temperature grows. An experimental check, although not trivial at all, is therefore highly required.

At the borders of the trap (where the condensate density vanishes) and for a given temperature, the non condensate density takes on a finite value which is a quite abrupt behavior. Although this meets the fact that the thermal cloud is actually surrounding the condensate, it is by no means conclusive. But this is also a shortcoming of the TF approximation as a whole since it is known to break down at the boundaries of the condensate. Indeed, reinjecting the second derivatives of the densities will entail a more

physical behavior.

These results are quite satisfactory considering the drastic simplifications that occur, as compared for instance to the full self-consistent HFB calculations. Indeed, even if our overall density profiles are smoother and broader than what they should be, we know precisely the reasons and how to incorporate gradually what is missing. In order to apprehend better the advantages of our approach and owing to its importance to account for many-body effects, many Analytic and numeric studies in the static cases at finite and zero temperature taken a cont the kinetic energy have been done after such as [313, 314, 315] they show that at low temperatures, the anomalous fraction is larger than the non condensate one. The former necessarily plays a major role in the Bose-Einstein condensation phenomenon. Any approach neglecting the anomalous fraction at low temperatures will inevitably lead to inconsistencies.

At finite temperature, the Hartree Fock Bogoliubov (HFB) approximation and its generalizations, being selfconsistent and gapless, are known to be very good candidates for the description of the thermal behaviour of the gas [303, 306], except perhaps near the transition where some controversies still persist . There remain, however, many unanswered questions. One of the most challenging is the effect of the thermal cloud on the condensate, especially the compression effect, and the correlation between these two components (commonly referred to as the anomalous average). Recent experiments focusing on these effects [307, 309]report clear evidence that the GrossPitaevskii equation supplemented with the Castin Dum model for free expansion [310] does not provide definite answers for, say, the condensate radius or the aspect ratio. They indeed predict constant values for both quantities, which is reminiscent of the ThomasFermi (TF) behavior. Most importantly, a recent numerical study based on the classical field approximation [311] reports that the previous experiments are not in mutual agreement and some of them do not coincide with the numerical results.

The numerical difficulties are twofold. First, one has to handle more and more quantum states as the temperature is increased. The code developed in [312] becomes rapidly unstable with growing N . It therefore requires to be improved in order to handle atom numbers as high as $10^4 - 10^5$. Secondly, the UV divergences that appear in the anomalous density for high atom numbers must be regularized. The heuristic regularization method employed in [312] ceases to be efficient as soon as $N \geq 10^3$ and hence it also needs to be improved. So to get an excellent result we need a very performance code. So for this reasons in the second part of our thesis we prefer to keep the numerical calculation and try to understand before very well the generalized Gross Pitaevskii Equation (Schrodinger equation) using a mathematical tools and go back to the numerical study in the future.

Part II

Solitonic Solutions of Higher-Order Nonlinear Schrödinger equations and their Special cases

Introduction

Soliton theory is an important branch of nonlinear science. On one hand, it describes various kinds of stable motions appearing in nature, such as solitary water wave, solitary signals in optical fibre etc. It has many applications in science and technology (like optical signal communication). On the other hand, it gives many effective methods of obtaining explicit solutions of nonlinear partial differential equations. Therefore, it has attracted much attention from physicists as well as mathematicians. Nonlinear partial differential equations appear in many scientific problems. obtaining explicit solutions is usually a difficult task. Only in certain special cases can the solutions be written down explicitly. However, for many soliton equations, people have found quite a few methods to get explicit solutions. The most famous ones are the inverse scattering transform (IST) method, Bäcklund transformation etc. The IST method is based on the spectral theory of ordinary differential equations. The Cauchy problem of many soliton equations can be transformed to solving a system of linear integral equations. Explicit solutions can be derived when the kernel of the integral equation is degenerate. The Bäcklund transformation gives a new solution from a known solution by solving a system of completely integrable partial differential equations. Some complicated nonlinear superposition formula arise to substitute the superposition principle in linear science.

However, if the kernel of the integral equation is not degenerate, it is very difficult to get the explicit expressions of the solutions via the inverse scattering method. For the Bäcklundtransformation, the nonlinear superposition formula is not easy to be obtained in general. In late 1970s, it was discovered by V. B. Matveev that a method given by G. Darboux a century ago for the spectral problem of second order ordinary differential equations can be extended to some important soliton equations. This method was called Darboux transformation. After that, it was found that this method is very effective for many partial differential equations. It is now playing an important role in mechanics, physics and differential geometry.

The complete integrability of a system of partial differential equations has been a topic of active research over the last forty or so years. Even today there is no one generally accepted definition of integrability. Many approaches have been advocated, all of which have their merits but none seem to encapsulate the essence of integrability. However one concept has appeared in many different approaches; the Lax pair. This is a reformulation of the original system of nonlinear equations as the compatibility condition for a system of linear equations.

The story of Lax pairs begins with the discovery by Lax of such a linear system for the ubiquitous KdV equation. This equation models a variety of nonlinear wave phenomena, including shallow water waves and ion-acoustic waves in plasmas. Lax's discovery sheds light on the then newly discovered inverse scattering transform method to solve the KdV equation. It allowed this method to be extended to a variety of integrable equations. In 1979 it was realised that the Lax pair could be interpreted as a zero curvature condition on an appropriate connection. This led to generalisations of the method of inverse scattering transforms. In the 1980s, the algebraic structure of Lax pairs was elucidated. The connection between Lax pairs and Kac-Moody algebras was given in . Subsequent applications for Lax pairs include Bäcklund-Darboux transformations, recursion operators and generating integrable hierarchies via the root method. However there was a problem; finding the Lax pair in the first place. In the following, we outline the remaining chapters of this part

- In chapter 5, we present general notions about the solitons, where we give a short history and background of the soliton.
- In chapter 6, we present a general formalism for the Darboux transformation as a method for solving the linear and nonlinear equation by using the Lax Pair, and then we illustrate it by an example.
- In chapter 7 we use the Lax Pair and Darboux transformation to derive the solitonic solutions of the HNLS equation with cubic nonlinearity, complex potentials, and time-dependent coefficients by applying the Darboux transformation, solitonic solutions are then also derived for some of the well-known nonlinear Schrödinger equations, Hirota equation (HE), and Sasa-Satsuma equation (SSE) as special cases.
- Some concluding remarks of our method are given at the conclusion.

Chapter 5

Soliton theory and nonlinear Schrödinger equation

5.1 Solitons, a brief history of

In 1834, a young Scottish engineer named John Scott Russell was conducting experiments on the Union Canal (near Edinburgh) to measure the relationship between the speed of a boat and its propelling force, with the aim of finding design parameters for conversion from horse power to steam. One August day, a rope parted in his measurement apparatus and [60, 61]. the boat suddenly stopped not so the mass of water in the channel which it had put in motion; it accumulated round the prow of the vessel in a state of violent agitation, then suddenly leaving it behind, rolled forward with great velocity, assuming the form of a large solitary elevation, a rounded, smooth and well defined heap of water, which continued its course along the channel without change of form or diminution of speed.

Russell did not ignore this unexpected phenomenon, but "followed it on horseback, and overtook it still rolling on at a rate of some eight or nine miles an hour, preserving its original figure some thirty feet long and a foot to a foot and a half in height" until the wave became lost in the windings of the channel. He continued to study the solitary wave in tanks and canals over the following decade, finding it to be an independent dynamic entity moving with constant shape and speed. Using a wave tank he demonstrated four facts [60, 61]:

- Solitary waves have the shape $h \operatorname{sech}^2[k(x - vt)]$;
- A sufficiently large initial mass of water produces two or more independent solitary waves;
- Solitary waves cross each other "without change of any kind";
- A wave of height h and travelling in a channel of depth d has a velocity given by the expression

$$v = \sqrt{g\sqrt{d+h}} \tag{5.1}$$

(where g is the acceleration of gravity) implying that a large amplitude solitary wave travels faster than one of low amplitude.

Although confirmed by observations on the Canal de Bourgogne, near Dijon, most subsequent discussions of the hydrodynamic solitary wave missed the physical significance of Russell's observations. Evidence that to the end of his life Russell maintained a much broader and deeper appreciation of the importance of his discovery is vided by a posthumous work where among several provocative ideas he correctly estimated the height of the earth's atmosphere from Equation Eqs. (5.1) and the fact that "the sound of a cannon travels faster than the command to fire it" [60, 61]. In 1895, Korteweg and de Vries [62] published a theory of shallow water waves that reduced Russell's problem to its essential features. One of their results was the nonlinear partial differential equation

$$\frac{\partial u}{\partial t} + c \frac{\partial u}{\partial x} + \epsilon \frac{\partial^3 u}{\partial x^3} + \gamma u \frac{\partial u}{\partial x} = 0, \quad (5.2)$$

which would play a key role in soliton theory [62]. In this equation, $u(x, t)$ is the wave amplitude, $c = \sqrt{gd}$ is the speed of small amplitude waves, ($\epsilon \equiv c(\frac{d^2}{6}) - \frac{T}{2\rho g}$) is a dispersive parameter, $\gamma \equiv \frac{3c}{2d}$ is a nonlinear parameter, and T and ρ are respectively the surface tension and the density of water. The authors showed that Equation Eqs. (5.2) has a family of exact travelling wave solutions of the form $u(x, t) = \tilde{u}(x - vt)$, where \tilde{u} is Russell's "rounded, smooth and well defined heap" and v is the wave speed. If the dispersive term ϵ and the nonlinear term γ in Equation Eqs. (5.2) are both zero, then the Korteweg-de Vries (KdV) equation becomes linear ($u_t + cu_x = 0$) with a travelling wave solution for any pulse shape at the fixed speed $v = c = \sqrt{gd}$. In general Equation Eqs. (5.2) is nonlinear with exact travelling wave solutions

$$u(x, t) = \hbar \operatorname{sech}^2[k(x - vt)] \quad (5.3)$$

Where $k = \sqrt{\frac{\gamma \hbar}{12\epsilon}}$; implying that higher amplitude waves are more narrow. With this shape, the effects of dispersion balance those of nonlinearity at an adjustable value of the pulse speed. Thus the solitary wave is recognized as an independent dynamic entity, maintaining a dynamic balance between these two influences. Interestingly, solitary wave velocities are related to amplitudes by

$$v = c + \frac{\gamma \hbar}{3} = \sqrt{gd} \left(1 + \frac{\hbar}{2d}\right) \quad (5.4)$$

in accord with Russell's empirical results[60, 61], given in Equation Eqs. (5.1), to $O(\hbar)$. Although unrecognized at the time, such an energy conserving solitary wave is related to the existence of a Backlund transform (BT), which was also studied during the late 19th century [96]. In such a transform, a known solution generates a new solution through a single integration, after which the new solution can be used to generate another new solution, and so on. It is straightforward to find a BT for any linear partial differential equation (PDE), which introduces a new eigenfunction into the total solution with each application of the transform. Only special nonlinear PDEs are found to have BTs, but late nineteenth mathematicians knew that these include

$$\frac{\partial^2 u}{\partial x^2} = \sin u \quad (5.5)$$

which arose in research on the geometry of curved surfaces [97]. In 1939 Frenkel and Kontorova introduced a seemingly unrelated problem arising in solid state physics to model the relationship between dislocation dynamics and plastic deformation of a crystal[98] . From this study, an equation describing dislocation motion is

$$\frac{\partial_2 u}{\partial x^2} - \frac{\partial_2 u}{\partial t^2} = \sin u \quad (5.6)$$

Where $u(x, t)$ is atomic displacement in the x-direction and the "sin" function represents periodicity of the crystal lattice. A travelling wave solution of Equation Eqs. (5.6), corresponding to the propagation of a dislocation, is

$$u(x, t) = 4 \arctan[\exp(\frac{x-vt}{\sqrt{1-v^2}})] \quad (5.7)$$

with velocity v in the range $(-1, +1)$. Since Equation Eqs. (5.6) is identical to Equation Eqs. (5.5) after an independent variable transformation $\xi = \frac{x-t}{2}$ and $\tau = \frac{x+t}{2}$, exact solutions of Equation Eqs. (5.6) involving arbitrary numbers of dislocation components as in Equation Eqs. (5.7) can be generated through a succession of Bäcklund transforms, but this was not known to Frenkel and Kontorova.

In the late 1940s, Fermi and Ulam suggested one of the first scientific problems to be assigned to the Los Alamos MANIAC computing machine: the dynamics of energy equipartition in a slightly nonlinear crystal lattice, which is related to thermal conductivity. The system they chose was a chain of 64 equal mass particles connected by slightly nonlinear springs, so from a linear perspective there were 64 normal modes of oscillation in the system. It was expected that if all the initial energy were put into a single vibrational mode, the small nonlinearity would cause a gradual progress toward equal distribution of the energy among all modes (thermalization), but the numerical results were surprising. If all the energy is originally in the mode of lowest frequency, it returns almost entirely to that mode after a period of interaction among a few other low frequency modes. In the course of several numerical refinements, no thermalization was observed [99] . Pursuit of an explanation for this "FPU recurrence" led Zabusky and Kruskal to approximate the nonlinear spring-mass system by the KdV equation. In 1965 they reported numerical observations that KdV solitary waves pass through each other with no change in shape or speed, and coined the term "soliton" to suggest this property [100]. Zabusky and Kruskal were not the first to observe nondestructive interactions of energy conserving solitary waves. Apart from Russell's tank measurements [60], Perring and Skyrme, had studied solutions of Equation Eqs. (5.6) comprising two solutions as in Equation Eqs. (5.7) undergoing a

collision. In 1962 they published numerical results showing perfect recovery of shapes and speeds after a collision and went on to discover an exact analytical description of this phenomenon [101]. This result would not have surprised nineteenth century mathematicians; it is merely the second member of the hierarchy of solutions generated by a Bäcklund transform. Nor would it have been unexpected by Seeger and his colleagues, who had noted in 1953 the connections between the nineteenth century work [97] and that of Frenkel and Kontorova [102]. Since Perring and Skyrme were interested in Equation Eqs. (5.6) as a nonlinear model for elementary particles of matter, however, the complete absence of scattering may have been disappointing. Throughout the 1960s, Equation Eqs. (5.6) arose in a variety of problems including the propagation of ferromagnetic domain walls, self-induced transparency in nonlinear optics, and the propagation of magnetic

flux quanta in long Josephson transmission lines. Eventually Equation Eqs. (5.6) became known as the "sine-Gordon" (SG) equation (a nonlinear version of the Klein-Gordon equation: $u_{xx} - u_{tt} = u$)

Perhaps the most important contribution made by Zabusky and Kruskal in their 1965 paper was to recognize the relation between nondestructive soliton collisions and the riddle of FPU recurrence. Viewing KdV solitons as independent and localized dynamic entities, they

explained the FPU observations as follows. The initial condition generates a family of solitons with different speeds, moving apart in the x-t plane. Since the system studied was of finite length with perfect reflections at both ends, the solitons could not move infinitely far apart; instead they eventually reassembled in the x-t plane, approximately recreating the initial condition after a surprisingly short"recurrence time." By 1967, this insight had led Kruskal and his colleagues to devise a nonlinear generalization of the Fourier transform method for constructing solutions of the KdV emerging from arbitrary initial conditions [103]. Called the inverse scattering (or inverse spectral) method (ISM), this approach proceeds in three steps.

- The nonlinear KdV dynamics are mapped onto an associated linear problem, where each eigenvalue of the linear problem corresponds to the speed of a particular KdV soliton.

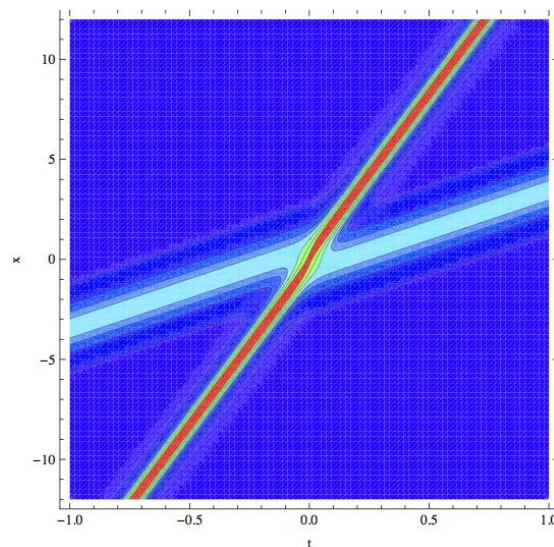


Figure 5.1: . A soliton collision via the KdV equation; Notice how the amplitude and direction of the waves is the same before and after the collision, but phase shift

- Since the associated problem is linear, the time evolution of its solution is readily computed.
- An inverse calculation then determines the time evolved KdV dynamics from the evolved solution of the linear associated problem. Thus the solution of a nonlinear problem is found from a series of linear computations.

Another development of the 1960s was Toda's discovery of exact two-soliton interactions on a nonlinear spring-mass system [104]. As in the FPU system, equal masses were

assumed to be interconnected with nonlinear springs, but Toda chose the potential

$$V = \left(\frac{a}{b}\right)[\exp^{-b u_j} - 1] + a u_j \quad (5.8)$$

Where $u_j(t)$ is the longitudinal extension of the j -th spring from its equilibrium value and both a and b are adjustable parameters. (In the limit $a \rightarrow \infty$ and $b \rightarrow 0$ with ab finite, this reduces to the quadratic potential of a linear spring. In the limit $a \rightarrow 0$ and $b \rightarrow \infty$ with ab finite, it describes the interaction between hard spheres.) Thus by the late 1960s it was established although not widely known that solitons were not limited to PDEs (KdV and SG). Local solutions of difference differential equations could also exhibit the unexpected properties of unchanging shapes and speeds after collisions.

These events are only the salient features of a growing panorama of nonlinear wave activities that became gradually less parochial during the 1960s. Solid state physicists began to see relationships between their solitary waves (magnetic domain walls, selfshaping pulses of light, quanta of magnetic flux, polarons, etc.), and those from classical hydrodynamics and oceanography, while applied mathematicians began to suspect that the ISM might be used for a broader class of nonlinear wave equations. It was amid this intellectual ferment that Newell and his colleagues organized the first soliton research workshop during the summer of 1972[105]. Interestingly, one of the most significant contributions to this conference came by post. From the Soviet Union arrived a paper by Zakharov and Shabat [63]formulating Kruskal's ISM for the nonlinear PDE [63]

$$i \frac{\partial^2 u}{\partial t^2} + \frac{\partial^2 u}{\partial x^2} + 2|u|^2 u = 0 \quad (5.9)$$

In contrast to KdV, SG and the Toda Lattice, the dependent variable in this equation is complex rather than real, so the evolutions of two quantities (magnitude and phase of u) are governed by the equation. This reflects the fact that Equation Eqs. (5.9) is a nonlinear generalization of a linear equation $i u_t + u_{xx} + u = 0$ solutions of which comprise both an envelope and a carrier wave. Since this linear equation is a Schrödinger equation for the quantum mechanical probability amplitude of a particle (like an electron) moving through a region of uniform potential, it is natural to call Equation Eqs. (5.9) the nonlinear Schrödinger(NLS) equation. When the NLS equation is used to model wave packets in such fields as hydrodynamics, nonlinear optics, nonlinear acoustics, plasma waves and biomolecular dynamics, however, its solutions are devoid of quantum character. Upon appreciating the Zakharov and Shabat paper, many left the 1972 conference convinced that four nonlinear equations (KdV, SG, NLS, and the Toda lattice) display solitary wave behavior with the special properties that led Zabusky and Kruskal to coin the term soliton [105]. Within two years, ISM formulations had been constructed for the SG equation and also for the Toda lattice. Since the mid-1970s, the soliton concept has become established in several areas of applied science, and dozens of dynamic systems are now known to be integrable through the ISM. Even if a system is not exactly integrable, additionally, it may be close to an integrable system, allowing analytic insight to be gleaned from perturbation theory. Thus one is no longer surprised to find stable spatially localized regions of energy, balancing the opposing effects of nonlinearity and dispersion and displaying the essential properties of objects. Current soliton studies are focused on working out the details of such object-like behavior in a wide range of research areas [106].

5.2 different types of solitons

About thirty years ago a remarkable discovery was made in Los Alamos. Enrico Fermi, John Pasta, and Stan Ulam were calculating the flow of energy in a one dimensional lattice consisting of equal masses connected by nonlinear springs. They conjectured that energy initially put into a long-wavelength mode of the system would eventually be thermalized, that is, be shared among all modes of the system. This conjecture was based on the expectation that the nonlinearities in the system would transfer energy into higher harmonic modes. Much to their surprise the system did not thermalize but rather exhibited energy sharing among the few lowest modes and long time near recurrences of the initial state. This discovery remained largely a mystery until Norman Zabusky and Martin Kruskal started to investigate the system again in the early sixties. The fact that only the lowest order (long-wavelength) modes of the discrete Fermi-Pasta-Ulam lattice were active led them in a continuum approximation to the study of the nonlinear partial differential equation

$$\frac{\partial u}{\partial t} + u \frac{\partial u}{\partial x} + \frac{\partial^3 u}{\partial x^3} = 0 \quad (5.10)$$

This equation (the KdV equation) had been derived in 1885 by Korteweg and de Vries to describe long-wave propagation on shallow water. But until recently its properties were not well understood. From a detailed numerical study Zabusky and Kruskal found that stable pulse-like waves could exist in a system described by the KdV equation. A remarkable quality of these solitary waves was that they could collide with each other and yet preserve their shapes and speeds after the collision. This particle-like nature led Zabusky and Kruskal to name such waves solitons. The first success of the soliton concept was explaining the recurrence in the Fermi-Pasta-Ulam system. From numerical solution of the KdV equation with periodic boundary conditions (representing essentially a ring of coupled nonlinear springs), Zabusky and Kruskal made the following observations. An initial profile representing a long-wavelength excitation would break up into a number of solitons, which would propagate around the system with different speeds. The solitons would collide but preserve their individual shapes and speeds. At some instant all of the solitons would collide at the same point, and a near recurrence of the initial profile would occur.

This success was exciting, of course, but the soliton concept proved to have even greater impact. In fact, it stimulated very important progress in the analytic treatment of initial-value problems for nonlinear partial differential equations describing wave propagation. During the past fifteen years a rather complete mathematical description of solitons has been developed. The amount of information on nonlinear wave phenomena obtained through the fruitful collaboration of mathematicians and physicists using this description makes the soliton concept one of the most significant developments in modern mathematical physics. The non dispersive nature of the soliton solutions to the KdV equation arises not because the effects of dispersion are absent but because they are balanced by nonlinearities in the system. The presence of both phenomena can be appreciated by considering simplified versions of the KdV equation. Eliminating the nonlinear term $u(\frac{\partial u}{\partial x})$ yields the linearized version

$$\frac{\partial u}{\partial t} + \frac{\partial^3 u}{\partial x^3} = 0 \quad (5.11)$$

The most elementary wave solution of this equation is the harmonic wave

$$u(x, t) = A \exp^{i(kx + \omega t)} \quad (5.12)$$

Where k is the wave number and ω is the angular frequency. In order for the displacement $u(x, t)$ given by equation Eqs. (5.10) to be solution of equation Eqs. (5.11), ω and k must satisfy the relation

$$\omega = k^3 \quad (5.13)$$

Such a dispersion relation is a very handy algebraic description of a linear system since it contains all the characteristics of the original differential equation, Two important concepts connected with the phase velocity $v_p = \omega/k$ and the group velocity $v_g = \frac{\partial \omega}{\partial k}$. The phase velocity measures how fast a point of constant phase is moving, while the group velocity measures how fast the energy of the wave moves. The waves described by Eqs. (5.11) are said to be dispersive because a wave with large k will have larger phase and group velocities than a wave with small k . Therefore, a wave composed of a superposition of elementary components with different wave numbers (different values of k in Eqs. (5.24)) will disperse, or change its form. as it propagates. Now, we eliminate the dispersive term $\frac{\partial^3 u}{\partial x^3}$ and consider the equation

$$\frac{\partial u}{\partial t} + u \frac{\partial u}{\partial x} = 0 \quad (5.14)$$

This simple nonlinear equation also admits wave solutions, but they are now of the form $u(x, t) = f(x - ut)$, where the function f is arbitrary. (that $f(x - ut)$) is a solution of Eqs. (5.14) For waves of this form, the important thing to note is that the velocity of a point of constant displacement u is equal to that displacement. As a result, the wave breaks; that is, portions of the wave undergoing greater displacements move faster than, and therefore overtake, those undergoing smaller displacements, This multivaluedness is a result of the nonlinearity and, like dispersion, leads to a change in form as the wave propagates. A remarkable property of the KdV equation is that dispersion and nonlinearity balance each other and allow wave solutions that propagate without changing form, An example of such a solution is

$$u(x, t) = 3c \operatorname{sech}^2[c^{\frac{1}{2}}(x - ct)/2] \quad (5.15)$$

where the velocity c can take any positive value. This is the one soliton solution of the KdV equation. not all nonlinear partial differential equations have soliton solutions. Those that do are generic and belong to a class for which the general initial-value problem can be solved by a technique called the inverse scattering transform, a brilliant scheme developed by Kruskal and his coworkers in 1967. With this method, which can be viewed as a generalization of the Fourier transform to nonlinear equations, general solutions can be produced through a series of linear calculations. During the solution process it is possible to identify new nonlinear modesgeneralized Fourier modes that are the soliton components of the solution and, in addition, modes that are purely dispersive and therefore often called radiation. Equations that can be solved by the inverse scattering transform are said to be completely integrable. The manifestation of balance between dispersion and nonlinearity can be quite different from system to system. Other equations thus have soliton solutions that are distinct from the bell-shaped solitons of the KdV equation. An

example is the so-called nonlinear Schrodinger (NLS) equation. This equation is generic to all conservative systems that are weakly nonlinear but strongly dispersive. It describes the slow temporal and spatial evolution of the envelope of an almost monochromatic wave train. We present here a heuristic derivation of the NLS equation that shows how it is the natural equation for the evolution of a carrier-wave envelope. Consider a dispersion relation for a harmonic wave that is amplitude dependent:

$$\omega = \omega(k, |E|^2) \quad (5.16)$$

Here $E = E(x, t)$ is the slowly varying envelope function of a situation described by Eqs. (5.16) occurs, for example. in nonlinear optical phenomena, where the dielectric constant of the medium depends on the intensity of the electric signal. Other examples include surface waves on deep water, electrostatic plasma waves, and bond-energy transport in proteins. By expanding Eqs. (5.16) in a Taylor's series about ω_0 and k_0 , we obtain

$$\omega - \omega_0 = \left. \frac{\partial \omega}{\partial k} \right|_0 (k - k_0) + \frac{1}{2} \left. \frac{\partial^2 \omega}{\partial k^2} \right|_0 (k - k_0)^2 + \left. \frac{\partial \omega}{\partial (|E|^2)} \right|_0 |E|^2 \quad (5.17)$$

We have expanded only to the first order in the nonlinearity but to the second order in the dispersion term, as we shall see only represents undistorted propagation of the wave with the group velocity $v_g = \left. \frac{\partial \omega}{\partial k} \right|_0$. If we now substitute the operators $i \left(\frac{\partial}{\partial t} \right)$ for $\omega - \omega_0$ and $-i \left(\frac{\partial}{\partial x} \right)$ for $k - k_0$ in Eqs. (5.17) and let resulting expression operate on E , we get

$$i \left[\frac{\partial E}{\partial t} + \left. \frac{\partial \omega}{\partial k} \right|_0 \frac{\partial E}{\partial x} \right] + \frac{1}{2} \left. \frac{\partial^2 \omega}{\partial k^2} \right|_0 \frac{\partial^2 E}{\partial x^2} - \left. \frac{\partial \omega}{\partial (|E|^2)} \right|_0 |E|^2 E = 0 \quad (5.18)$$

This is the nonlinear Schrodinger equation, so called because of its resemblance to the Schrodinger equation even though its derivation often has nothing to do with quantum mechanics. The first term of Eqs. (5.18) represents undistorted propagation of the wave at the group velocity. and the second and third terms represent its linear and nonlinear distortion. respectively. This crude derivation of the NLS equation shows how it arises in systems with amplitude-dependent dispersion relations. It is often preferable to express Eqs. (5.18) in a neater form. For this purpose we transform the variables x and t into z and τ , where $z = x - \left. \frac{\partial \omega}{\partial k} \right|_0 t$ is a coordinate moving with group velocity and $\tau = \frac{1}{2} \left. \frac{\partial^2 \omega}{\partial k^2} \right|_0 t$ is the normalized time Eqs. (5.18) then reduced

$$i \frac{\partial E}{\partial \tau} + \frac{\partial^2 E}{\partial \tau^2} + 2k |E|^2 E = 0 \quad (5.19)$$

where

$$k = \frac{-\left[\left. \frac{\partial \omega}{\partial (|E|^2)} \right|_0 \right]}{\left[\left. \frac{\partial^2 \omega}{\partial k^2} \right|_0 \right]} \quad (5.20)$$

The NLS equation like the KdV equation is completely integrable and has soliton solutions. The analytic form for a single-soliton solution is given by

$$E(z, \tau) = 2\eta \operatorname{sech}[2\eta(\theta_0 - \eta z - 4\zeta\eta\tau)] \exp^{-2i[\phi_0 + 2(\zeta^2 - \eta^2)t + \zeta z]} \quad (5.21)$$

where $\zeta, \eta, \theta_0, \phi_0$ are free parameters determining the speed, amplitude, initial position, and initial phase, respectively, of the soliton. Any initial excitation for the NLS equation will decompose into solitons and/or dispersive radiation. A monochromatic wave train solution $E(z, \tau) = E(\tau)$ is thus unstable to any z dependent perturbation and breaks up into separate and localized solitons. This phenomenon is called the Benjamin-Feir instability and is well known to any surfer on the beach who has noticed that every, say, seventh wave is the largest. The NLS equation is in a way more universal than the KdV equation since an almost monochromatic, small-amplitude solution of the KdV equation will evolve according to the NLS equation. The last type of soliton we mention, which is distinctly different from the kdv or NLS solitons, is one that represents topologically invariant quantities in a system. Such an invariant can be a domain wall or a dislocation in a magnetic crystal or a shift in the bond-alternation pattern in a polymer. The prototype of equations for such solitons is the Sine-Gordon equation,

$$\frac{\partial^2 u}{\partial x^2} - \frac{\partial^2 u}{\partial t^2} = \sin u \quad (5.22)$$

notice that this equation allows for an infinite number of trivial solution, namely $u = 0 \pm 2\pi \pm 4\pi$ systems with a multitude of such degenerate ground states also allow solutions that connect two neighboring ground states. Solutions of this type are often called kinks, and for the sine-Gordon equation they are exact solitons; that is, they collide elastically without generation of dispersive radiation. The analytic form is given by

$$u_{\pm}(x, t) = 4 \tan^{-1} \exp[\pm (x - x_0 - ct)/(1 - c^2)^{\frac{1}{2}}] \quad (5.23)$$

where the solution u is often called an antikink. The parameter c ($1 < c < 1$) determines the velocity and x_0 the initial position, Other equations with degenerate ground states also have kink and antikink solutions, but they are not exact solitons like those of the sine-Gordon equation. It is interesting to note that small-amplitude solutions of the sine-Gordon equation also can be shown to evolve according to the NLS equation.

5.3 Optical Solitons

5.3.1 Introduction

Optical solitary waves, temporal and spatial solitons, have been the subject of intense theoretical and experimental studies in recent years. Solitons - localized pulses in time or bounded self-guided beams in space - evolve from a nonlinear change in the refractive index of a material induced by the light intensity distribution. When the combined effects of the refractive nonlinearity and the pulse dispersion (in the case of temporal solitons) or beam diffraction (in the case of spatial solitons) exactly compensate each other, the pulse or beam propagates without change in shape and is said to be self-trapped. Nonlinear effects responsible for soliton formation in optical fibers are, in general, weak and Kerr-like, i.e. they induce a local index change directly proportional to the light intensity. In this case the main nonlinear equation governing the pulse evolution is the famous cubic nonlinear Schrödinger (NLS) equation for the complex amplitude envelope of the electric field which, depending on the sign of the group-velocity dispersion, has two distinct types of localized solutions, bright or dark solitons. These two types of waves look like two members of

a general family of localized solutions, and this idea manifests itself in the drawing of Marc Haelterman, see Fig.8.2 However, these two types of solitary waves are in fact very different, they have completely different nature and result from quite different physics. In the case of temporal solitons observed in optical fibers [64, 65], the group velocity dispersion is known to vanish at a wavelength of about 1.3 μm and is positive at larger wavelengths and negative at shorter ones. As a result, since silica optical fibers have always a positive Kerr coefficient, the two different signs of group-velocity dispersion support two different types of solitons, dark, in the former case, and bright, in the latter case. A similar situation occurs for self-guided beams or spatial optical solitons [66, 67] observed in planar waveguides or in a bulk medium. Here diffraction plays a role analogous to dispersion in the temporal domain, but now the nonlinearity may be either positive, for the so-called self-focusing nonlinear medium, or negative, for self-defocusing medium. This again gives rise to two distinct types of solitons, bright and dark, respectively [68]. When the group-

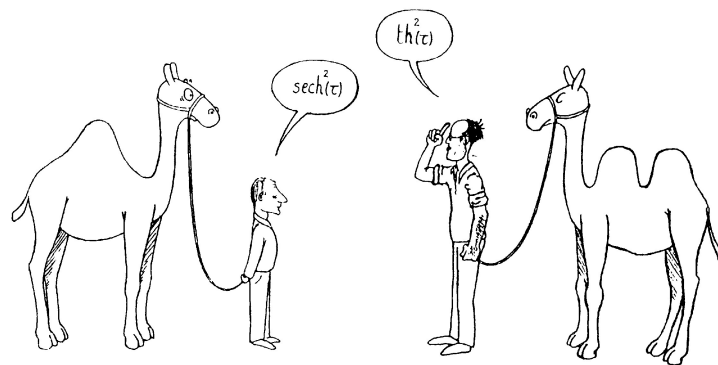


Figure 5.2: Do these 'animals' belong to the same soliton family? (the drawing made by Marc Haelterman in 1989).

velocity dispersion in an optical fiber is anomalous (or, similarly, when the nonlinearity of a planar waveguide is self-focusing), a constant amplitude continuous wave is unstable due to the modulational instability [64], and breaks down into a sequence of localized pulses (or beams for the spatial domain). These pulses are bright solitons. Propagation of bright solitons in optical fibers has been verified in a number of elegant experiments, [69], as well as more recent investigations of long-distance soliton transmission in periodically amplified fibers [70]. These results have been presented in several review papers and books [64, 65, 71, 72]. In the case of normal group-velocity dispersion in fibers (or a self-defocusing nonlinearity in waveguides), bright solitons do not exist, instead initial pulses (or spatially localized beams) undergo enhanced dispersion (or diffraction) induced broadening and chirping. In this case a constant amplitude wave is modulationally stable and localized pulses can appear only as holes on a continuous wave (cw) background, i.e., as dark solitons. Interest in the behaviour of such dark solitons has been motivated by several experimental observations of temporal dark solitons in optical fibers [73, 74, 75] and spatial dark solitons in bulk media and waveguides [76, 77, 78, 79, 80, 81, 82, 83, 84]. Although there has now been many successful experiments in which dark solitons have been observed in optical systems because of the relative ease of producing high intensity light beams or short (ps or fs) optical pulses, it should be remembered that the basic physics behind dark-soliton propagation on a modulationally stable background wave is quite fundamental and it applies to nonlinear problems with a different physical context.

5.3.2 Why temporal and spatial solitons are different?

Usually, the stationary beam propagation in planar waveguides is considered as the phenomenon similar to the pulse propagation in fibers referring to the so-called spatio-temporal analogy in wave propagation [85, 86]. This means that the propagation coordinate z is treated as the evolution variable and the spatial beam profile along the transverse direction, for the case of waveguides, is similar to the temporal pulse profile, for the case of fibers. This analogy has been developed by many researchers, and it is based on a simple notion that both beam and pulse propagation can be described by the cubic NLS equation [87, 88]. However, contrary to the accepted opinion, there exists a crucial difference between these two phenomena. Indeed, in the case of the nonstationary pulse propagation in fibers, the operation wavelength is usually selected near the zero of the group-velocity dispersion. This means that the absolute value of the fiber dispersion is small enough to be compensated by a weak nonlinearity such as that produced by the (very weak) Kerr effect in optical fibers which leads to a nonlinearity-induced change in the refractive index by the order of 10^{-10} . Therefore, nonlinearity in fibers is always weak and it is well modeled by the cubic NLS equation, which is known to be integrable by means of the inverse scattering transform [89, 90, 91]. However, for very short (fs) pulses the cubic NLS equation should be corrected to include some additional (but still small) effects such as higher-order dispersion, induced Raman scattering, etc. [92, 94]. Thus, in fibers nonlinear effects are very weak and they become important on large distances (of order of hundred meters or even kilometers). Contrary to the pulse propagation in optical fibers, the physics underlying the stationary beam propagation in planar waveguides and a bulk medium is different. In this case the nonlinear change in the refractive index should compensate for the beam spreading caused by diffraction which is not a small effect. That is why to observe spatial solitons much larger nonlinearities are usually required, and very often such nonlinearities are not of the Kerr type (e.g. they saturate at higher intensities). This leads to the models of generalized non-linearities with the properties of solitary waves different from those described by the integrable cubic NLS equation. For example, unlike the solitons of the integrable cubic NLS equation, solitary waves of generalized nonlinearities may be unstable, they also show some interesting properties such as fusion due to collision, etc.

5.3.3 Quantitative consideration

In the modern experimental and theoretical studies of solitons, the most significant progress has been achieved in optics and, most recently, in Bose-Einstein condensates (BECs). A milestone achievement was the creation of bright temporal solitons in nonlinear optical fiber in 1980, after this possibility had been predicted seven years earlier. In the realm of nonlinear optics, this was followed by the creation of dark solitons in fiber, bright spatial solitons in planar nonlinear waveguides, and gap solitons (GSs) in fiber Bragg gratings [57]. In all these cases, the soliton is supported by interplay between the chromatic dispersion (in the temporal domain) or diffraction (for spatial solitons) of the electromagnetic wave and cubic self-focusing nonlinearity, induced by the Kerr effect. The latter may be realized as an effective positive correction, $\Delta n(I)$, to the local refractive index (RI) of the material medium, which is proportional to the local intensity, I , of that very electromagnetic wave on which the RI acts, i.e., $\Delta n(I) = n_2 I$ with a positive coefficient n_2 . Besides the self-focusing sign of the Kerr effect $\Delta n(I) > 0$, its essential property in normal optical materials is the instantaneous character (no temporal delay between $\Delta n(I)$

and I). In view of fundamental importance of the temporal and spatial optical solitons supported by this mechanism, it is relevant to present a short quantitative explanation for it here.

In the course of the propagation in the nonlinear medium, the light pulse accumulates a phase shift that, through the correction $n_2 I$ to the RI, mimics the temporal shape of the pulse, $I = I(t)$. To understand this feature in a more accurate form, one may start from the normalized wave equation for the electric field E [93].

$$E_{zz} + E_{xx} + E_{yy} - (n^2 E)_{tt} = 0 \quad (5.24)$$

where the subscripts stand for the partial derivative, z is the propagation distance, x and y are transverse coordinates, t is time, and n is the above-mentioned RI (detailed derivation of the wave equation can be found, e.g., in book [93]). A solution to Eqs. (5.24) for a one-dimensional wave, which must be a real function, is looked for as

$$E(z, t) = u(z) \exp(i k_0 z - i \omega_0 t) + u^*(z) \exp(-i k_0 z + i \omega_0 t) \quad (5.25)$$

where $\exp(i k_0 z - i \omega_0 t)$ represent a rapidly oscillating carrier wave, the asterisk stands for the complex conjugation, and $u(z, t)$ is a slowly varying complex local amplitude. Substituting this in Eqs. (5.24), in the lowest approximation one obtains the dispersion relation between the propagation constant (wave number) k and frequency ω , $k_0^2 = (n_0 \omega_0)^2$, with n_0 the RI in the linear approximation. The next-order approximation, which takes into regard the above correction to the RI, $n = n_0 + n_2 I$, yields an evolution equation for the amplitude,

$$i \frac{du}{dz} + \frac{n_0 n_2}{k_0} \omega_0^2 I u = 0 \quad (5.26)$$

. Actually, this equation is a nonlinear one, as the intensity is tantamount to the squared amplitude, $I = |u|^2$. A solution to Eqs. (5.26) is simply $\Delta \Phi = (n_0 n_2) (\omega_0^2 / k_0) I z$, where $\Delta \Phi$ is a nonlinear contribution to the wave's phase (the accumulation of the non-linear phase is usually called self-phase modulation, SPM). The corresponding SPM-induced frequency shift being $\Delta \omega = -\partial \Delta \Phi / \partial t$, one obtains an expression for it,

$$\Delta \omega = -n_0 n_2 \frac{\omega_0^2}{k_0} \frac{dI}{dt} z \quad (5.27)$$

. It follows from Eqs. (5.27) that the lower-frequency components of the pulse, with $\Delta \omega < 0$, develop near its front, where $dI/dt > 0$ (the intensity grows with time), while higher frequencies, with $\Delta \omega > 0$, develop close to the rear of the pulse, where $dI/dt < 0$. On the other hand, the dielectric response of the material medium is not strictly instantaneous, featuring a finite temporal delay. This implies that the linear part, $\epsilon \equiv n_0^2$, of the multiplier n^2 in the wave equation Eqs. (5.24) (the dynamics dielectric permeability) is, as a matter of fact, a linear operator, rather than simply a multiplier. The accordingly modified form of the linear term $(\epsilon E)_{tt}$ in Eqs. (5.24) becomes $(\int_0^\infty \epsilon(\tau) E(t - \tau) d\tau)_{tt}$, where τ is the delay time. Finally, approximating this nonlocal-in-time expression by a quasi-local expansion, $\epsilon_0 E_{tt} + \epsilon_2 E_{ttt} + \dots$, which is justified when the

actual delay in the dielectric response is very small, gives rise to the second-and higher-order group-velocity-dispersion (GVD), alias chromatic-dispersion, terms in the eventual propagation equation, which can be translated into the corresponding linear dispersion relation, $k = k(\omega)$ [93]. In particular, the normal (positive)GVD (which means that waves with a higher frequency have a smaller group velocity, as expressed by the condition that the second-order-dispersion coefficient is positive, $\beta_2 \equiv d^2k/d\omega^2 > 0$) reinforces the above (nonlinearity-induced) trend to the temporal separation between the low-and high-frequency components of the pulse, contributing to its rapid spread. on the contrary, anomalous (negative)GVD $\beta_2 < 0$, which also occurs in real materials, may compensate the nonlinearity-induced spreading. with the magnitudes of the dispersion and intensity properly matched, the balance may be perfect, giving rise to very robust pulse, i.e., solitons.

5.3.4 Modulational instability and solitons

The dimensionless form of the standard cubic NLS equation is [95]

$$i \frac{\partial u}{\partial z} + \frac{1}{2} \frac{\partial^2}{\partial x^2} \pm |u|^2 u = 0 \quad (5.28)$$

where $z = \frac{z}{Z_0}$, $x = \frac{(t - \frac{z}{v_g})}{t_c}$, z is the normalized distance along the fiber, and the time variable t is a retarded time measured in the reference frame moving along the fiber with the group velocity.

The most frequently used normalized units are $Z_0 = 0.322 \frac{\pi c T^2}{\lambda_0^2 D}$, $t_c = \frac{T}{1.763}$, $v_g^{-1} = 2 \left\{ \frac{dk}{d\omega} \right\}_{\omega=\omega_0}$ and $D = \frac{2\pi}{\lambda_0^2} \left\{ \frac{d^2k}{d\omega^2} \right\}_{\omega=\omega_0}$

the NLS equation has simplest solution in the form of a continuous wave (cw) given by the expression

$$u = u_0 \exp^{i k x - i A z}, \quad A = \frac{1}{2} k^2 \pm u_0^2 \quad (5.29)$$

where the sign stands for the type of nonlinearity. Let us investigate the linear stability of the exact solution, Eqs. (5.29), against small perturbations. To do so, we follow the standard procedure and look for solutions describing small variations around the exact solution, Eqs. (5.29), in the form,

$$u = (u_0 + \xi) \exp^{i k x - i A z + i \psi} \quad (5.30)$$

where the function ξ and derivatives of the phase ψ are assumed to be small. Substituting Eqs. (5.30) into the NLS Eqs. (5.28), we come to a system of two coupled linear equations for ξ and ψ . Looking for solutions to these functions in the form, $\xi, \psi \sim \exp^{i \Omega z - i Q x}$, we obtain the dispersion relation

$$(\Omega - k Q)^2 = Q^2 \left(\pm u_0^2 + \frac{1}{4} Q^2 \right) \quad (5.31)$$

which shows that small excitations on the cw background, Eqs. (5.30), are absolutely stable only for the case of the defocusing medium (the sign +), whereas they become

unstable for the focusing nonlinearity provided $Q^2 < 4u_0^2$. In the former case, the small-amplitude waves can propagate along the background and these waves are characterized by the minimum (sound) velocity $c^2 = u_0^2$. This property of modulational instability of the cw background is closely connected with the existence and type of solitary wave solutions of the NLS equation. Namely, spatially localized solutions with vanishing asymptotics are possible only for the case when the plane wave solution is unstable, i.e., only for the focusing nonlinearity.

In the case of anomalous dispersion the cw solution is unstable and therefore the appropriate boundary conditions to Eqs. (5.30) is $|u| \rightarrow 0$ at $x \rightarrow \pm\infty$. For these conditions [89] showed that Eqs. (5.30) is exactly integrable by means of the inverse scattering transform, and it possesses localized solutions called bright solitons. General solution for the bright soliton has the form,

$$u(z, x) = \frac{a \exp^{i v x / 2 - i (v^2 / 4 - a^2) z}}{\cosh[a(x - v z)]} \quad (5.32)$$

where a is the soliton amplitude and v is its velocity. At $v = 0$ this soliton has a simplified structure referred to as the fundamental bright soliton (see Fig. 2a)

$$u(z, x) = \frac{a \exp^{i a^2 z}}{\cosh(a x)} \quad (5.33)$$

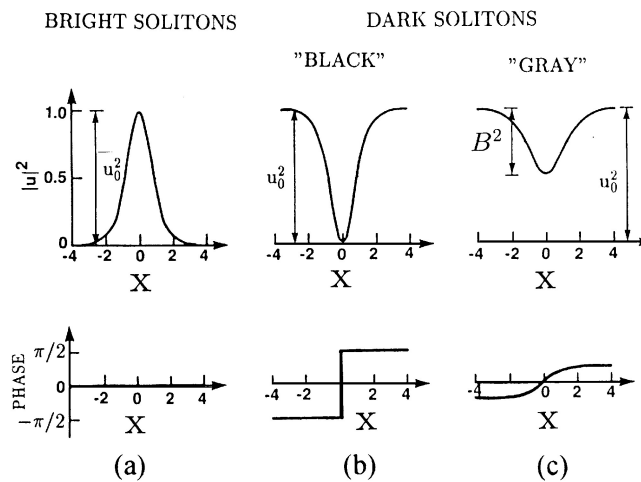


Figure 5.3: Intensity and phase as functions of normalized coordinate x for bright (a), black (b) and (c) gray solitons [adapted from Tomlinson et al. (1989)] .

For normal dispersion the cw solution $|u| = u_0$ is always stable against small modulations of its shape. The NLS equation with the boundary conditions $|u| = u_0$ is also exactly integrable by the inverse scattering technique[90] and its one-soliton solution for a single dark soliton can be written in the form,

$$u(z, x) = u_0 [A \tanh \Theta + i F] \exp^{i u_0^2 z} \quad (5.34)$$

where

$$\Theta = u_0 F (x - A u_0 z) \quad (5.35)$$

. Parameters A and F are connected by a simple relation, $A^2 + F^2 = 1$, so that instead of two parameters we can use only one, introducing $A = \sin \phi$ and $F = \cos \phi$. The effective angle ϕ corresponds to the total phase shift across the dark soliton, 2ϕ Soliton solution, Eqs. (5.34) and Eqs. (5.35), has, unlike the bright soliton, Eqs. (5.32), the only parameter ϕ and the function $F^2 = \cos^2 \phi$ characterizes the soliton intensity at the center, i.e., the minimum soliton intensity relative to the background intensity. The soliton intensity profile $|u|^2$ has the dip-like shape (see Fig. 9.3b and Fig. 9.3c)

$$|u|^2 = u_0^2 \left(1 - \frac{\cos^2 \phi}{\cosh^2 \Theta}\right) \quad (5.36)$$

We distinguish two limit cases of the dark soliton solution, Eqs. (5.34). The so-called fundamental dark soliton (at $\phi = 0$)

$$u(z, x) = u_0 \tanh(u_0 x) \exp^{i u_0^2 z} \quad (5.37)$$

is the anti-symmetric function of x with the π phase shift and zero intensity at its center (see Fig. 8.3b). Another limit case, when $\cos^2 \phi < 1$, corresponds to the so-called gray solitons (see Fig. 8.3c) when the minimum intensity does not drop to zero. As may be seen in Fig. 8.3, one of the major differences between bright and dark solitons is in the phase dependence: Bright solitons have a constant phase across the localized region but dark solitons have a nontrivial distribution of their phase, so that there exists a finite phase jump across the localized region.

5.3.5 Nonlinear Schrödinger equation and solitons

Putting all the above ingredients together, and assuming that the amplitude u in Eqs. (5.25) is a slowly varying function of z and "reduced time", $\tau \equiv t - k'_\omega z$ (here and below, the value of the derivative k'_ω is calculated at the carrier-wave's frequency, $\omega = \omega_0$), one arrives at the nonlinear Schrödinger (NLS) equation which governs the evolution of $u(z, \tau)$,

$$i u_z - \frac{1}{2} \beta u_{\tau\tau} + \gamma |u|^2 u = 0, \quad (5.38)$$

. Where β replaces β_2 (the replacement will not lead to confusion, as higher-order dispersion, which is different from β_2), is not dealt with below), and $\gamma \equiv n_2 \sqrt{\epsilon_0 \omega_0^2 / k_0}$. The introduction of τ instead of t is necessary to eliminate a term with the first derivative in t (the group-velocity term), thus casting the NLS equation in the simplest possible form, namely, the one given by Eqs. (5.38). Below, a number of models will be considered that may be viewed as various generalizations of the NLS equation Eqs. (5.38) two-component systems, equations with different nonlinearities, multidimensional systems, etc. A very recent succinct review of equations of the NLS type can be found in article [105]. An elementary property of the NLS equation is its Galilean invariance: any given solution $u(z, t)$ automatically generates a family of moving solutions by means of the Galilean boost that depends on an arbitrary real parameter c (it is an inverse-velocity shift, relative to the inverse group velocity, k'_ω , of the carries wave):

$$u(z, t; c) = u(z, \tau - cz) \exp\left(\frac{ic^2}{2\beta} z - \frac{ic}{\beta} \tau\right). \quad (5.39)$$

. Another simple property of Eqs. (5.38) is the modulational instability of CW(continuous-wave)solution, $u_{CW} = A_0 \exp(i \gamma A_0^2 z)$ with an arbitrary amplitude A_0 : although the CW solution does not contain the GVD coefficient β , it is stable in the case of $\beta \gamma < 0$, and unstable (against τ -dependent perturbations) in the opposite case. The NLS equation has natural Lagrangian and Hamiltonian representations:

$$i u_z = \frac{\delta H}{\delta u^*}, \quad (5.40)$$

. where $\delta/\delta u^*$ is the functional derivative, the asterisk stands for the complex conjugation, and the Hamiltonian,

$$H = -\frac{1}{2} \int_{-\infty}^{+\infty} (\beta |u_\tau|^2 + \gamma |u|^4) d\tau, \quad (5.41)$$

. is considered as a functional of two formally independent arguments, $u(\tau)$ and $(u(\tau))^*$. The Hamiltonian is a dynamical invariant of Eqs. (5.38), i.e., $dH/dz = 0$. Two other straightforward dynamical invariants of the NLS equation are energy E , alias norm of the solution (in the context of fiber optics, the energy is different from the Hamiltonian). and momentum P .

$$E \equiv \frac{1}{2} \int_{-\infty}^{+\infty} |u(\tau)|^2 d\tau, \quad (5.42)$$

$$P \equiv i \frac{1}{2} \int_{-\infty}^{+\infty} u u_\tau^* d\tau, \quad (5.43)$$

. Due to the fact that NLS equation is exactly integrable by means of the IST, it has an infinite set of higher-order dynamical invariants, in addition to E, P and H . [176]

In the case of the anomalous GVD, $\beta < 0$ (it is assumed that γ is positive), i.e., when the CW solution are unstable, a commonly known family of solitons to Eqs. (5.38) is

$$u_{sol}(z, \tau) = \frac{\eta}{\sqrt{\gamma}} \operatorname{sech}\left(\eta\left(\frac{\tau}{|\beta|} - cz\right)\right) \exp\left(i\left[\frac{c\tau}{\sqrt{|\beta|}} + \frac{1}{2}(\eta^2 - c^2)z\right]\right), \quad (5.44)$$

. where η and c are arbitrary real parameters, that determine the soliton's amplitude and the above-mentioned inverse-velocity shift. The function sech (hyperbolic secant) in this solution provides for the localization of the soliton. In the experiment, the temporal soliton is observed as a localized pulse running along the fiber with the velocity $V = 1/(K'_\omega + c \sqrt{|\beta|})$. The entire soliton family Eqs. (5.44) is stable against small perturbations. The applications of the IST yields solutions of the NLS equation more complex than the fundamental soliton Eqs. (5.38). In particular, the initial condition (in the case of $\beta < 0$)

$$u_0(\tau) = n \frac{\eta}{\sqrt{\gamma}} \operatorname{sech}\left(\frac{\eta}{\sqrt{\beta}} \beta\right) \quad (5.45)$$

. with integer n and arbitrary η , that the fundamental soliton for $n = 1$, gives rise to higher-order "n-solitons" for $n \geq 2$ [154]. Analytical expressions for these solitons with $n \geq 3$ are cumbersome. A relatively simple analytical solution describes the 2-soliton,

$$u_{2\text{sol}} = \frac{4\eta \cosh(3\eta\tau/\sqrt{|\beta|}) + 3 \exp(4\eta^2 z) \cosh(3\eta\tau/\sqrt{|\beta|})}{\sqrt{\gamma} \cosh(4\eta\tau/\sqrt{|\beta|}) + 4 \cosh(2\eta\tau/\sqrt{|\beta|}) + 3 \cos(4\eta^2 z)} \exp\left(\frac{i}{2}\eta^2 z\right) \quad (5.46)$$

. As seen from this expression, the shape of the 2-soliton, i.e., the distribution of the power in the soliton, $|u(z, \tau)|^2$, oscillates in z with the period

$$z_{\text{sol}} = \frac{\pi}{2\eta^2} \quad (5.47)$$

. which is called the soliton period. It can be demonstrated that all the exact n -soliton solutions generated by the initial condition Eqs. (5.45) with $N \geq 2$ oscillate with exactly the same period Eqs. (5.47), irrespective of the integer value of n . In fact, z_{sol} is also an estimate for the propagation distance which is necessary for formation (self-trapping) of the fundamental soliton from an initial pulse of a generic form. As well as the fundamental soliton Eqs. (5.44), the 2-soliton Eqs. (5.46) single-humped at any z (i.e., $|u(z, \tau)|^2$) always has a single maximum as a function of τ . However, the 3-soliton solution periodically splits into a double-humped structure and recombines into a sharp single-peak one, see Fig. 5.4 in book [15]. In terms of the IST, the 2-soliton Eqs. (5.46) may be regarded as a nonlinear bound state of two fundamental solitons, with the amplitudes

$$\eta_1^{(n=2)} = 3\eta, \eta_2^{(n=2)} = \eta \quad (5.48)$$

. Similarly, the 3-soliton is a bound state of three fundamental solitons, with

$$\eta_1^{(n=3)} = 5\eta, \eta_2^{(n=3)} = 3\eta, \eta_3^{(n=3)} = \eta \quad (5.49)$$

. Note that the energy Eqs. (5.42) of the n -soliton Eqs. (5.44) is

$$E_n = \frac{2\sqrt{|\beta|}}{\gamma} n^2 \eta \quad (5.50)$$

. As follows from the above and Eqs. (5.51), for $n = 2$ and $n = 3$ (actually, for any n) the energy of the n -soliton is exactly equal to the sum of energies of the constituent fundamental solitons, if they are separated from each other. To understand if the bound state is stable against splitting into the separate fundamental solitons, one can identify its binding potential, as a difference between the value of the Hamiltonian Eqs. (5.45) for the n -soliton which is

$$E_n = \frac{2\sqrt{|\beta|}}{\gamma} n^2 \eta \quad (5.51)$$

. and the sum of the values of H for the separated constituent solitons. The result is that the binding potential is exactly equal to zero for all the n -solitons. For this reason, they are considered as unstable states. Indeed, an initial perturbation which imparts infinitely small velocities to the constituent solitons will result in splitting. However, this is a slowly growing instability, rather than exponential growth of perturbations, which would imply usual dynamical instability. For this reason, n -solitons may be physically meaningful objects. In the case of normal GVD, $B > 0$, localized (bright) solitons do not exist, but a

dark soliton (DS) is found in this case, in the form of a dark spot ("hole") against a uniform CW background. It is described by the following exact soliton to the NLS equation Eqs. (5.38)

$$H_n = \frac{\sqrt{\eta}}{\sqrt{\gamma}} \tanh\left(\frac{\eta}{\sqrt{\beta}\tau}\right) \exp(i\eta^2 z) \quad (5.52)$$

where η is an arbitrary amplitude of the background which supports the dark soliton. The DSs are stable, which is possible because the CW background supporting them is itself modulationally stable for $B > 0$, as mentioned above. DSs were created experimentally in nonlinear optical fibers [60,98,172], about a decade after the first observation of the bright solitons in fibers was reported.

5.4 Solitons in Bose Einstein Condensates

After the experimental realization of a Bose-Einstein condensate (BEC) [107] in a trapped ultracold Bose gas of alkali atoms (such as Rb, Na and Li), the study of solitons in this intrinsically nonlinear system has become a topic of current interest, both experimentally [108, 109] and theoretically [110, 111]. A BEC is characterized by the macroscopic occupation of bosons in a single quantum level, usually the ground state. This condensed state is a matter wave analogous to a laser where all atoms in the condensate are phase coherent. Thus, widely spaced atoms can have an interference pattern, with quantum effects manifested on a macroscopic scale. The nonlinear effects in a BEC depend crucially on the type of interaction between the bosons. A certain class of nonlinear evolution equations can support solitary wave/soliton solutions. The Gross-Pitaevskii equation (GPE) describing the evolution of the Bose-Einstein condensate (BEC) order parameter for weakly interacting bosons supports dark solitons for repulsive interactions and bright solitons for attractive interactions.

5.4.1 Interacting Bose system

The many-body Hamiltonian for a system of interacting bosons is given by

$$H = - \int \psi^\dagger \left[\frac{\hbar^2 \nabla^2}{2m} + \mu \right] \psi \, dr + \frac{1}{2} \int \psi^\dagger(r) \psi^\dagger(\hat{r}) v(\hat{r} - r) \Psi(r) \Psi(\hat{r}) \, d\hat{r} \, dr \quad (5.53)$$

Where ψ is the boson field operator satisfying the commutation relation $[\psi(r), \psi(\hat{r})] = \delta(r - \hat{r})$, $v(\hat{r} - r)$ is the two body interaction, and μ is the chemical potential. The dynamics is found to be

$$i \hbar \frac{\partial \psi}{\partial t} = [\psi, H] = \left[-\frac{\hbar^2}{2m} \nabla^2 + \int \psi^\dagger(\hat{r}) v(\hat{r} - r) \psi(\hat{r}) \, d\hat{r} - \mu \right] \psi(r) \quad (5.54)$$

5.4.2 Weakly interacting Bosons: Gross-Pitaevskii equation (GPE) for the condensate order parameter

Consider a dilute gas whose range of interatomic forces $r_0 \ll$ average distance between atoms $d = n^{-\frac{1}{3}}$ where $n = \text{density}$. For large d , the asymptotic expression for the wave

function, which depends on the scattering amplitude, can be used. For $T < T_c$, since relevant momenta are small, the scattering amplitude becomes independent of energy, and is replaced by its low-energy value, determined by the s-wave scattering length \bar{a} . An effective soft potential V_{eff}

which has the same low-energy scattering properties as $V(r - \hat{r})$ is introduced. It is defined using $g = \int V_{eff}(r) dr = \frac{4\pi\hbar^2\bar{a}}{m}$ where m is the atomic mass. In effect $V(r - \hat{r})$, can be replaced by a contact potential $g\delta(r - \hat{r})$ in the dynamical equation Eqs. (5.54). Next, after making the transformation $\psi \rightarrow \psi \exp(\frac{i\mu t}{\hbar})$ and by just replacing the operator Ψ by its expectation value $\psi = \langle \Psi \rangle$ the following Gross-Pitaevskii equation (GPE) is obtained for the time evolution of the condensate order parameter ψ , in the case of weakly interacting bosons:

$$i\hbar \frac{\partial \psi}{\partial t} + \frac{\hbar^2}{2m} \nabla^2 \psi - g |\psi|^2 \psi \quad (5.55)$$

This is a nonlinear partial differential equation, with the interaction term g giving rise to the nonlinearity. Note that $\bar{a} > 0$ ($g > 0$) implies a repulsive interaction, while $\bar{a} < 0$ ($g < 0$) implies attractive interaction. As is obvious in this case $\rho = \langle \Psi^\dagger \Psi \rangle = \psi^* \psi$. Thus the total density is equal to the condensate density, and hence both quantum fluctuations and depletion are absent in GPE dynamics. Although GPE has an underlying quantum nature, the condensate order parameter has a macroscopic extent, suggesting observation of quantum effects on a macroscopic, classical scale.

5.4.3 Linear excitations in GPE

At very low temperatures, the energy-momentum dispersion relation for the small amplitude excitations can be found from the frequencies of the linearized GPE with plane wave solutions. Small deviations around the background density ρ are studied by setting $\psi(r, t) = \sqrt{\rho_0} + \delta\psi$, in Eqs. (5.55), with

$$\delta\psi = A \exp i(kr - \omega t) + B \exp -i(kr - \omega t) \quad (5.56)$$

The dispersion relation is found to be

$$\omega^2(k) = \frac{\rho_0 g}{m} k^2 + \frac{\hbar^2 k^4}{4m^2} \quad (5.57)$$

Two cases arise:

1. Repulsive interaction ($g > 0$): This leads to the following Bogoliubov spectrum:

$$\omega(k) = \sqrt{c^2 k^2 + \frac{\hbar^2 k^4}{4m}} \quad (5.58)$$

where

$$c = \sqrt{\frac{\rho_0 g}{m}} \quad (5.59)$$

is called the Bogoliubov sound velocity. This is because for small momenta, the excitations are phonon-like, with $\omega = ck$, linear in k . For large k , $\omega = \frac{\hbar^2 k^2}{2m}$, quadratic in k . These excitations are dynamically stable for all k , since $\omega^2 \geq 0$

2. Attractive interaction ($g < 0$): In this case, there is dynamical stability only if $-\frac{\rho_0|g|}{m}k^2 + \frac{\hbar^2 k^4}{4m^2} \geq 0$. On substituting for g , this leads to the condition $k^2 \geq 16\pi\rho_0\bar{a}$ for stability. In other words, there is no associated sound velocity such as Eqs. (5.59) for the attractive case. For a particle in a box of length L , the lowest nonzero momentum is $\frac{2\pi}{L}$, which leads to the condition $N|\bar{a}|L \leq (\frac{\pi}{4})$.

5.4.4 Nonlinear excitations of the GPE

In this section, we review the known exact results for soliton solutions of the GPE Eqs. (5.55), for the condensate of bosons with weak repulsive interaction ($g > 0$) and weak attractive interaction ($g < 0$), by studying unidirectional dynamics in quasi-one dimensional traps. **a. Repulsive interaction ($g > 0$):** Dark solitons By looking for unidirectional traveling wave solutions of Eqs. (5.55) of the form $\psi(z) = \sqrt{\rho(z)} \exp^{i\phi(z)}$, where $z = (x - vt)$

xi is a dimensionless variable, we get $\xi = \hbar/\sqrt{2mg\rho_0}$. Here ξ is the healing length and ρ_0 is the background density. (ξ turns out to be the typical length scale of interaction obtained by equating kinetic and potential energies, i.e., $\frac{p^2}{2m} = \frac{(\frac{\hbar}{\xi})^2}{2m} = g\rho_0$.) Imposing the boundary conditions $|\psi(z)|^2 \rightarrow \rho_0$ and $\frac{d\psi}{dz} \rightarrow 0$, as $z \rightarrow \pm\infty$ one obtains

$$\psi(z) = \sqrt{\rho_0}(\gamma \tanh \frac{\gamma z}{\sqrt{2}} + i \frac{v}{c}) = \sqrt{\rho_0} \exp^{i\phi(z)}. \quad (5.60)$$

. Here, $\gamma = \sqrt{(1 - \frac{v^2}{c^2})}$, where $c = \sqrt{g\rho_0/m}$ is the Bogoliubov sound velocity that appeared in Eqs. (5.59). The solution Eqs. (5.60) shows that both the density profile $\rho(z)$ and the phase profile $\phi(z)$ travel with the same speed v . For $v \leq c$, γ is real, and the condensate wave function $\psi(z)$ takes on different constant complex values as $z \rightarrow \pm\infty$. However, when $v = 0$, the complex order parameter ψ becomes a real kink solution with asymptotic values $\pm\sqrt{\rho_0}$ as z goes to $\pm\infty$. In general, Eqs. (5.60) corresponds to the following density profile:

$$\rho(z) = |\psi(z)|^2 = \rho_0[1 - \gamma^2 \text{sech}^2[\frac{\gamma z}{\sqrt{2}}]]. \quad (5.61)$$

. For $v \leq c$, $\rho(z) \rightarrow \rho_0$ as $z \rightarrow \pm\infty$. There is a suppression of density (i.e. absence of atoms) at the center of the BEC soliton, with respect to the background value ρ_0 , for all $0 < v < c$. As $v \rightarrow 0$, $\rho(z)$ dips to zero at the soliton center. This is called a dark soliton. As v increases, the width of the soliton increases. $\rho(z)$ dips to a non-zero value $\rho_0[1 - \gamma^2]$ at the center. This is sometimes called a gray soliton. As $v \rightarrow c$, $\rho(z) \rightarrow \rho_0$ for all z . Thus the dark soliton flattens out and disappears as $v \rightarrow c$.

b. Attractive interaction ($g < 0$): Bright solitons

Unidirectional traveling wave solutions of Eqs. (5.55) with $g = -|g|$ have the following form:

$$\psi = A_0 \text{sech}[\sqrt{\frac{|g|}{2}}(x - u_d t)A_0] \exp[iu_d(x - u_p t)/2]. \quad (5.62)$$

. In Eqs. (5.62), u_d and u_p are the speeds of the density profile and phase profile, respectively. u_d, u_p can be positive or negative. $A_0 = \sqrt{u_d(u_d - 2u_p)/2|g|}$. This leads to the density profile

$$\rho(z) = A_0^2 \text{sech}^2[\sqrt{\frac{|g|}{2}}(x - u_d t)A_0]. \quad (5.63)$$

Chapter 6

Darboux transformation and Lax pairs: General formalism

6.1 Darboux transformation and Lax pair: General formalism

6.1.1 Introduction

The soliton theory is an important branch of nonlinear science. On one hand, it describes various kinds of stable motions appearing in nature, such as solitary water wave, solitary signals in optical fibre etc., and has many applications in science and technology (like optical signal communication). On the other hand, it gives many effective methods of getting explicit solutions of nonlinear partial differential equations. Therefore, it has attracted much attention from physicists as well as mathematicians.

Nonlinear partial differential equations appear in many scientific problems. Getting explicit solutions is usually a difficult task. Only in certain special cases can the solutions be written down explicitly. However, for many soliton equations, people have found quite a few methods to get explicit solutions. The most famous ones are the inverse scattering method, Bäcklund transformation etc.. The inverse scattering method is based on the spectral theory of ordinary differential equations. The Cauchy problem of many soliton equations can be transformed to solving a system of linear integral equations. Explicit solutions can be derived when the kernel of the integral equation is degenerate. The Bäcklund transformation gives a new solution from a known solution by solving a system of completely integrable partial differential equations. Some complicated nonlinear superposition formula arise to substitute the superposition principle in linear science.

However, if the kernel of the integral equation is not degenerate, it is very difficult to get the explicit expressions of the solutions via the inverse scattering method. For the Bäcklund transformation, the nonlinear superposition formula is not easy to be obtained in general. In late 1970s, it was discovered by V. B. Matveev that a method given by G. Darboux a century ago for the spectral problem of second order ordinary differential equations can be extended to some important soliton equations. This method was called Darboux transformation. After that, it was found that this method is very effective for many partial differential equations. It is now playing an important role in mechanics, physics and differential geometry. V. B. Matveev and M. A. Salle published an important monograph [112] on this topic in 1991. Besides, an interesting monograph of C. Rogers and W. K. Schief [119] with many recent results was published in 2002.

Peter Lax became interested in the mathematical properties of the nonlinear PDEs and their solutions. In his seminal 1968 paper [120], Lax introduced the concept of a Lax pair as a way to linearize these complicated PDEs. A Lax pair takes a higher order, completely integrable, non-linear PDE and expresses it as a system of linear equations involving a pair of differential operators or as a system of first-order linear differential equations written in matrix form

The Darboux transformation, or analogously Bäcklund or dressing transformation, applies only to systems of linear differential equations and cannot be applied directly to nonlinear differential equations. To be able to apply the Darboux transformation to a certain nonlinear differential equation, one finds a linear system of equations that is equivalent to a nonlinear differential equation. The relation between the linear system and the nonlinear differential equation is established through a consistency condition satisfied by the linear system. The Darboux transformation is then applied to the linear system resulting in transforming the equivalent nonlinear equation as well. The linear system is usually represented in terms of a pair of matrices called the Lax pair which must satisfy a consistency condition that is equivalent to the differential equation at hand. The difficulty is usually in finding this Lax pair. It is known for some nonlinear differential equations such as the Kortwegde Vries (KdV) equation, the sine-Gordon equation and the nonlinear Schrödinger equation [112]. In addition to the Lax pair, one also needs to know an exact solution of the nonlinear differential equation. This exact solution is then used as a seed for the Darboux transformation to generate other exact solutions [113]. In this part, we present a method of obtaining these two essential ingredients for performing the Darboux transformation, namely the Lax pair and the seed solution the calculus was doing by Usama Alkhawadja in his paper [113].

6.1.2 Darboux Transformation for Linear Ordinary Differential Equations

Schrödinger Equation With a Harmonic Potential

Consider the equation

$$-\Psi_{xx}(x) + x^2 \Psi = \lambda \Psi(x), \quad (6.1)$$

With Seed solution $\Psi_1 = \exp(\frac{x^2}{2})$ and $\lambda_1 = -1$. Applying DT on Ψ and $u = x^2$, we get

$$\begin{aligned} \Psi[1] &= \left(\frac{d}{dx} - x\right) \Phi, \\ u[1] &= x^2 - 2, \end{aligned} \quad (6.2)$$

Which satisfy the equation

$$-\Psi[1]_{xx} + x^2 \Psi[1] = (\lambda + 2) \Psi(x), \quad (6.3)$$

For example: $\Psi = \exp(\frac{x^2}{2})$ with $\lambda = 1$, gives

$$\Psi[1] = -2x \exp\left(\frac{-x^2}{2}\right) \quad (6.4)$$

With eigenvalue $\lambda + 2 = 3$. Applying the DT on $\Psi[1]$ we get

$$\Psi[2] = (4x^2 - 2) \exp\left(\frac{-x^2}{2}\right) \quad (6.5)$$

With eigenvalue $\lambda + 2 = 5$. Applying the DT on $\Psi[1]$ n -times, we get

$$\Psi[n] = -H_n \exp\left(\frac{-x^2}{2}\right) \quad (6.6)$$

With eigenvalue $\lambda + 2 = 2n + 1$, where

$$H_n = (-1)^n \exp\left(\frac{x^2}{2}\right) \left(\frac{d}{dx} - x\right)^n \exp\left(\frac{-x^2}{2}\right) \quad (6.7)$$

is the Hermite polynomial of order n .

6.1.3 Darboux Transformation for Nonlinear Partial Differential Equations

For nonlinear partial differential equations, Darboux transformation is applied in an indirect manner. One starts by finding a linear system of equations for an auxiliary field ψ in the form $\psi_x = U \cdot \psi$ and $\psi_t = V \cdot \psi$ where the order of the matrices U and V depends on the equation to be solved as will be seen next. The pair and the matrices U and V known as the Lax pair, are functionals of the solution of the differential equation. The consistency condition of the linear system $\psi_{xt} = \psi_{tx}$ should be equivalent to the differential equation. The linear system and hence its consistency condition are covariant under the Darboux transformation. Therefore, applying the Darboux transformation on the linear system results in a new consistency condition which is equivalent to a new differential equation that is covariant with the old one. The new differential equation is satisfied by a new solution. In the following we describe this procedure in a more detailed manner.

Lax pair Consider the general form of the nonlinear partial differential equation

$$F[Q(x, t), Q^*(x, t), Q_t(x, t), Q_{xx}(x, t)] = 0 \quad (6.8)$$

The auxiliary field is represented by a 2×2 matrix

$$\Psi = \begin{pmatrix} \psi_1(x, t) & \psi_2(x, t) \\ \phi_1(x, t) & \phi_2(x, t) \end{pmatrix}, \quad (6.9)$$

Where $\psi_{1,2}(x, t)$ and $\phi_{1,2}(x, t)$ are its components. The linear system of equations of the auxiliary field is formally written as an expansion in powers of the constant eigenvalues matrix

$$\Lambda = \begin{pmatrix} \lambda_1 & 0 \\ 0 & \lambda_2 \end{pmatrix}, \quad (6.10)$$

as follows

$$\Psi_x = \mathbf{U}_0 \cdot \Psi + \mathbf{U}_1 \cdot \Psi \cdot \Lambda \quad (6.11)$$

and

$$\Psi_t = \mathbf{V}_0 \cdot \Psi + \mathbf{V}_1 \cdot \Psi \cdot \Lambda + \mathbf{V}_2 \cdot \Psi \cdot \Lambda^2 \quad (6.12)$$

Here $U_{0,1}$ and $V_{0,1,2}$ are in principle functionals of Q and Q^* and their partial derivatives. The expansions were terminated at the linear and quadratic powers of Λ (6.11) and (6.12) respectively. To satisfy both (6.11) and (6.12), ψ must obey the consistency condition $\psi_{xt} = \psi_{tx}$ which leads to

$$\mathbf{U}_{0t} - \mathbf{V}_{0x} + [\mathbf{U}_0, \mathbf{V}_0] = \mathbf{0}, \quad (6.13)$$

$$\mathbf{U}_{1t} - \mathbf{V}_{1x} + [\mathbf{U}_0, \mathbf{V}_1] + [\mathbf{U}_1, \mathbf{V}_0] = \mathbf{0}, \quad (6.14)$$

$$\mathbf{V}_{2x} + [\mathbf{V}_2, \mathbf{U}_0] + [\mathbf{V}_1, \mathbf{U}_1] = \mathbf{0}, \quad (6.15)$$

$$[\mathbf{U}_1, \mathbf{V}_3] = \mathbf{0}, \quad (6.16)$$

where $[\mathbf{X}, \mathbf{Y}]$ denotes the commutator of \mathbf{X} and \mathbf{Y} . These equations are obtained by equating the coefficients $\Lambda^0, \Lambda^1, \Lambda^2$ and Λ^3 in ψ_{xt} to the corresponding ones in ψ_{tx} . The matrices U_0 and V_0 are the lax pair of (6.8). It is the consistency condition, (6.13), that should be equivalent to the differential equation

$$\mathbf{U}_{0t} - \mathbf{V}_{0x} + [\mathbf{U}_0, \mathbf{V}_0] = \begin{pmatrix} 0 & F \\ -F^* & 0 \end{pmatrix}, \quad (6.17)$$

Darboux transformation

Consider the following version of the Darboux transformation

$$\psi[1] = \psi \Lambda - \sigma \psi, \quad (6.18)$$

where $\psi[1]$ is the transformed field, Λ is a constant diagonal matrix and $\sigma = \psi_0 \Lambda \psi_0^{-1}$. Here ψ_0 is a known solution of the linear system, (6.11) and (6.12). To be able to find such a solution the coefficients of the linear system should be known explicitly. These coefficients are functionals of the solution of the differential equation Q . Thus, determining the coefficients of the linear system requires knowing an exact solution of the differential equation. This solution is known as the seed solution. Which we denote here by Q_0 . It is in the very nature of the Darboux transformation method that new exact solutions are only obtained from other exact solutions. The transformed field $\psi[1]$ is required to be a solution of a linear system that is covariant with the system (6.11) and (6.12), namely

$$\Psi[1]_x = \mathbf{U}_0[1] \cdot \Psi[1] + \mathbf{U}_1[1] \cdot \Psi[1] \cdot \Lambda \quad (6.19)$$

and

$$\Psi[1]_t = \mathbf{V}_0[1] \cdot \Psi[1] + \mathbf{V}_1[1] \cdot \Psi[1] \cdot \Lambda + \mathbf{V}_2[1] \cdot \Psi[1] \cdot \Lambda^2 \quad (6.20)$$

Requiring the system (6.19) and (6.20) to be covariant with the system (6.11) and (6.12) leads to a consistency condition

$$\mathbf{U}_0[1]_t - \mathbf{V}_0[1]_x + [\mathbf{U}_0[1], \mathbf{V}_0[1]] = \mathbf{0}, \quad (6.21)$$

that is covariant with (6.13) Similar to(6.17), this new consistency condition will be equivalent to a differential equation that is covariant with (6.8).

$$\mathbf{U}_0[\mathbf{1}]_t - \mathbf{V}_0[\mathbf{1}]_x + [\mathbf{U}_0[\mathbf{1}], \mathbf{V}_0[\mathbf{1}]] = \begin{pmatrix} 0 & F \\ -F^* & 0 \end{pmatrix} = \mathbf{0}, \quad (6.22)$$

This means that $Q[1]$ is a new solution of the same differential equation that Q_0 is a solution for. To find $U_0[1]$ and $V_0[1]$ and hence $Q[1]$ we substitute for $\psi[1]$ from (6.18)in (6.19) and (6.20) using (6.11) and (6.12) and then equating the coefficients of Λ^0 and Λ^1 to zero we get

$$\mathbf{U}_0[\mathbf{1}] = \sigma \mathbf{U}_0 \sigma^{-1} + \sigma_x \sigma^{-1}, \quad (6.23)$$

$$\mathbf{U}_0[\mathbf{1}] = \mathbf{U}_0 + [\mathbf{U}_1, \sigma], \quad (6.24)$$

Where σ^{-1} is the inverse of σ . The new solution $Q[1]$ can be calculated using either of these two equations which can be shown to be equivalent. Notice that the quantities on the right-hand side are calculated using the seed solution Q_0 .

To summarize, a nonlinear differential equation can be solved with the Darboux transformation method by first finding an exact (seed) solution, Q_0 , to the differential equation and finding a linear system for an auxiliary field ψ that is associated to the differential equation through its consistency condition. Using the seed solution, a solution of the linear system, ψ_0 , is found. The linear system is then transformed into a new one via the Darboux transformation. Thus, the coefficients of the new linear system which are functionals of the new solution of the differential equation, $Q[1]$ will be related to the coefficients of the original linear system which are functionals of Q_0 . This relation gives the new solution $Q[1]$ in terms of the seed solution Q_0 . In the following section we try to illustrate further this procedure by an example doing by Usama El khawadja in his paper[113] .

a. The GrossPitaevskii equation:

The mean-field equation of motion governing the evolution of the wave function of the Bose Einstein condensate is the so-called time-dependent GrossPitaevskii equation [114, 115]

$$i \hbar \frac{\partial \psi(r, t)}{\partial t} = -\frac{\hbar^2}{2m} \nabla^2 \psi(r, t) + \frac{1}{2} m (\omega_x^2 x^2 + \omega_y^2 y^2 + \omega_z^2 z^2) \psi(r, t) + g |\psi(r, t)|^2 \psi(r, t) = 0. \quad (6.25)$$

which is basically a Schrödinger equation but with a nonlinear term. Here, g is the effective two-particle interaction which is proportional to the s-wave scattering length a according to $g = \frac{4\pi a \hbar^2}{m}$, where m is the mass of an atom, and ω_x, ω_y and ω_z are the trap frequencies in the x, y and z directions, respectively. For axially symmetric elongated traps, where the confining along, say, the y and z directions is much stronger than along the x direction, namely $\omega_y = \omega_z = \omega_{\perp} \geq \omega_x$, , the condensate is quasi one dimensional. The GrossPitaevskii equation can then be integrated over the transverse directions to reduce to a one-dimensional nonlinear Schrödinger equation [116, 117]

$$i \hbar \frac{\partial \psi(r, t)}{\partial t} = -\frac{\hbar^2}{2m} \frac{\partial^2 \psi(r, t)}{\partial^2 x} + \frac{g}{2\pi a_{\perp}^2} |\psi(r, t)|^2 \psi(r, t) = 0. \quad (6.26)$$

Where $a_{\perp} = \sqrt{\frac{\hbar}{m\omega_{\perp}}}$ and ω_{\perp} are the characteristic length and frequency of the harmonic trap in the transverse direction, respectively. Scaling length to a_{\perp} , time to $\frac{2}{\omega_{\perp}}$ and $\psi(r, t)$ to $\frac{1}{\sqrt{2a_{\perp}}}$, the last equation takes the dimensionless form

$$i\hbar \frac{\partial\psi(r, t)}{\partial t} = -\frac{\partial^2\psi(r, t)}{\partial^2x} + \frac{1}{4}\lambda^2x^2\psi(x, t) + 2a|\psi(r, t)|^2\psi(r, t). \quad (6.27)$$

Where $\lambda = \frac{2\omega_x}{\omega_{\perp}}$. In the homogeneous case, $\lambda = 0$, exact bright and dark solitonic solutions can be obtained for attractive interatomic interaction, $a < 0$, and repulsive interactions, $a > 0$, respectively [116, 117]. For an expulsive harmonic potential, it was shown by Liang et al [118] that an exact solitonic solution can also be obtained provided that the scattering length is given by $a(t) = a_0 \exp(\lambda t)$ where a_0 is the scattering length at $t = 0$. In this case, the Gross-Pitaevskii equation takes the form

$$i\hbar \frac{\partial\psi(r, t)}{\partial t} + \frac{\partial^2\psi(r, t)}{\partial^2x} + \frac{1}{4}\lambda^2x^2\psi(x, t) + 2a_0 \exp(\lambda t) |\psi(r, t)|^2\psi(r, t) = 0. \quad (6.28)$$

$$i\hbar \frac{\partial\psi(r, t)}{\partial t} + \frac{\partial^2\psi(r, t)}{\partial^2x} + \frac{1}{4}\lambda(x)^2\psi(x, t) + 2a(t) |\psi(r, t)|^2\psi(r, t) = 0. \quad (6.29)$$

Where $a(t) = a_0 \exp(\gamma(t)t)$ and $\lambda(x)$ and $\gamma(t)$ are assumed to be independent general functions of x and t , respectively. For the special case of $\lambda(x) = \lambda x$ and $\gamma(t) = \lambda$, the expulsive potential case, Eqs. (6.28) are retrieved.

Lax pair for Gross Pitaevskii equation with expulsive harmonic potential:

Darboux transformation is a method used to obtain exact solutions of nonlinear partial differential equations [112]. In this method, a linear system of equations for a field $\phi(x, t)$ is written in the form

$$\phi_x = U \phi \quad (6.30)$$

$$\phi_t = V \phi \quad (6.31)$$

where the matrices, U and V , are called the Lax pair. The subscripts x and t denote, here and throughout, position and time derivatives, respectively. The consistency condition $\phi_{xt} = \phi_{tx}$ requires that U and V obey

$$U_t - V_x + [U, V] = 0 \quad (6.32)$$

The Lax pair is expressed in terms of the wavefunction $\psi(x, t)$ such that the consistency condition, Eqs. (6.32), is equivalent to the Gross-Pitaevskii equation. Once the Lax pair is obtained, the Darboux transformation can be applied to the linear system Eqs. (6.30) and Eqs. (6.31). In the Darboux transformation method, one of the solutions of the linear system, denoted by ϕ_1 , is chosen as a seed to perform the following functional transform on the field ϕ :

$$\phi[1] = \phi \Lambda - \sigma \phi, \quad (6.33)$$

where ϕ_1 is the transformed field, Λ is a constant diagonal matrix and $\sigma = \phi_1 \Lambda \phi_1^{-1}$. For the system Eqs. (6.30) and Eqs. (6.31) to be covariant with respect to the Darboux transformation, the Lax

$$\phi[1]_x = U[1] \phi[1], \quad (6.34)$$

$$\phi[1]_t = V[1] \phi[1], \quad (6.35)$$

is satisfied. As a result, the consistency condition is also covariant under the Darboux transformation and takes the form of Eqs. (6.32) but with the Lax pair, U and V , being replaced by the transformed Lax pair $U[1]$ and $V[1]$. This means that the new wavefunction $\psi[1]$ is also a solution of the GrossPitaevskii equation. Thus, using the Darboux transformation, we obtain one exact solution from another. In some cases, this leads to classes of solutions. The difficulty in this method is in finding the Lax pair that corresponds to a given differential equation. Usually, one starts with a Lax pair and then discovers what differential equation it represents. For the inhomogeneous case, with an expulsive potential the Lax pair corresponding to Eqs. (6.28) was found to be [118]

$$\mathbf{U} = \begin{pmatrix} \zeta & \sqrt{a_0}Q \\ \sqrt{a_0}Q^* & \zeta \end{pmatrix}, \quad (6.36)$$

$$\mathbf{V} = \begin{pmatrix} 2\imath\zeta^2 + \lambda x \zeta + \imath a_0|Q|^2 & \sqrt{a_0}[(\lambda x + 2\imath\zeta)Q + \imath Q_x] \\ \sqrt{a_0}[-(\lambda x + 2\imath\zeta)Q^* + \imath Q_x^{star}] & -2\imath\zeta^2 - \lambda x \zeta - \imath a_0|Q|^2 \end{pmatrix}, \quad (6.37)$$

Here, $Q(x, t) = \exp(\lambda t/2 - \imath \lambda x^2/4) \psi(x, t)$ and $\zeta(t) = \xi_0 \exp(\lambda t)$ where ξ_0 is an arbitrary constant. The consistency condition generates Eqs. (6.32). The Lax pair of the homogeneous Gross-Pitaevskii equation can be obtained simply by setting $\lambda = 0$ in Eqs. (6.36) and Eqs. (6.37).

Liang et al have applied the Darboux transformation on the Lax pair Eqs. (6.36) and Eqs. (6.37) to derive a solitonic solution of Eqs. (6.28).

Lax pair for general form of Gross Pitaevskii : In this example Usama Alkhawadja [113] attempt to find the Lax pair of a Gross Pitaevskii of the general form Eqs. (6.29). The method is summarized as follows. He calculate the matrix resulting from substituting the Lax pair for the expulsive potential case, Eqs. (6.36) and Eqs. (6.37), in the consistency condition Eqs. (6.32). He modify the resulting matrix such that, when equating it to zero, the general Gross Pitaevskii equation, Eqs. (6.29), is obtained. Then He express the unknown Lax pair in terms of second-order polynomials in the wavefunction $\psi(x, t)$ with unknown function coefficients. Calculating the consistency condition using this Lax pair and requiring the result to be equal to the modified matrix, He obtain equations for the unknown coefficients. By solving these equations, He obtain the Lax pair equivalent to Eqs. (6.29). This approach reproduces the previously found Lax pairs of the expulsive potential and homogeneous potential cases [112, 118], in addition to a new Lax pair for the linear potential case. Calculating the consistency condition for the expulsive potential case by substituting the Lax pair Eqs. (6.36) and Eqs. (6.37) into Eqs. (6.32), we obtain

$$\begin{pmatrix} 0 & -\sqrt{a_0} \exp((\lambda t/2 + \imath \lambda x^2/4)) A[\psi, \Psi^*] \\ -\sqrt{a_0} \exp((\lambda t/2 - \imath \lambda x^2/4)) A^*[\psi, \Psi^*] & 0 \end{pmatrix} = 0, \quad (6.38)$$

Where $A[\psi, \psi^*]$ is the left -hand side of equation Eqs. (6.28). This leads to $A[\psi, \psi^*] = 0$ and $A^*[\psi, \Psi^*] = 0$ which are the Gross-Pitaevskii equation, Eqs. (6.28), and its complex

conjugate, respectively. The prefactors of $A[\psi, \psi^*]$ and $A^*[\psi, \Psi^*]$ result from the functional transformation $Q(x, t) = \exp((\lambda t/2 - \imath \lambda x^2/4))\psi(x, t)$. In the general case, equation Eqs. (6.29) is accounted for if we modify this matrix into

$$\begin{pmatrix} 0 & -\sqrt{a_0} \exp(\gamma(t) t/2 + \imath f(x)) B[\psi, \Psi^*] \\ -\sqrt{a_0} \exp(\gamma(t) t/2 - \imath f(x)) B^*[\psi, \Psi^*] & 0 \end{pmatrix} = 0, \quad (6.39)$$

where $B[\psi, \Psi^*]$ is the left-hand side of equation Eqs. (6.29). Similar to the expulsive potential case, it turns out that it is more convenient to express the wavefunction $\psi(x, t)$ in terms of the function $Q(x, t)$ as follows:

$$\psi(x, t) = \exp(-\imath f(x) - \gamma(t) t/2) Q(x, t). \quad (6.40)$$

This equation is a generalization of the analogous transformation in the expulsive potential case. The real function $f(x)$ appears only in the prefactors of $B[\psi, \Psi^*]$ and $B^*[\psi, \Psi^*]$, i.e., the resulting GrossPitaevskii equation is independent of $f(x)$. However, it turns out that the Lax pair depends on $f_x(x)$. Thus, we can choose a certain form of $f(x)$ such that the Lax pair is simplified without changing the differential equation that it corresponds to.

He expand the Lax pair in powers of Q , Q_x and their complex conjugates as follows:

$$\mathbf{U} = \begin{pmatrix} f_1 + f_2 Q & f_3 + f_4 Q \\ f_5 + f_6 Q^* & f_7 + f_8 Q^* \end{pmatrix}, \quad (6.41)$$

$$\mathbf{V} = \begin{pmatrix} g_1 + g_2 Q + g_3 Q_x + g_4 Q Q^* & g_5 + g_6 Q + g_7 Q_x + g_8 Q Q^* \\ g_9 + g_{10} Q + g_{11} Q_x + g_{12} Q Q^* & g_{13} + g_{14} Q + g_{15} Q_x + g_{16} Q Q^* \end{pmatrix}, \quad (6.42)$$

Where $f_{1-8}(x, t)$ and $g_{1-16}(x, t)$ are the unknown functions. The matrices U and V are expanded up to the linear and quadratic order, respectively, since their product should account for the cubic term in Eqs. (6.29). He has terminated the expansion of U at the linear order and excluded many terms from both expansions. This is because when He employed the full expansions of both U and V up to the third order, many of the coefficients vanished since they resulted in terms that are not present in Eqs. (6.29). For example, having a Q_x term in U would lead, when calculating the consistency condition, to the term Q_{xt} which is not present in the differential equation. Even in the present form, many of the coefficients of the Lax pair Eqs. (6.41) and Eqs. (6.42) turn out to be zero. Consequently, the expansions in Eqs. (6.36) and Eqs. (6.37) are more than sufficient to give rise to the cases of quadratic, linear and homogeneous potentials. We substitute the Lax pair Eqs. (6.41) and Eqs. (6.42) in the consistency condition Eqs. (6.32) and use Eqs. (6.40) to express the matrix of equation Eqs. (6.39) in terms of $Q(x, t)$ and then we require the left-hand-side of the consistency condition Eqs. (6.32) to be equal to the matrix of Eqs. (6.39). Equating the coefficients of Q , Q_x , Q_{xx} , Q_t , $|Q|^2 Q$, and their complex conjugates on both sides of the resulting equation, we obtain 24 equations for 24 unknown coefficients $f_{1-8}(x, t)$ and $g_{1-16}(x, t)$. This results in many of the coefficients to be equal to zero or constant, namely: $f_2 = f_3 = f_5 = f_8 = g_2 = g_3 = g_5 = g_8 = g_9 = g_{12} = g_{14} = g_{15} = 0$, $f_4 = -f_6 = \sqrt{a_0}$, $g_7 = g_{11} = \sqrt{a_0 \imath}$, $g_4 = -g_{16} = a_0 \imath$. Using these constant values, the equations for the rest of the coefficients simplify to

$$g_{10} = -g_6 \quad (6.43)$$

$$f_{1t} - g_{1x} = 0 \quad (6.44)$$

$$(6.45)$$

$$g_{10x} + (f_7 - f_1)g_{10} + \sqrt{a_0}(g_{13} - g_1) - \sqrt{a_0}[-\iota \lambda^2/4 - (\gamma - 2\iota f_x^2 + \gamma_t + 2f_{xx}/2)] = 0 \quad (6.46)$$

$$g_{10x} - (f_7 - f_1)g_{10} - \sqrt{a_0}(g_{13} - g_1) + \sqrt{a_0}[-\iota \lambda^2/4 - (\gamma + 2\iota f_x^2 + \gamma_t + 2f_{xx}/2)] = 0 \quad (6.47)$$

$$g_{10} + \iota\sqrt{a_0}(f_1 - f_7) + 2\sqrt{a_0}f_x = 0 \quad (6.48)$$

In the following, we solve this system of equations. Adding equations Eqs. (6.47) and Eqs. (6.46), we find

$$g_{10} = -\sqrt{a_0}(\gamma x + 2f_x + \gamma_t t x)/2 + c_1 \quad (6.49)$$

Where $c_1(t)$ is a constant of integration resulting from integrating over x . Equation Eqs. (6.44) and Eqs. (6.45) can be both satisfied by assuming $f_7 = \alpha_1 f_1 + \alpha_2$ and $g_{13} = \alpha_1 g_1 + \alpha_3$, where α_1, α_2 and α_3 are the arbitrary constants. For $\alpha_1 = 1$, equations Eqs. (6.44) and Eqs. (6.45) become equivalent and decouple from equation Eqs. (6.46) to Eqs. (6.48). Therefore, the solutions of equations Eqs. (6.43) to Eqs. (6.48) are expected to differ significantly when $\alpha_1 = 1$ and $\alpha_1 \neq 1$. solution.

a. $\alpha_1 \neq 1$:

Substituting for g_{10} from equation Eqs. (6.49) into equation Eqs. (6.48), we get an equation for f_1 whose solution is given by

$$f_1 = \frac{\iota}{2(\alpha_1 - 1)(2\iota\alpha_2 + \gamma x - \frac{2c_1}{\sqrt{a_0}} - 2f_x + \gamma_t t x)} \quad (6.50)$$

Subtracting equations Eqs. (6.46) and Eqs. (6.47), and using the above expression for f_1 , we find

$$g_1 = \frac{-\iota}{4(\alpha_1 - 1)a_0}[-4c_1^2 + 4\sqrt{a_0}c_1(\gamma + \gamma_t t)x + a_0(\lambda^2 - 4\iota\alpha_3 - (\gamma + \gamma_t t)^2 x^2)]. \quad (6.51)$$

Substituting for f_1 and g_1 into equation Eqs. (6.44), we find

$$\frac{2}{\sqrt{a_0}}[(\gamma + \gamma_t t)c_1 - c_{1t}] + \lambda \lambda_x + [2\gamma_t - (\gamma + \gamma_t t)^2 + \gamma_{tt}t]x = 0 \quad (6.52)$$

For this equation to be satisfied, the function $\lambda(x)$ must be of the form where λ_0, λ_1 and λ_2 are the constants. Substituting this expression for $\lambda(x)$ into equation Eqs. (6.50) it take the form

$$\frac{2}{\sqrt{a_0}} \left[\frac{a_0}{2} \lambda_1 + (\gamma + \gamma_t t) c_1 - c_{1t} \right] + [\lambda_2^2 + 2\gamma_t - (\gamma + \gamma_t t)^2 + \gamma_{tt} t] x = 0 \quad (6.53)$$

Here again, the cases of $\lambda_2 \neq 0$ and $\lambda_2 = 0$ should be treated separately.

a.1. $\lambda_2 \neq 0$:Equating separately the first and the second lines of equation Eqs. (6.53)to zero, and solving for $\gamma(t)$ and then for c

$$\gamma(t) = \lambda_2 - \frac{1}{t} \ln(c_2 \exp(2 \lambda_2 t) + c_3), \quad (6.54)$$

and

$$c_1(t) = \frac{4 c_4 \lambda_2 \exp(\lambda_2 t) - \sqrt{a_0 \lambda_1 (c_3 - c_2 \exp(2 \lambda_2 t))}}{4 \lambda_2 (c_3 + c_2 \exp(2 \lambda_2 t))} \quad (6.55)$$

Where $c_2, c_3,$ and c_4 are the constants of integration (independent of x and t). Using the last two equations to substitute for $c_1(t)$ and $\gamma(t)$ into equation Eqs. (6.49)to Eqs. (6.50),we obtain explicit expressions for $f_1(x, t), g_1(x, t)$ and $g_{10}(x, t)$:

$$f_1(x, t) = \frac{i \eta_2}{4 \lambda_2 (\alpha_1 - 1) \eta_1}, \quad (6.56)$$

$$g_1(x, t) = \frac{i [(c_2^2 \zeta^4 + c_3^2) \eta_4 - 2 c_4 c_3 \zeta^2 \eta_5]}{16 (\alpha_1 - 1) \lambda_2^2 \eta_1^2}, \quad (6.57)$$

$$g_{10}(x, t) = -\frac{\sqrt{a_0 \eta_6}}{4 \lambda_2 \eta_1}, \quad (6.58)$$

Where $\eta_1 = c_3 + c_2 \zeta^2$, $\eta_2 = -4 \lambda_2 f_x \eta_1 + (\lambda_1 + 2 \lambda_2^2 x) \eta_3$, $\eta_3 = c_3 - c_2 \zeta^2$, $\eta_4 = \lambda_1^2 - 4 \lambda_0 \lambda_2^2$, $\eta_5 \lambda_1^2 + \lambda_2^2 (4 \lambda_0 + 8 \lambda_1 x + 8 \lambda_2^2 x^2)$, $\eta_6 = 4 \lambda_2 f_x \eta_1 + (\lambda_1 + 2 \lambda_2^2 x) \eta_2$ and $\zeta = \exp(\lambda_2 t)$. It should be noted here that since α_2 and α_3 do not appear in the Gross Pitaevskii equation, they have been readily set to zero. This completes the determination of the unknown coefficient functions f_{1-7} and g_{1-16} . Substituting for these coefficients into equations (Eqs. (6.41)) and (Eqs. (6.42)), we obtain the Lax pair

$$\mathbf{U} = \begin{pmatrix} f_1 & f_3 + \sqrt{a_0} Q \\ -\sqrt{a_0} Q^* & \alpha_1 f_1 \end{pmatrix}, \quad (6.59)$$

$$\mathbf{V} = \begin{pmatrix} g_1 + i a_0 |Q|^2 & -g_{10} Q + i \sqrt{a_0} Q_x \\ g_{10} Q^* + i \sqrt{a_0} Q^* & \alpha_1 g_1 - i a_0 |Q|^2 \end{pmatrix}, \quad (6.60)$$

Calculating the consistency condition (Eqs. (6.32)) using this Lax pair, we obtain the Gross-Pitaevskii equation

$$i \frac{\partial \psi(x, t)}{\partial t} + \frac{\partial^2 \psi(x, t)}{\partial^2 x} + \frac{1}{4}(\lambda_0 + \lambda_1 x + \lambda_2^2 x^2) \psi(x, t) + \frac{2 a_0}{c_2 \exp(\lambda_2 t) |\psi(x, t)|^2 \psi(x, t)} = 0. \quad (6.61)$$

The Lax pair (Eqs. (6.41))and (Eqs. (6.42))corresponding to this Gross Pitaevskii equation is a generalization to the previous cases of homogeneous potential [112] and quadratic potential [118].

a.2. $\lambda_2 = 0$ In this case, the solutin of equation Eqs. (6.52)gives

$$\gamma(t) = -\frac{1}{t} \ln(c_2 t + c_3), \quad (6.62)$$

$$c_1(t) = \frac{8 c_4 + \sqrt{a_0} \lambda_1 \eta_2 t}{8 \eta_1} \quad (6.63)$$

The resulting Lax pair is again gives by Eqs. (6.59) with

$$f_1(x, t) = -\frac{i(4 c_2 x + 2 c_3 \lambda_1 t + c_2 \lambda_1 t^2 + 8 \lambda_1 f_x)}{8(\alpha_1 - 1) \eta_1}, \quad (6.64)$$

$$g_1(x, t) = \frac{i(4 c_3^2 \eta_2 + 4 c_2 c_3 \eta_3 t + c_2^2 \eta_4)}{64(\alpha_1 - 1) \eta_1^2}, \quad (6.65)$$

$$g_{10}(x, t) = \frac{\sqrt{a_0}}{8 \eta_1} (4 c_2 x + 2 c_3 \lambda_1 t + c_2 \lambda_1 t^2 - 8 \eta_1 f_x). \quad (6.66)$$

Here $\eta_1 = c_3 + c_2 t$, $\eta_2 = \lambda_1(\lambda_1 t^2 - 4x) - 4\lambda_0$, $\eta_3 = \eta_2 - 4\lambda_0$ and $\eta_4 = \lambda_1^2 t^4 - 8\lambda_1 x t^2 - 16\lambda_0 t^2 + 16x^2$. The Gross Pitaevskii equation corresponding to this case is

$$i \frac{\partial \psi(x, t)}{\partial t} + \frac{\partial^2 \psi(x, t)}{\partial^2 x} + \frac{1}{4}(\lambda_0 + \lambda_1 x) \psi(x, t) + \frac{2 a_0}{c_2 t + c_3} |\psi(x, t)|^2 \psi(x, t) = 0. \quad (6.67)$$

b. $\alpha_1 = 1$: For $\alpha = 1$, Eqs. (6.44)to Eqs. (6.49)reduce to

$$f_{1t} - g_{1x} = 0 \quad (6.68)$$

$$g_{10t} + \alpha_2 g_{10} + \sqrt{a_0(\alpha_3 + i\lambda^2/4 + \gamma/2 - i f_x^2 + \gamma_t t/2 + f_{xx})} = 0 \quad (6.69)$$

$$g_{10t} - \alpha_2 g_{10} - \sqrt{a_0(\alpha_3 + i\lambda^2/4 - \gamma/2 - i f_x^2 - \gamma_t t/2 - f_{xx})} = 0 \quad (6.70)$$

$$g_{10} - \iota \sqrt{a_0} \alpha_2 + 2 \sqrt{a_0} f_x = 0 \quad (6.71)$$

Subtracting Eqs. (6.69) and Eqs. (6.70) and substituting for g_{10x} using Eqs. (6.70), we get a second-order differential equation for $f(x)$, with a solution

$$f_x = (\gamma + \gamma_t t x^2/4 + c_2 x + c_1), \quad (6.72)$$

where c_1 and c_2 are the constants. Adding Eqs. (6.69) and Eqs. (6.70) and using the last equation to substitute for $f(x)$, we get

$$g_{10}(x, t) = 4 \alpha_3 + \iota \lambda(x)^2 - \iota (2 c_2 + \gamma x + \gamma_t t x)^2 \quad (6.73)$$

Substituting for $g_{10}(x, t)$ from the last equation and for $f(x)$ from Eqs. (6.72) into Eqs. (6.71), we obtain

$$\begin{aligned} & -4\iota \alpha_2^2 - 4 \alpha_3 + 8 \alpha_2 c_2 - \iota (\lambda_0 - 4c_2^2) + [-\iota \lambda_1 + 4(\alpha_2 \\ & + \iota c_2)(\gamma + \gamma_t t)]x^2 + [-\iota(\lambda_2^2 - \gamma^2 - 2\gamma \gamma_t t - \gamma_t^2 t^2)]x^2 = 0, \end{aligned} \quad (6.74)$$

Equating the first line of this equation to zero, we obtain $\alpha_2 = \alpha_3 = 0$ and $c_2 = \sqrt{a_0/2}$. Equating the coefficient of x to zero, we find

$$\gamma(t) = \frac{\lambda_2}{4 c_2} + \frac{c_1}{t} \quad (6.75)$$

and equating the coefficient of x^2 to zero, we get

$$\gamma(t) = \pm \lambda_2 + \frac{c_1}{t}. \quad (6.76)$$

Substituting this solution into equation Eqs. (6.72), the term $\gamma + \gamma_t$ vanishes and thus $f(x)$ becomes a function of x only as it should be. The last two equations indicate that $c_2 = \pm \lambda_1/4 \lambda_2 = \sqrt{\lambda_0}/2$. Eqs. (6.68) is decoupled from Eqs. (6.69) to Eqs. (6.73), and thus can be satisfied by setting an arbitrary expression for $f_1(x, t)$ and then solving for $g_1(x, t)$. Since the choice of $f_1(x, t)$ is arbitrary and will not affect the resulting Gross Pitaevskii equation, make the simple choice $f_1(x, t) = g_1(x, t) = 0$. The resulting Lax Pair is given by

$$U = \begin{pmatrix} 0 & \sqrt{a_0} Q \\ -\sqrt{a_0} Q^* & 0 \end{pmatrix}, \quad (6.77)$$

$$V = \begin{pmatrix} \iota a_0 |Q|^2 & \sqrt{a_0} [\iota Q_x + (\sqrt{\lambda_0} \pm \lambda_2 x) Q] \\ \sqrt{a_0} [\iota Q_x^* - (\sqrt{\lambda_0} \pm \lambda_2 x) Q^*] & -\iota a_0 |Q|^2 \end{pmatrix}, \quad (6.78)$$

where $Q(x, t) = \exp[(2c_1 + 2\iota \sqrt{\lambda_0} x \pm 2 \lambda_2 t \pm \iota \lambda_2 x^2)/4] \psi(x, t)$. The corresponding Gross Pitaevskii equation is calculated to be

$$\iota \frac{\partial \psi(x, t)}{\partial t} + \frac{\partial^2 \psi(x, t)}{\partial x^2} + \frac{1}{4} (\lambda_0 \pm \lambda_1 x)^2 \psi(x, t) + 2 a_0 \exp(c_3 \pm \lambda_2 t) |\psi(x, t)|^2 \psi(x, t) = 0. \quad (6.79)$$

Substituting $c_2 = 0$ and $f_x(x) = \lambda_2 x/2$ into equation Eqs. (6.59) and Eqs. (6.60) of the case $\alpha_1 \neq 1$, we obtain Eqs. (6.77) and Eqs. (6.78) of the present case with a positive sign of λ_2 . For $c_3 = 0$ and $f_x(x) = -\lambda_2 x/2$, we obtain equations Eqs. (6.77)-Eqs. (6.79) with the negative sign of λ_2 . Thus, Eqs. (6.77), Eqs. (6.79) are just special cases of Eqs. (6.59), Eqs. (6.60) and Eqs. (6.61).

Seed solution: we derive a solution of the general Gross Pitaevskii equation [113], Eqs. (6.29), to be used as a seed to the Darboux transformation. This can be achieved by writing $\psi(x, t)$ in the form

$$\psi(x, t) = A \exp[h_1(x, t) + i h_2(x, t)], \quad (6.80)$$

where A is a real constant and $h_1(x, t)$ and $h_2(x, t)$ are the real functions. Substituting this expression for $\psi(x, t)$ into Eqs. (6.29), the real and imaginary parts are

$$8 A^2 \exp(2 h_1) a_0 \gamma(t) + \lambda(x)^2 - 4 (h_{2t} - h_{1x}^2 + h_{2x}^2 - h_{1xx}), \quad (6.81)$$

$$h_{1t} + 2 h_{1x} h_{2x} + h_{2xx} = 0. \quad (6.82)$$

Using the assumption $h_1(x, t) = h_1(t)$, the last two equations simplify to

$$8 A^2 \exp(2 h_1) a_0 \gamma(t) + \lambda(x)^2 - 4 (h_{2t} + h_{2x}^2), \quad (6.83)$$

$$h_{1t} + h_{2xx} = 0. \quad (6.84)$$

Solving the last equation for $h_2(x, t)$, we obtain

$$h_2(x, t) = c_1(t) + c_2(t)x - \frac{1}{2}x^2 h_{1t}. \quad (6.85)$$

Substituting this expression for h_2 into Eqs. (6.83) we get

$$8 A^2 \exp(2 h_1) a_0 \gamma(t) + \lambda(x)^2 - 4 [(c_2 - x h_{1t}^2)^2 + c_{1t} + x c_{2t} - \frac{1}{2}x^2 h_{1tt}], \quad (6.86)$$

This equation can be solved by expanding $\lambda(x)^2$, in powers of x , up to the second order, as in equation. Substituting this expression into Eqs. (6.86) and equating to zero the coefficients of x^0 , x^1 and x^2 , we obtain

$$\lambda_0 + 8 A^2 \exp(2 h_1) a_0 \gamma(t) - 4 c_2^2 - 4 c_{1t} = 0, \quad (6.87)$$

$$\lambda_1 + 8 c_2 h_{1t} - 4 c_{2t} = 0, \quad (6.88)$$

$$\lambda_2^2 - 4 h_{1t}^2 + 2 h_{1tt} = 0, \quad (6.89)$$

The solution of the last equation is

$$h_1(t) = c_4 - \frac{1}{2} \ln \cosh[\lambda_2(2c_3 + t)] = 0. \quad (6.90)$$

Substituting this solution into Eqs. (6.85), we get

$$c_2(t) = c_5 \operatorname{sech} \eta_1 + \frac{\lambda_1}{4 \lambda_2} \tanh \eta_1. \quad (6.91)$$

and Eqs. (6.84) leads to

$$c_1(t) = c_6 + \frac{1}{16 \lambda_2^3} \lambda_2 (c_7 - t) (\lambda_1^2 - 4 \lambda_0 \lambda_2^2) + 8 c_5 \lambda_1 \lambda_2 (\operatorname{sech} \eta_1 - \operatorname{sech} \eta_2) + (\lambda_1^2 - 16 c_5^2 \lambda_2^2) (\tanh \eta_1 - \tanh \eta_2) + 2 A^2 \exp(2c_4) g_0 \int_{c_7}^t (\gamma(t') \operatorname{sech}[2c_3 + t']) dt' \quad (6.92)$$

where $\eta_1 = \lambda_2(2c_3 + t)$, $\eta_2 = \lambda_2(2c_3 + c_7)$ and c_{3-7} are constants of integration. Having determined the unknown function $h_1(t)$ and $h_2(x, t)$, the seed solution take the form

$$\psi(x, t) = A \sqrt{\operatorname{sech}[\lambda_2(2c_3 + t)]} \exp c_4 + i [c_1(t) + c_2(t)x + \lambda_2 \tanh[\lambda_2(2c_3 + t)]x^2/4]. \quad (6.93)$$

where $c_1(t)$ and $c_2(t)$ are given by Eqs. (6.89) and Eqs. (6.88).

Darboux transformation of Gross-Pitaevskii equation:

we find the Lax pair and an exact solution of the dimensionless Gross Pitaevskii equation, known as the seed solution. Fortunately, the trivial solution can be used as a seed, leading to nontrivial solutions. Using the Lax pair and the seed solution, the linear system is then solved and the components of ψ are found. The new solution is expressed in terms of these components and the seed solution.

the Gross-Pitaevskii equation take the dimensionless form

$$i \frac{\partial \psi(x, t)}{\partial t} = \left[-\frac{1}{2} \frac{\partial^2}{\partial x^2} + \frac{1}{2} p(t) x^2 - a q(t) |\psi(x, t)|^2 \right] \psi(x, t). \quad (6.94)$$

where a is the scaled scattering length. The dimensionless general functions $p(t)$ and $q(t)$ are introduced to account for the time dependencies of the strengths of the trapping potential and the interatomic interaction. The equation is integrable only if $p(t)$ and $q(t)$ are related as follows: $p(t) = \ddot{\gamma}(t) - \dot{\gamma}(t)^2$ and $q(t) = \exp(\gamma(t))$, where $\gamma(t)$ is an arbitrary real function. Using Lax pair search method used in the previous section, we find the linear system which corresponds to the class of Gross-Pitaevskii equations we are interested in:

$$\psi_x = \zeta \cdot J \cdot \psi \Lambda + U \cdot \psi, \quad (6.95)$$

$$\psi_t = i \zeta^2 \cdot J \cdot \psi \cdot \Lambda \cdot \Lambda + \zeta (i U + x \gamma(t) J) \cdot \psi \cdot \Lambda + V \cdot \psi \quad (6.96)$$

where

$$\psi(x, t) = \begin{pmatrix} \psi_1(x, t) & \psi_2(x, t) \\ \phi_1(x, t) & \phi_2(x, t) \end{pmatrix}, \quad (6.97)$$

$$J = \begin{pmatrix} 1 & 0 \\ 0 & -1 \end{pmatrix}, \quad (6.98)$$

$$\Lambda = \begin{pmatrix} \lambda_1 & 0 \\ 0 & \lambda_2 \end{pmatrix}, \quad (6.99)$$

$$U = \begin{pmatrix} 0 & \sqrt{a_0}Q \\ -\sqrt{a_0}Q^* & 0 \end{pmatrix}, \quad (6.100)$$

$$V = \begin{pmatrix} i\sqrt{a}|Q|^2/2 & \sqrt{a}\lambda x\dot{\gamma}Q(x, t) + i\sqrt{a}Q_x(x, t)/2 \\ -\sqrt{a}\lambda x\dot{\gamma}Q(x, t)^* + i\sqrt{a}Q_x^*(x, t)/2 & -i\sqrt{a}|Q|^2/2 \end{pmatrix}, \quad (6.101)$$

$\zeta = \exp(\gamma(t))$, and λ_1 and λ_2 are arbitrary constants. Where $Q(x, t) = \psi(x, t) \exp(\gamma(t) + i\gamma(t)x^2)/2$. It should be emphasized that while applying the Darboux transformation is almost straightforward, finding a linear system that corresponds to the differential equation at hand is certainly not a trivial matter. Usually, this is found by trial and error, or by starting from a certain linear system and then finding the differential equation it corresponds to. In [113], Usama Al khawaja introduced a systematic approach to find the linear system which we describe here. The partial derivatives of the auxiliary field, ψ_x and ψ_t , are expanded in powers of Λ with unknown matrix coefficients. The expansions are terminated at the first order for ψ_x and the second order for ψ_t since this will be sufficient to generate the class of Gross Pitaevskii equations under consideration. The higher order matrix coefficients turn out to be essentially determined by the zeroth-order matrix coefficients U and V . To find the matrices U and V , we expand them in powers of the wavefunction $\psi(x, t)$, its complex conjugate, and their partial derivatives. The coefficients of the expansions are unknown functions of x and t . Substituting these expansions in the consistency condition we find a set of equations for the unknown function coefficients. Finally, by solving these equations the Lax pair and consequently the linear system will be determined. For ψ to be a solution of both equations Eqs. (6.95) and Eqs. (6.96), the consistency condition $\psi_{xt} = \psi_{tx}$ must be satisfied. This condition leads to the following relation between the matrices U and V :

$$U_t - V_x + [U, V] = 0 \quad (6.102)$$

Where $[U, V]$ is the commutator of U and V . Substituting the above expressions for U and V in the last equation, we obtain the Gross-Pitaevskii equation

$$i\frac{\partial}{\partial t}\psi(x, t) = \left[-\frac{1}{2}\frac{\partial^2}{\partial x^2} + \frac{1}{2}(\ddot{\gamma}(t) - \dot{\gamma}(t))x^2\psi(x, t) - a \exp^{\gamma(t)} |\psi(x, t)|\right], \quad (6.103)$$

and its complex conjugate. This equation shows that the functions $p(t)$ and $q(t)$ are related to each other through the general function $\gamma(t)$. We focus here on the specific case of only a harmonic trapping potential and constant dispersion. The linear system of eight equations, Eqs. (6.95) and Eqs. (6.96) read explicitly,

$$\psi_{1x} - \phi_1 \sqrt{a} \exp^{\frac{1}{2}(\imath \dot{\gamma} x^2 + \gamma)} \psi_0 - \sqrt{2} \lambda_1 \psi_1 \exp^\gamma = 0 \quad (6.104)$$

$$\psi_{2x} - \phi_2 \sqrt{a} \exp^{\frac{1}{2}(\imath \dot{\gamma} x^2 + \gamma)} \psi_0 - \sqrt{2} \lambda_1 \psi_2 \exp^\gamma = 0 \quad (6.105)$$

$$\phi_{1x} + \sqrt{2} \lambda_1 \exp^\gamma \phi_1 + \psi_0^* \psi_1 \sqrt{a} \exp^{\frac{1}{2}(\gamma - \imath x^2 \dot{\gamma})} = 0 \quad (6.106)$$

$$\phi_{2x} + \sqrt{2} \lambda_2 \exp^\gamma \phi_2 + \psi_0^* \psi_2 \sqrt{a} \exp^{\frac{1}{2}(\gamma - \imath x^2 \dot{\gamma})} = 0 \quad (6.107)$$

$$\begin{aligned} & \psi_{1t} - \imath \psi_1 \exp^\gamma (2 \exp^\gamma \lambda_1^2 - \imath \sqrt{2} x \dot{\gamma} \lambda_1 + \frac{1}{2} |\psi_0|^2 a) \\ & - \frac{1}{2} \phi_1 \sqrt{a} \exp(\frac{1}{2}(\imath \dot{\gamma} x^2 + \gamma)) (\imath \psi_{0x} + \psi_0 (2 \imath \sqrt{2} \exp(\gamma) \lambda_1 + x \dot{\gamma})) = 0, \end{aligned} \quad (6.108)$$

$$\begin{aligned} \psi_{2t} - \imath \psi_2 \exp^\gamma (2 \exp^\gamma \lambda_2^2 - \imath \sqrt{2} x \dot{\gamma} \lambda_2 + \frac{1}{2} |\psi_0|^2 a) - \frac{1}{2} \phi_2 \sqrt{a} \exp(\frac{1}{2}(\imath \dot{\gamma} x^2 + \gamma)) (\imath \psi_{0x} \\ + \psi_0 (2 \imath \sqrt{2} \exp(\gamma) \lambda_2 + x \dot{\gamma})) = 0 \end{aligned} \quad (6.109)$$

$$\begin{aligned} \phi_{1t} + \frac{1}{2} \psi_1 \sqrt{a} \exp^{\frac{1}{2}(\gamma - \imath x^2 \dot{\gamma})} (\psi_0^* (2 \imath \sqrt{2} \exp^\gamma \lambda_1 + x \dot{\gamma}) - \imath \psi_{0x}^*) + \frac{1}{2} \phi_1 \exp^\gamma (\imath |\psi_0|^2 a \\ + 2 \lambda_1 (2 \imath \exp^\gamma \lambda_1 + \sqrt{2} x \dot{\gamma})) = 0 \end{aligned} \quad (6.110)$$

$$\begin{aligned} \phi_{2t} + \frac{1}{2} \psi_2 \sqrt{a} \exp^{\frac{1}{2}(\gamma - \imath x^2 \dot{\gamma})} (\psi_0^* (2 \imath \sqrt{2} \exp^\gamma \lambda_2 + x \dot{\gamma}) - \imath \psi_{0x}^*) + \frac{1}{2} \phi_2 \exp^\gamma (\imath |\psi_0|^2 a \\ + 2 \lambda_2 (2 \imath \exp^\gamma \lambda_2 + \sqrt{2} x \dot{\gamma})) = 0 \end{aligned} \quad (6.111)$$

Where $\psi_0(x, t)$ is an exact seed solution of Eqs. (6.98). These equations reduce to an equivalent system of four equations with nontrivial solution by making the following substitutions: $\lambda_1 = -\lambda_2^*$, $\psi_2 = \phi_1^*$ and $\phi_2 = -\psi_1^*$. Using the trivial solution, $\Psi_0(x, t) = 0$, as seed, the linear system will have the solution

$$\psi_1(x, t) = c_1 \exp^{(2i\lambda_1^2)} \int \exp^{(2\gamma(t))} dt + \exp^{\gamma(t)} \lambda_1 x \quad (6.112)$$

where c_1 and c_2 are real arbitrary constants of integration.

Consider the following version of the Darboux transformation[36]:

$$\psi[1] = \psi.\Lambda - \sigma \psi, \quad (6.113)$$

Eqs. (6.99-Eqs. (6.106. For the transformation field $\psi[1]$ to be a solution of the linear system, the matrix U for instance must be transformed as

$$U[1] = \sigma.U.\sigma^{-1} + \sigma_x.\sigma^{-1}, \quad (6.114)$$

Where σ^{-1} is the inverse of σ .This equation gives the new solution in terms of the seed solutions of the Gross Pitaevskii equation, $\psi_0(x, t)$, and the linear system, ψ_0 ,which reads

$$\psi(x, t) = \psi_0(x, t) + \frac{2}{a}(\lambda_1 + \lambda_1^*) \exp^{-i\gamma(t)x^2/4+\gamma(t)/2} \frac{\phi_1 \psi_1^*}{|\phi_1|^2 + |\psi_1|^2} \quad (6.115)$$

Chapter 7

Solitonic Solution of higher-order nonlinear Schrödinger equations

7.1 Introduction

The nonlinear Schrödinger equation (NLSE) plays a vital role in different fields of science, e.g., physics, chemistry, biology, etc [25]. In physics NLSEs describe the dynamics of optical pulses in dielectric media or optical fibers[26], matter waves in Bose-Einstein condensates[27], solitary and rogue waves in the ocean [28]. The discovery of integrability of this equation by Zakharov and Shabat in 1971 has made a big impact on the studies of all these areas. Complete integrability of the NLSE through the existence of a pair of matrices, known as Lax pair [50], which are functionals of the solution of the NLSE and its time and space derivatives [29]. In fiber optics, where solitons are the data carriers, one of the most important challenges is to increase the bit-rate by stacking as much solitons as possible along the fiber. This requires to use femto-second solitons, which have shorter pulse widths. Due to the short pulse width, higher-order effect such as third order dispersion, Raman scattering, self-steepening, etc., become important. As a result the higher-order terms describing the mentioned effects are to be included in the NLSE to correctly describe the propagation of optical pulses in optical fibers. Therefore, it is necessary to solve NLSEs with higher-order terms. In this chapter, we derive the solitonic solution of the nonlinear Schrödinger equation with higher-order terms, complex external potentials, and time dependent coefficients by applying the Darboux transformation this end need to find first the Lax Pairs and integrability conditions. The solution for some of the well-known nonlinear Schrödinger equation are then derived as special cases such as Nonlinear Schrödinger equation, NLSE, Hirota equation, HE, Sasa-Satsuma equation, SSE. In the following we use a systematic search approach to calculate the Lax pairs of HNLSE with cubic nonlinearity

7.2 A Systematic search approach to find the Lax pair

In this section we consider the most general NLSE with qubic nonlinearity [32, 33, 34, 26, 35]. In the presence of damping or gain and external potential, the general NLSE can be written as

$$i \psi_t + a_1 \psi_{xx} + a_2 |\psi|^2 \psi + i a_3 \psi_{xxx} + i a_4 |\psi|^2 \psi_x + i a_5 \psi^2 \psi_x^* + i \Gamma \psi + V_{ext} \psi = 0. \quad (7.1)$$

In Refs. [36, 37]. Here all the coefficients $a_i \equiv a_i(t)$ are initially assumed to be complex functions of time, but it turns out that integrability restricts them to be real. The functions $V_{ext} \equiv V_{ext}(x, t)$ and $\Gamma \equiv \Gamma(t)$ are real and account for the external potential and the damping or gain in the system, respectively. Equation Eq. (7.1) describes the evolution of the electric field envelope of an optical pulse through an optical fiber. The second term denotes the chromatic or group velocity dispersion, the third term denotes the Kerr nonlinearity or self phase modulation (arises due to intensity dependent refractive index), and the fourth term denotes the third-order dispersion. The fifth and the sixth terms are related to the self steepening and self-frequency shift due to the Raman scattering. The Lax pair is the most important ingredient in solving a NLSE using the DT. The method is described in the previous chapter here we summarize the basic equations explained before there is only difference by put the third order of Λ in the equation of ψ_t because HNLSE is solved only if Λ is 3×3 matrices. In order to derive the Lax pair we start by writing the following two equations

$$\Psi_x = \mathbf{U}_0 \cdot \Psi + \mathbf{U}_1 \cdot \Psi \cdot \Lambda \quad (7.2)$$

and

$$\Psi_t = \mathbf{V}_0 \cdot \Psi + \mathbf{V}_1 \cdot \Psi \cdot \Lambda + \mathbf{V}_2 \cdot \Psi \cdot \Lambda^2 + \mathbf{V}_3 \cdot \Psi \cdot \Lambda^3 \quad (7.3)$$

for an auxiliary field Ψ . Here subscripts t and x represent the derivative with respect to time and position, respectively. The matrices \mathbf{U}_0 , \mathbf{U}_1 , \mathbf{V}_0 , \mathbf{V}_1 , \mathbf{V}_2 , and \mathbf{V}_3 are functions of the solution of the given NLSE and its space derivatives. The matrix Λ denotes the spectral parameters and is given by

$$\Lambda = \begin{pmatrix} \lambda_1 & 0 & 0 \\ 0 & \lambda_2 & 0 \\ 0 & 0 & \lambda_3 \end{pmatrix}, \quad (7.4)$$

The order of the matrices depends on the NLSE to be solved as will be seen next. The compatibility condition $\Psi_{xt} = \Psi_{tx}$, which leads to the following set of equations

$$\mathbf{U}_{0t} - \mathbf{V}_{0x} + [\mathbf{U}_0, \mathbf{V}_0] = \mathbf{0}, \quad (7.5)$$

$$\mathbf{U}_{1t} - \mathbf{V}_{1x} + [\mathbf{U}_0, \mathbf{V}_1] + [\mathbf{U}_1, \mathbf{V}_0] = \mathbf{0}, \quad (7.6)$$

$$\mathbf{V}_{2x} + [\mathbf{V}_2, \mathbf{U}_0] + [\mathbf{V}_1, \mathbf{U}_1] = \mathbf{0}, \quad (7.7)$$

$$\mathbf{V}_{3x} + [\mathbf{V}_3, \mathbf{U}_0] + [\mathbf{V}_2, \mathbf{U}_1] = \mathbf{0}, \quad (7.8)$$

$$[\mathbf{V}_3, \mathbf{U}_1] = \mathbf{0}, \quad (7.9)$$

Existence of the Lax pair assures the integrability of the given NLSE, i.e., the given NLSE can be solved analytically. In Ref [113], the author devised a systematic approach to find the Lax pair. In this approach, the Lax pair \mathbf{U}_0 and \mathbf{V}_0 is constructed in terms of ψ the solution of the NLSE and its time and position derivatives with unknown coefficients up to a certain order depending on the given NLSE. By equating the compatibility condition matrix, Eq. (7.5), and the matrix constructed from the original NLSE, we get a set of equations for the unknown coefficients in \mathbf{U}_0 and \mathbf{V}_0 in terms of the coefficients of the original NLSE. Solving this set of equations gives \mathbf{U}_0 and \mathbf{V}_0 for the given NLSE.

In the second step, we construct arbitrary \mathbf{U}_1 and \mathbf{V}_1 as we do for \mathbf{U}_0 and \mathbf{V}_0 . Using the second compatibility condition, Eq. (7.6), we get a set of equations for the unknown coefficients. By solving this set of equations for unknown coefficients, we get \mathbf{U}_1 and

\mathbf{V}_1 . In the same manner we find the matrix \mathbf{V}_2 by solving the two compatibility conditions, Eq (7.7) and Eq (7.8) by solving the last equation we get \mathbf{V}_3 . Employing the systematic search approach we find the complete set of matrices for Eq. (7.1):

$$\mathbf{U}_0 = \begin{pmatrix} 0 & -c_3 e^{-G} \psi & c_3 e^G \psi^* \\ c_3 e^G \psi^* & 0 & 0 \\ -c_3 e^{-G} \psi & 0 & 0 \end{pmatrix}, \quad (7.10)$$

$$\mathbf{U}_1 = \begin{pmatrix} c_1 & 0 & 0 \\ 0 & c_1 + c_2 & 0 \\ 0 & 0 & c_1 + c_2 \end{pmatrix}, \quad (7.11)$$

$$\mathbf{V}_0 = \begin{pmatrix} v_{011} & v_{012} & v_{013} \\ v_{021} & v_{022} & v_{023} \\ v_{031} & v_{032} & v_{033} \end{pmatrix}, \quad (7.12)$$

where

$$\begin{aligned} v_{011} &= v_{023} = v_{032} = 0, \\ v_{012} &= v_{031} = \frac{i c_3^3 e^{-G} (Q_1 + Q_2)}{9\sqrt{2} a_2 a_3}, \\ v_{013} &= v_{021} = \frac{i c_3^3 e^{-G} (Q_1^* + Q_2^*)}{9\sqrt{2} a_2 a_3}, \\ v_{022} &= \frac{a_2}{6 a_1} (3 a_3 [\psi^* \psi_x - \psi \psi_x^*] - 2 i a_1 |\psi|^2), \\ v_{033} &= \frac{a_2}{6 a_1} (3 a_3 [\psi \psi_x^* - \psi_x \psi^*] + 2 i a_1 |\psi|^2), \end{aligned}$$

here

$$\begin{aligned} Q_1 &= 18 a_2 a_3^2 |\psi|^2 \psi + 2 a_1^3 \psi, \\ Q_2 &= 9 a_1 a_3^2 \psi_{xx} - 6 i a_1^2 a_3 \psi_x, \end{aligned}$$

$$\mathbf{V}_1 = \begin{pmatrix} v_{111} & v_{112} & v_{113} \\ v_{121} & v_{122} & v_{123} \\ v_{131} & v_{132} & v_{133} \end{pmatrix}, \quad (7.13)$$

$$v_{111} = \frac{c_2 a_2 a_3 |\psi|^2}{a_1} + \frac{c_2 a_1^2}{6 a_3},$$

$$v_{112} = \frac{1}{3\sqrt{2}} c_2 c_3 e^{-G} (a_1 \psi + 3 i a_3 \psi_x) \quad (7.14)$$

$$v_{113} = \frac{1}{3\sqrt{2}} c_2 c_3 e^G (a_1 \psi^* - 3 i a_3 \psi_x^*) \quad (7.15)$$

$$v_{121} = -\frac{1}{3\sqrt{2}} c_2 c_3 e^G (a_1 \psi^* - 3i a_3 \psi_x^*) \quad (7.16)$$

$$v_{122} = -\frac{c_2}{6 a_1 a_3} (a_1^3 + 3 a_2 a_3^2 |\psi|^2) \quad (7.17)$$

$$v_{123} = \frac{c_2}{2 a_1} e^{2G} a_2 a_3 (\psi^*)^2 \quad (7.18)$$

$$v_{131} = -\frac{1}{3\sqrt{2}} c_2 c_3 e^{-G} (a_1 \psi + 3i a_3 \psi_x) \quad (7.19)$$

$$v_{132} = \frac{c_2}{2 a_1} e^{-2G} a_2 a_3 \psi^2 \quad (7.20)$$

$$v_{133} = -\frac{c_2}{6 a_1 a_3} (a_1^3 + 3 a_2 a_3^2 |\psi|^2) \quad (7.21)$$

$$\mathbf{V}_2 = \begin{pmatrix} c_4 & -i c_2^2 c_3 a_3 e^{-G} \psi & i c_2^2 c_3 a_3 e^G \psi^* \\ i c_2^2 c_3 a_3 e^G \psi^* & c_4 & 0 \\ -i c_2^2 c_3 a_3 e^{-G} \psi & 0 & c_4 \end{pmatrix}, \quad (7.22)$$

and

$$\mathbf{V}_3 = \begin{pmatrix} c_2^3 a_3 + c_5 & 0 \\ 0 & c_5 & 0 \\ 0 & 0 & c_5 \end{pmatrix}. \quad (7.23)$$

Here, $c_2 = \sqrt{2 a_5 - a_4 / (6 a_3)}$, $c_3 = \sqrt{a_5 / (2 a_3)}$, $c_5 = -(2 c_2^2 a_1 + a_2) / a_5$, and $G = i a_1 x / (3 a_3)$, and c_1 is a arbitrary time-independent constant. When we use \mathbf{U}_0 and \mathbf{V}_0 in Eq. (7.5) we get back Eq. (7.1) with

$$\Gamma = \frac{\dot{a}_2}{2 a_2} - \frac{\dot{a}_1}{2 a_1} \quad (7.24)$$

and

$$V_{ext} = \frac{a_3 \dot{a}_1 - a_1 \dot{a}_3}{3 a_3^2} x + \frac{2 a_1^3}{27 a_3^2}. \quad (7.25)$$

The remaining two integrability conditions are

$$a_4 = \frac{9 a_2 a_3}{2 a_1} \quad (7.26)$$

and

$$a_5 = \frac{3 a_2 a_3}{2 a_1}. \quad (7.27)$$

Therefore Eq. (7.1) is integrable only with three independent parameters a_1 , a_2 , and a_3 . One point worths mentioning here is that the damping or gain, Γ , and the linear part of the potential, V_{ext} , arise due to the time variation of the coefficients a_1 , a_2 , and a_3 .

7.3 Darboux transformation

Applying the DT describing in the previous chapter on the Lax pair of Eq. (7.1) and using zero as a trivial seed solution the following solitonic solution can be derived

$$\psi(x, t) = \frac{A}{\cosh(2x - b)} e^{i \frac{a_1}{3a_3} (x + \frac{\pi}{2})}, \quad (7.28)$$

where $A = 2\sqrt{a_1/a_2}$ and

$$b = \int \left(\frac{2a_1^2}{3a_3} + 8a_3 \right) dt - \frac{1}{2} \log 2. \quad (7.29)$$

The amplitude A depends on the ratio of the coefficients of the chromatic dispersion and the nonlinearity. The phase is position dependent and depends on the ratio of the coefficients of the chromatic and third-order dispersions. For repulsive interaction, i.e., $a_2 < 0$, the equation supports diverging solutions, one of which is given by

$$\psi(x, t) = \frac{A}{\sinh(2x - b)} e^{i \frac{a_1}{3a_3} (x + \frac{\pi}{2})}, \quad (7.30)$$

where $A = 2\sqrt{-a_1/a_2}$ and b is given by Eq. (7.29).

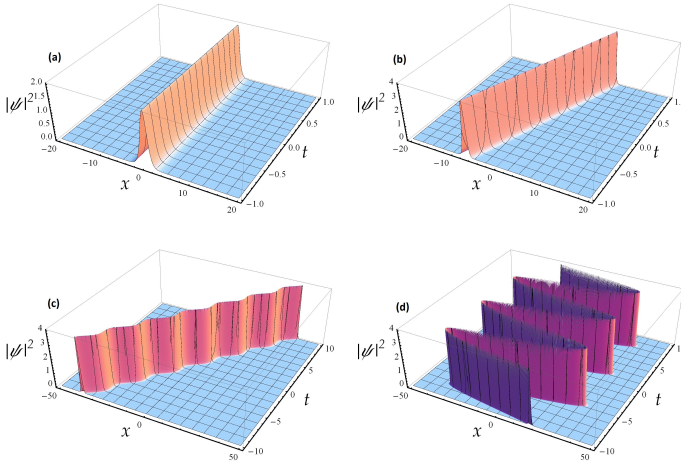


Figure 7.1: (Color online) (a) Solitonic solution of HNSLE with constant coefficients, $a_1 = 1$ and $a_2 = 1$. (b) The solution of Eq. (9) with constant coefficients, namely, $a_1 = 1$, $a_2 = 1$, and $a_3 = 0.05$. (c) Trigonometric time dependence for $a_1 = \cos(t)$, $a_2 = \cos(t)$ and constant third order dispersion $a_3 = 0.05$. (d) All the three coefficients are trigonometric time dependent $a_1 = \cos(t)$, $a_2 = \cos(t)$, and $a_3 = 0.05 \cos(t)$.

In both the attractive and repulsive cases the third-order dispersion coefficient controls the phase of the envelope. One important factor to note that the self steepening and the Raman scattering terms arise due to the third-order dispersion through the relations given by Eqs. (7.26) and (7.27). The group velocity of the envelope, depends on the coefficients a_1 and a_3 . Therefore, we can control the group velocity i.e., the center of mass motion of the soliton, by properly choosing the chromatic dispersion and the third-order dispersion. This interesting fact can be used to manipulate soliton motion without the need of an external potential.

Figure 1 shows the solitonic solutions given by Eq. (14). For comparison, Fig. 1(a) shows the solitonic solution of NLSE with constant coefficients, i.e., without any damping and external potential. In Fig. 1(b), we choose all the three coefficients a_1 - a_3 be time independent and take a_3 very small compared to a_1 and a_2 . In this particular case $\Gamma = 0$ and $V_{ext} = 2a_1^2/27a_3^2$ and the center of mass velocity of the soliton is a constant. We assume trigonometric time dependence for a_1 and a_2 [35] and constant a_3 in Fig. 1(c). The soliton moves with a constant velocity with oscillation around it. In Fig. 1(d), we assume all the coefficients be trigonometric time dependent and the center of mass velocity oscillates. From Figs. 1(b) -(c), it is obvious that the center of mass velocity can be controlled by appropriate choice of the third order dispersion coefficient a_3 .

In the next Section the solution, Lax pairs and integrability conditions for some of the well-known nonlinear Schrödinger equations are then derived as special cases such as , NLSE equation, Hirota equation (HE), and Sasa-Satsuma equation (SSE), we use in all cases seed solution equal to zero .

7.4 Special cases

1. Nonlinear Schrödinger equation, NLSE: If we set $a_3 = a_4 = a_5 = 0$ in Eq. (7.1) we get the standard NLSE or GPE with damping or gaining and potential, which can be written as

$$i\psi_t + a_1\psi_{xx} + a_2|\psi|^2\psi + i\Gamma\psi + V_{ext}\psi = 0. \quad (7.31)$$

This is one of the most well-known NLSEs in the optical [26], Bose-Einstein [27], and ocean wave communities [28]. The Lax pair for Eq. (7.31)with time-independent coefficient and without damping and potential was first found by Zakharov and Shabat [38] and was then widely used in the Darboux transformation to find exact solutions. The damping is given by $\Gamma = \dot{a}_2/(2a_2) - \dot{a}_1/(2a_1)$ and the potential is given by $V_{ext} = c_1^2 a_1 - \dot{c}_1 x$.

$$\mathbf{U}_0 = \begin{pmatrix} 0 & -c_4(t) e^G \psi(x, t) \\ -c_4(t) e^{-G} \psi^*(x, t) & 0 \end{pmatrix}, \quad (7.32)$$

$$\mathbf{V}_0 = \begin{pmatrix} \frac{i}{2} a_2(t) |\psi(x, t)|^2 & -c_4(t) e^G [c_1(t) \psi(x, t) + i \psi_x(x, t)] \\ c_4(t) e^{-G} [c_1(t) \psi^*(x, t) + i \psi_x^*(x, t)] & -\frac{i}{2} a_2(t) |\psi(x, t)|^2 \end{pmatrix}, \quad (7.33)$$

$$\mathbf{U}_1 = \begin{pmatrix} c_2 & 0 \\ 0 & c_2 + c_3 \end{pmatrix}, \quad (7.34)$$

$$\mathbf{V}_1 = \begin{pmatrix} -c_3 c_1(t) a_1(t) & i c_3 c_4(t) e^G \psi(x, t) \\ -i c_3 c_4(t) e^{-G} \psi^*(x, t) & c_3 c_1(t) a_1(t) \end{pmatrix}, \quad (7.35)$$

and

$$\mathbf{V}_2 = \begin{pmatrix} \frac{1}{2} i c_3^2 a_1(t) & 0 \\ 0 & -\frac{1}{2} i c_3^2 a_1(t) \end{pmatrix}, \quad (7.36)$$

where $c_4(t) = \sqrt{\frac{a_2(t)}{2a_1(t)}}$ and $G = i c_1(t) x$. Here $c_1(t)$ is a time-dependent parameter and c_2 and c_3 are two time-independent constants.

Using the DT Eq. (7.1) supports solitonic solutions, one such solutions is given by

$$\psi(x, t) = \frac{A}{\cosh[c_3 x + b]} e^{i[c_3^2 \int a_1 dt - c_1 x]}, \quad (7.37)$$

where $A = -4 c_3 \sqrt{2 a_1/a_2}$ and $b = \sqrt{2} c_3 \int c_1 a_1 dt$. Similar results are also found by H. Kumar *et al.* [39]. U. Al Khawaja found solution of Eq. (7.31) with quadratic potential, periodic potential, and different types of solution with linear potential. It is well-known

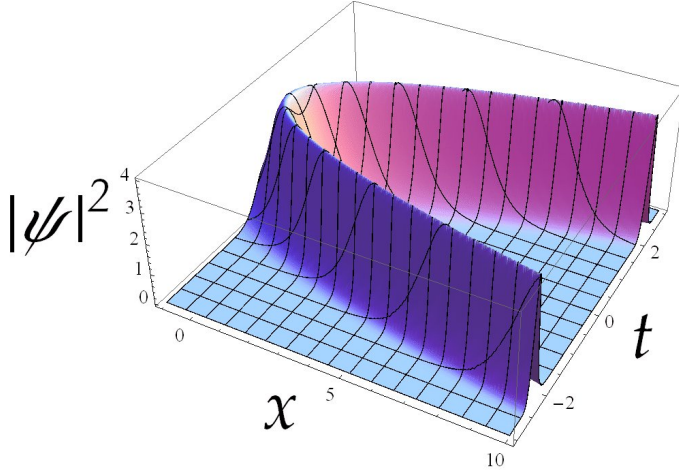


Figure 7.2: Solitonic solution of NLSE with constant coefficients, $a_1 = 2$, $a_2 = 1$

that the NLSE or GPE with time-dependent coefficients is integrable with potential up to quadratic power in x [51, 47]. Here, we find the Lax pair for NLSE with linear potential $V_{ext} = c_1^2 a_1 - c_1 x$; this is due to the fact that we derive the Lax pair for the NLSE from that of the higher-order NLSE with cubic-quintic nonlinearity by taking appropriate limit of $a_3 = a_4 = a_5 = a_6 = 0$. The higher-order terms in higher-order NLSE restrict integrability to linear potentials. One of the original motivations of our work is to solve the most general NLSE with cubic-quintic nonlinearity and find the solutions for other well-known NLSE as special cases. However, we find that general NLSE with cubic-quintic nonlinearity is not solvable in the Lax pair sense.

2. Hirota equation, HE: If we set $a_5 = 0$ in Eq. (7.1) we get the HE [40], namely,

$$i \psi_t + a_1 \psi_{xx} + a_2 |\psi|^2 \psi + i a_3 \psi_{xxx} + i a_4 |\psi|^2 \psi_x + i \Gamma \psi + V_{ext} \psi = 0. \quad (7.38)$$

In this case we find that the equation is integrable only if $a_4 = 3 a_2 a_3/a_1$, $\Gamma = a_4/(2 a_4) - a_3/(2 a_3)$, and $V_{ext} = 0$.

The Lax pair and the all set of matrices for Hirota equation is given by

$$\mathbf{U}_0 = \begin{pmatrix} 0 & c_2(t) \psi(x, t) \\ -c_2(t) \psi^*(x, t) & 0 \end{pmatrix}, \quad (7.39)$$

$$\mathbf{V}_0 = \begin{pmatrix} v_{011} & v_{012} \\ v_{021} & v_{022} \end{pmatrix}, \quad (7.40)$$

where

$$v_{011} = c_2^2(t) \left\{ a_3(t) [\psi(x, t) \psi_x^*(x, t) - \psi_x(x, t) \psi^*(x, t)] + i a_1(t) |\psi(x, t)|^2 \right\},$$

$$v_{012} = -c_2(t) \left[\frac{a_2(t) a_3(t)}{a_1(t)} |\psi(x, t)|^2 \psi(x, t) - i a_1(t) \psi_x(x, t) + a_3(t) \psi_{xx}(x, t) \right],$$

$$v_{021} = c_2(t) \left[\frac{a_2(t) a_3(t)}{a_1(t)} |\psi(x, t)|^2 \psi^*(x, t) + i a_1(t) \psi_x^*(x, t) + a_3(t) \psi_{xx}^*(x, t) \right],$$

and

$$v_{022} = c_2^2(t) \left\{ a_3(t) [\psi_x(x, t) \psi^*(x, t) - \psi(x, t) \psi_x^*(x, t)] - i a_1(t) \psi(x, t) \psi^*[x, t] \right\}.$$

$$\mathbf{U}_1 = \begin{pmatrix} -\sqrt{\frac{3}{2}} c_1 & 0 \\ 0 & \sqrt{\frac{3}{2}} c_1 \end{pmatrix}, \quad (7.41)$$

$$\mathbf{V}_1 = \begin{pmatrix} c_1 c_2(t) \sqrt{3 a_3(t)} |\psi(x, t)|^2 & \sqrt{6} c_1 c_2(t) [a_3(t) \psi_x(x, t) - i a_1(t) \psi(x, t)] \\ \sqrt{6} c_1 c_2(t) [a_3(t) \psi_x^*(x, t) + i a_1(t) \psi^*(x, t)] & -c_1 c_2(t) \sqrt{3 a_3(t)} |\psi(x, t)|^2 \end{pmatrix}, \quad (7.42)$$

$$\mathbf{V}_2 = \begin{pmatrix} 3 i c_1^2 a_1(t) & -6 c_1^2 c_2(t) a_3(t) \psi(x, t) \\ 6 c_1^2 c_2(t) a_3(t) \psi^*(x, t) & -3 i c_1^2 a_1(t) \end{pmatrix}, \quad (7.43)$$

and

$$\mathbf{V}_3 = \begin{pmatrix} 3\sqrt{6} c_1^3 a_3(t) & 0 \\ 0 & -3\sqrt{6} c_1^3 a_3(t) \end{pmatrix}. \quad (7.44)$$

Here $c_1(t)$ is time-dependent constant and $c_2(t) = \sqrt{\frac{a_2(t)}{2 a_1(t)}}$.

Using the DT the one-soliton solution of the HE is given by

$$\psi(x, t) = \frac{A}{\cosh[\sqrt{6} x - b]} e^{6 i \int a_1 dt}, \quad (7.45)$$

where $A = -12 \sqrt{a_3/a_4}$ and $b = 6\sqrt{6} \int a_3 dt$. Similar result was also found by C. Dai *et al.* [41].

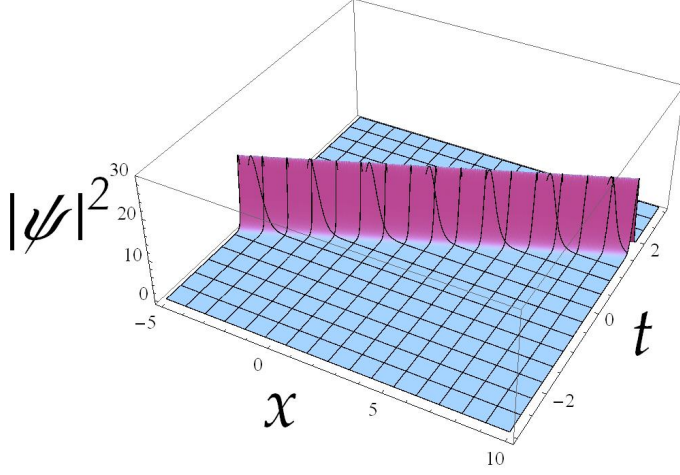


Figure 7.3: Solitonic solution of HE with constant coefficients, $a_1 = 1$, $a_2 = 1$ and $a_3 = 2$

3. Sasa-Satsuma equation, SSE:

Recent progress in the theory of integrable partial differential equations made a revolution in mathematics and expanded significantly the areas of physical application of these equations. Sasa-Satsuma equation (SSE) is one of the integrable extensions of the nonlinear Schrödinger equation (NLSE). Although with fixed relation between higher order terms, it contains the most essential contributions often found in various physical applications: deep water waves and pulse propagation in optical fibres. Namely, it contains the term with third order dispersion, the term with self-frequency shift and the term describing self steepening. These are the most general terms that have to be taken into account when extending the applicability of the NLSE.

If we set $a_1 = a_2 = 0$ in Eq. (7.1) we get the SSE [42], namely,

$$i \psi_t + i a_3 \psi_{xxx} + i a_4 |\psi|^2 \psi_x + i a_5 \psi^2 \psi_x^* + i \Gamma \psi + V_{ext} \psi = 0. \quad (7.46)$$

We find that the SSE is integrable for arbitrary values of a_3 , a_4 , and a_5 with $a_4 \neq 2 a_5$ and $\Gamma = V_{ext} = 0$.

For SSE, the set of matrices is given by

$$\mathbf{U}_0 = \begin{pmatrix} 0 & -i \frac{a_5}{3 a_3} \psi(x, t) & i \frac{a_5}{3 a_3} \psi^*(x, t) \\ -i \psi^*(x, t) & 0 & 0 \\ i \psi(x, t) & 0 & 0 \end{pmatrix} \quad (7.47)$$

$$\mathbf{U}_1 = \begin{pmatrix} c_1 & 0 & 0 \\ 0 & c_1 + c_2 & 0 \\ 0 & 0 & c_1 + c_2 \end{pmatrix} \quad (7.48)$$

$$\mathbf{V}_0 = \begin{pmatrix} v_{011} & v_{012} & v_{013} \\ v_{021} & v_{022} & v_{023} \\ v_{031} & v_{032} & v_{033} \end{pmatrix}, \quad (7.49)$$

where

$$v_{011} = v_{023} = v_{032} = 0 \quad (7.50)$$

$$v_{012} = \frac{i a_5}{9 a_3} [4 a_5 |\psi(x, t)|^2 \psi(x, t) + 3 a_3 \psi_{xx}(x, t)],$$

$$v_{013} = -\frac{i a_5}{9 a_3} [4 a_5 |\psi(x, t)|^2 \psi^*(x, t) + 3 a_3 \psi_{xx}^*(x, t)],$$

$$v_{021} = \frac{i}{3} [4 a_5 |\psi(x, t)|^2 \psi^*(x, t) + 3 a_3 \psi_{xx}^*(x, t)],$$

$$v_{022} = \frac{1}{3} a_5 [\psi_x(x, t) \psi^*(x, t) - \psi(x, t) \psi_x^*(x, t)],$$

$$v_{031} = -\frac{i}{3} [4 a_5 |\psi(x, t)|^2 \psi(x, t) + 3 a_3 \psi_{xx}(x, t)],$$

$$v_{033} = -\frac{1}{3} a_5 [\psi_x(x, t) \psi^*[x, t] - \psi(x, t) \psi_x^*(x, t)].$$

$$\mathbf{V}_1 = \begin{pmatrix} \frac{2}{3} c_2 a_5 |\psi(x, t)|^2 & -\frac{i}{3} c_2 a_5 \psi_x(x, t) & \frac{i}{3} c_2 a_5 \psi_x^*(x, t) \\ i c_2 a_3 \psi_x^*(x, t) & -\frac{1}{3} c_2 a_5 |\psi(x, t)|^2 & \frac{1}{3} c_2 a_5 \psi^{*2}(x, t) \\ -i c_2 a_3 \psi_x(x, t) & \frac{1}{3} c_2 a_5 \psi^2(x, t) & -\frac{1}{3} c_2 a_5 |\psi(x, t)|^2 \end{pmatrix}, \quad (7.51)$$

$$\mathbf{V}_2 = \begin{pmatrix} c_3(t) & \frac{i}{3} c_2^2 a_5 \psi(x, t) & -\frac{i}{3} c_2^2 a_5 \psi^*(x, t) \\ i c_2^2 a_3 \psi^*(x, t) & c_3(t) & 0 \\ -i c_2^2 a_3 \psi(x, t) & 0 & c_3(t) \end{pmatrix}, \quad (7.52)$$

and

$$\mathbf{V}_3 = \begin{pmatrix} c_2^2 a_3 + c_3(t) & 0 & \\ 0 & c_3(t) & 0 \\ 0 & 0 & c_3(t) \end{pmatrix}. \quad (7.53)$$

Using the DT the one-soliton solution of the SSE is given by

$$\psi(x, t) = \frac{i A}{\cosh(2 c_2 \lambda x - b)}, \quad (7.54)$$

where $A = \frac{2 c_1 c_2 \lambda_3}{c_3}$ and $b = 8 c_2^3 (t - 1) \lambda^3 a_3$. Similar result was found by C. Gilson, *et al.* [43].

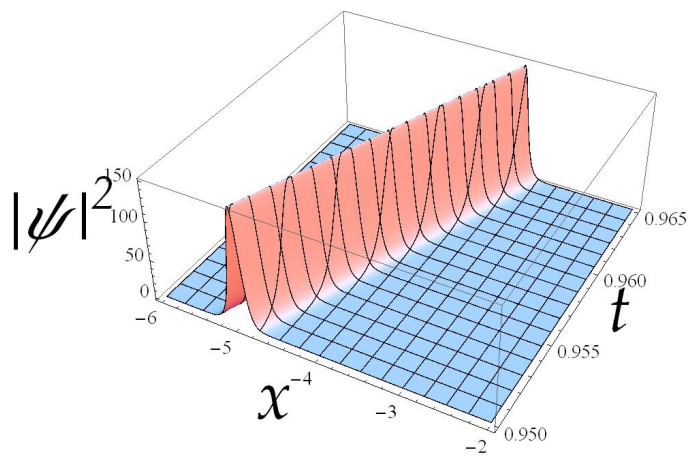


Figure 7.4: Solitonic solution of SSE with constant coefficients, $a_3 = 1$, $a_5 = 1$, $\lambda_3 = 5$, $c_1 = c_2 = c_3 = 1$

Conclusion

In this part we employ the Darboux transformation and Lax pair to solve the NLSE with cubic nonlinearity (HNLSE) and time-dependent coefficients. We investigate the integrability of HNLSE with damping and linear potential and find that it is integrable only with three independent coefficients, namely, dispersion, Kerr nonlinearity, and third-order dispersion coefficients. The coefficients for the Raman and self-steepening terms depend on the other three coefficients. The damping and linear part of the potential arise due to the time variation of the coefficients. This equation supports solitonic solution for focusing nonlinearity. For defocusing nonlinearity diverging non-solitonic solution exists. In both the cases the coefficient for the third-order dispersion can control the center of mass motion of the solutions. This findings can be used to control the motion of the soliton in the optical fiber without an external potential.

Using the same technique we are able to derive the solitonic solution for some of the well-known NLSEs, namely, Hirota, Sasa-Satsuma, and Nonlinear Schrödinger equations from the general equation by simply changing the parameter set . The Hirota and Sasa-Satsuma equations are not integrable with a linear potential, though the former is integrable with time-dependent coefficients. We check that the solutions of these equations are similar to those already found in the literature.

Bibliography

- [1] M. H. Anderson, J. R. Ensher, M. R. Matthews, C. E. Wieman and E. A. Cornell, *Science* **269**, 198 (1995).
- [2] K. B. Davis, M. O. Mewes, M. R. Andrews, N. J. Van Druten, D. S. Durfee, D. M. Kurn and W. Ketterle, *Phys. Rev. Lett.* **75**, 3969 (1995).
- [3] S. N. Bose, *Z. Phys.* **26**, 178 (1924); A. Einstein, *Akad. Wiss.* 1924, 261.
- [4] W. Krauth, *Phys. Rev. Lett.* **77**, (1996), 3695; A. B. Kuklov, N. Chencinski, A. M. Levine, W. M. Schreiber and J. L. Birman, *Phys. Rev.* **A55**, (1997), 488; N. V. Prokof'ev, B. V. Svistunov and I. S. Tupitsyn, *Sov. Phys. -JETP***87**, 310 (1998).
- [5] N. Bogoliubov, *J. Phys. USSR* **11** (1947), 23; A. L. Fetter and J. D. Walecka, "Quantum Theory of Many-Particle Systems", McGraw-Hill, NY, 1971; L. Pitaevskii and S. Stringari, "Bose-Einstein Condensation", International Series of Monographs on Physics, Oxford Science Publications, Clarendon Press, Oxford, 2003; C. J. Pethick and H. Smith, "Bose-Einstein Condensation in Dilute Gases", Cambridge University Press, Cambridge, UK, 2002.
- [6] V. N. Popov, *Sov. Phys. JETP* **20** (1965), 1185; "Functional Integrals and Collective Excitations", Cambridge Univ. Press, Cambridge, 1987; D. A. W. Hutchinson and E. Zaremba, *Phys. Rev.* **A57** (1998), 1280; S. A. Gardiner, *Phys. Rev.* **A56** (1997), 1414; S. A. Morgan, *J. Phys.* **B33** (2000), 3847.
- [7] S. T. Beliaev, *Soviet. Phys. JETP* **7** (1958), 289.
- [8] A. Griffin and H. Shi, *Phys. Rep.* **304** (1998), 1.
- [9] A. Griffin, *Phys. Rev.* **B53**, (1996), 9341; N. P. Proukakis and K. Burnett, *J. Res. Natl. Inst. Stand. Technol.* **101**, (1996), 457; D. A. W. Hutchinson, E. Zaremba and A. Griffin, *Phys. Rev. Lett.* **78**, (1997), 1842; D. S. Jin, M. R. Matthews, J. R. Ensher, C. E. Wieman and E. A. Cornell, *Phys. Rev. Lett.* **78**, (1997), 764; V. M. Perez-Garcia, H. Michinel, J. I. Cirac, M. Lewenstein and P. Zoller, *Phys. Rev.* **A56**, (1997), 1424; D. A. W. Hutchinson, R. J. Dodd and K. Burnett, *Phys. Rev. Lett.* **81** (11), (1998), 2298; T. Kita, *J. Phys. Soc. Jpn* **75**, 044603 (2006); V. I. Yukalov and H. Kleinert, *Phys. Rev.* **A75**, 063612 (2006).
- [10] D. A. W. Hutchinson, R. J. Dodd, K. Burnett, S. A. Morgan, M. Rusch, E. Zaremba, N.P. Proukakis, M. Edwards and C. W. Clark, *J. Phys.* **B33**, (2000), 3825.
- [11] A. K. Kerman and P. Tommasini, *Phys. Rev.* **B56**, (1997), 14733; *Ann. of Phys.* (N.Y.) **260** (1997), 250.

- [12] F. Dalfovo, S. Giorgini, L. P. Pitaevskii and S. Stringari, *Rev. Mod. Phys.* **71**, (1999), 463; J. Javanainen, *Phys. Rev.* **A54** (1996), 3722; A. Minguzzi and M. P. Tosi, *J. Phys.: Condens. Matter* **9** (1997), 10211; S. Giorgini, *Phys. Rev.* **A57** (1998), 2949.
- [13] M. Benarous, *Ann. of Phys. (N.Y.)* **320** (2005), 226.
- [14] R. Balian and M. Vénéroni, *Ann. of Phys. (N.Y.)* **187** (1988), 29; *Ann. of Phys. (N.Y.)* **195** (1989), 324.
- [15] E. P. Gross, *Nuovo Cimento* **20** (1961), 454; L. Pitaevskii, *Soviet Phys. JETP* **13** (1961), 451.
- [16] Y. Castin and R. Dum, *Phys. Rev.* **A57**, (1998), 3008.
- [17] N.P. Proukakis, K. Burnett and H. T. C. Stoof, *Phys. Rev.* **A57**, (1998), 1230.
- [18] F. Gerbier, J. H. Thywissen, S. Richard, M. Hugbart, P. Bouyer and A. Aspect, *Phys. Rev.* **A70**, (2004), 013607.
- [19] M. Benarous and H. Flocard, *Ann. of Phys. (N.Y.)* **273** (1999), 242.
- [20] V. Chernyak, S. Choi and S. Mukamel, *Phys. Rev.* **A67** (2003), 053604.
- [21] L. Pricoupenko, *Phys. Rev.* **A70** (2004), 013601.
- [22] G. Baym and C. J. Pethick, *Phys. Rev. Lett.* **76** (1996), 6; A. L. Fetter, *J. Low Temp. Phys.* **106** (1997), 643; E. Timmermans and P. Tommasini, *Phys. Rev.* **A55** (1997), 3645; S. Stenholm, *Phys. Rev.* **A57** (1998), 2942; P. Schuck and X. Vinas, *Phys. Rev.* **A61** (2000), 43603.
- [23] D. A. W. Hutchinson, Private communication.
- [24] F. Dalfovo, L. P. Pitaevskii and S. Stringari, *Phys. Rev.* **A54** (1996), 4213; A. L. Fetter and D. L. Feder, *Phys. Rev.* **A58** (1998), 3185;
- [25] A. Muñoz Mateo and V. Delgado, *Phys. Rev.* **A74** (2006), 065602.
- [26] A. Hasegawa and Y. Kodama, *Solitons in optical communications*, Oxford University Press (1995).
- [27] C. J. Pethick and H. Smith, *Bose-Einstein Condensation in Dilute Gases*, Cambridge University Press (2002).
- [28] C. Kharif, E. Pelinovsky, and A. Slunyaev, *Rogue Waves in the Ocean*, Springer (2010).
- [29] V. B. Matveev, M. A. Salle, *Darboux Transformations and Solitons*, Springer Series in Nonlinear Dynamics, Springer-Verlag, Berlin (1991).
- [30] U. Al Khawaja, *J. Phys. A* **39**, 9679 (2006).
- [31] A. Szameit and S. Nolte, *J. Phys. B* **43**, 163001 (2010).
- [32] Y. Kodama, *J. Stat. Phys.* **39**, 597 (1985).

- [33] Y. Kodama, A. Hasegawa, IEEE J. Quant. Electron. **QE-23**, 510 (1987).
- [34] M. J. Potasek, J. Appl. Phys. **65**, 941 (1989).
- [35] B. Tian, Y.-T. Gao, and H.-W. Zhu, Phys. Lett. A **366**, 223 (2007).
- [36] K. Porsezian and K. Nakkeeran, Phys. Rev. Lett. **76**, 3955 (1996).
- [37] A. Mahalingam and K. Porsezian, Phys. Rev. E **64**, 046608 (2001).
- [38] V. E. Zakharov and A. B. Shabat, Zh. Eksp. Teor. Fiz. **61**, 118 (1971).
- [39] Hitender Kumar, Anand Malik and Fakir Chand, Rramana journal of physics.**80**,No.2 (2013).pp.361-367.
- [40] R. Hirota, J. Math. Phys. **14**, 805 (1973).
- [41] Chao-Qing Dai and Jie-Fang Zhang, J. Phys. A: Math. Gen. **39**, 723 (2006).
- [42] N. Sasa and J. Satsuma, J. Phys. Soc. Jpn. **60**, 409 (1991).
- [43] C. Gilson, J. Hietarinta, J. Nimmo, and Y. Ohta Phys. Rev. E **68**, 016614 (2003).
- [44] H. Triki and A. Biswas, Waves in Random and Complex Media **21**, 151 (2011).
- [45] A. Choudhuri and K. Porsezian, Opt. Comm. **285**, 364 (2012).
- [46] A. Choudhuri and K. Porsezian, Phys. Rev. A **88**, 033808 (2013).
- [47] U. Al Khawaja, J. Math. Phys. **51**, 053506 (2010).
- [48] L. F. Mollenauer and J. P. Gordon, Solitons in Optical Fibers: Fundamentals and Applications, Academic Press (2006).
- [49] C. M. Soukoulis (edited by), Photonic Crystals and Light Localization in the 21st Century, Nato Science Series, Series C: Mathematical and Physical Sciences **563** (2000).
- [50] P. D. Lax, Comm. Pure Appl. Math. **21**, 467 (1968).
- [51] V. N. Serkin, A. Hasegawa, and T. L. Belyaeva, Phys. Rev. Lett. **98**, 074102 (2007).
- [52] D. J. Kaup and A. C. Newell, J. Math. Phys. **19**, 798 (1978).
- [53] Y. Tao and J. He, Phys. Rev. E **85**, 026601 (2012).
- [54] T. Brugarino and M. Sciacca, Opt. Comm. **262**, 250 (2006).
- [55] V. I. Kruglov, A. C. Peacock, and J. D. Harvey, Phys. Rev. Lett. **90**, 113902 (2003).
- [56] V. M. Pérez-García, P. J. Torres, and V. V. Konotop, Physica D **221**, 31 (2006).
- [57] S. A. Ponomarenko and G. P. Agrawal, Opt. Lett. **32**, 1659 (2007).
- [58] J. Belmonte-Beitia, V. M. Pérez-García, V. Vekslerchik, and V. V. Konotop, Phys. Rev. Lett. **100**, 164102 (2008).

- [59] A. Kundu, Phys. Rev. E **79**, 015601(R) (2009).
- [60] Russell, J.S. 1844. Report on Waves, 14th meeting of the British Association for the Advancement of Science, London: BAAS
- [61] Russell, J.S. 1885. The Wave of Translation in the Oceans of Water, Air and Ether, London: Trübner
- [62] Korteweg, D.J. and de Vries, H. 1895. On the change of form of long waves advancing in a rectangular canal, and on a new type of long stationary waves. Philosophical Magazine, 39: 422-43
- [63] Zakharov, V.E. and Shabat, A.B. 1972. Exact theory of two-dimensional self-focusing and one-dimensional self-modulation of waves in nonlinear media. Soviet Physics, JETP, 34: 62-69.
- [64] Hasegawa, A., 1989. Solitons in Optical Fibers. Springer, Berlin.
- [65] Hasegawa, A., Kodama, Y., 1995. Solitons in Optical Communications. Oxford University Press, Oxford
- [66] Chiao, R.Y., Garmire, E., Townes, C.H., 1964. Phys. Rev. Lett. 13, 479.
- [67] Chiao, R.Y., Deutsch, I.H., Garrison, J.C., Wright, E.M., 1993. In: Walter, H. et al. (Ed.), Frontiers in Nonlinear Optics (The Sergei Akhmanov Memorial Volume). Institute of Physics Publishing, Bristol, p. 151.
- [68] Yuri S. KIVSHAR DARK OPTICAL SOLITONS: PHYSICS AND APPLICATIONS , Barry LUTHER-DAVIES” Physics Reports 298 (1998) 81-197
- [69] Mollenauer, L.F., Stolen, R.H., Gordon, J.P., 1980. Phys. Rev. Lett. 45, 1095.
- [70] Mollenauer, L.F., Neubelt, M.J., Evangelides, S.G., Gordon, J.P., Simpson, J.R., Cohen, L.G., 1990. Opt. Lett. 15, 1203.
- [71] Agrawal, G., 1989. Nonlinear Fiber Optics. Academic Press, Boston, MA.
- [72] Haus, H.A., Wong, W.S., 1996. Rev. Mod. Phys. 68, 423.
- [73] Emplit, Ph., Hamaide, J.P., Reynaud, F., Froehly, G., Barthelemy, A., 1987. Opt. Commun. 62, 374.
- [74] Krökel, D., Halas, N.J., Giuliani, G., Grischkowsky, D., 1988. Phys. Rev. Lett. 60, 29.
- [75] Weiner, A.M., Heritage, J.P., Hawkins, R.J., Thurston, R.N., Kirschner, E.M., Learid, D.E., Tomlinson, W.J., 1988. Phys. Rev. Lett. 61, 2445.
- [76] Andersen, D.R., Hooton, D.E., Swartzlander, G.A. Jr., Kaplan, A.E., 1990. Opt. Lett. 15, 783.
- [77] Swartzlander, G.A. Jr., Andersen, D.R., Regan, J.J., Yin, H., Kaplan, A.E., 1991. Phys. Rev. Lett. 66, 1583.
- [78] Allan, G.R., Skinner, S.R., Andersen, D.R., Smirl, A.L., 1991. Opt. Lett. 16, 156.

- [79] Skinner, S.R., Allan, G.R., Andersen, D.R., Smirl, A.L., 1991. IEEE J. Quantum Electron. 27, 2211.
- [80] Luther-Davies, B., Yang, X., 1992a. Opt. Lett. 17, 496.
- [81] Luther-Davies, B., Yang, X., 1992b. Opt. Lett. 17, 1775.
- [82] Duree, G., Morin, M., Salamo, G., Segev, M., Crosignani, B., DiPorto, P., Sharp, E., Yariv, A., 1995. Phys. Rev. Lett. 74, 1978.
- [83] Taya, M., Bashaw, M.C., Feier, M.M., Segev, M., Valley, G.C., 1996. Opt. Lett. 21, 943.
- [84] Chen, Z., Mitchell, M., Segev, M., 1996b. Opt. Lett. 21, 716.
- [85] Akhmanov, S.A., Sukhorukov, A.P., Khokhlov, R.V., 1967. Usp. Fiz. Nauk 93, 19 [Sov. Phys. Uspekhi 10 (1968) 609].
- [86] Svelto, O., 1974. Self-focusing, self-trapping, and self-phase modulation of laser beams. In: Wolf, E. (Ed.), Progress in Optics, vol. XII, North-Holland, Amsterdam.
- [87] Boardman, A.D., Xie, K., 1993. Radio Sci. 28, 891.
- [88] Chiao, R.Y., Deutsch, I.H., Garrison, J.C., Wright, E.M., 1993. In: Walter, H. et al. (Ed.), Frontiers in Nonlinear Optics (The Sergei Akhmanov Memorial Volume). Institute of Physics Publishing, Bristol, p. 151.
- [89] Zakharov, V.E., Shabat, A.B., 1971. Zh. Eksp. Teor. Fiz. 61, 118 [Sov. Phys. JETP 34 (1972) 62].
- [90] Zakharov, V.E., Shabat, A.B., 1973. Zh. Eksp. Teor. Fiz. 64, 1627 [Sov. Phys. JETP 37 (1973) 823].
- [91] Zakharov, V.E., Manakov, S.V., Novikov, S.P., Pitaevskii, L.P., 1980. Theory of Solitons: The Inverse Scattering Transform. Nauka, Moscow (English Translation by Consultant Bureau, New York, 1984).
- [92] Hasegawa, A., 1989. Solitons in Optical Fibers. Springer, Berlin.
- [93] Soliton Management in periodic systems Boris A. Malomed.
- [94] Hasegawa, A., Kodama, Y., 1995. Solitons in Optical Communications. Oxford University Press, Oxford.
- [95] Yuri S. Kivshar and Barry Luther-Davies. Dark optical solitons: physics and applications Physics Reports 298 (1998) 81-197.
- [96] Lamb, G.L. Jr. 1976. Bäcklund transforms at the turn of the century. In Bäcklund Transforms, edited by R.M. Miura, Berlin and New York: Springer
- [97] Steuerwald, R. 1936. Über Enneper'sche Flächen und Bäcklund'sche Transformation. Abhandlungen der Bayerischen Akademie der Wissenschaften München 1-105.
- [98] Frenkel, J. and Kontorova, T. 1939. On the theory of plastic deformation and twinning. Phys. Z. Sowjetunion, 1: 137-49.

- [99] Fermi, E., Pasta, J.R. and Ulam, S.M. 1955. Studies of nonlinear problems, Los Alamos Scientific Laboratory Report No. LA-1940.
- [100] Zabusky, N.J. and Kruskal, M.D. 1965. Interactions of solitons in a collisionless plasma and the recurrence of initial states. *Physical Review Letters*, 15: 240-43.
- [101] Perring, J.K. and Skyrme, T.R.H. 1962. A model unified field equation. *Nuclear Physics*, 31: 550-55
- [102] Seeger, A., Donth, H. and Kochendörfer, A. 1953. Theorie der Versetzungen in eindimensionalen Atomreihen. *Zeitschrift für Physik*, 134: 173-93
- [103] Gardner, C.S., Greene, J.M., Kruskal, M.D. and Miura, R.M. 1967. Method for solving the Korteweg-de Vries equation. *Physical Review Letters*, 19: 1095-97.
- [104] Toda, M. 1967. Vibration of a chain with nonlinear interactions. *Journal of the Physical Society of Japan*, 22: 431-36; Wave propagation in anharmonic lattices. *Journal of the Physical Society of Japan*, 23: 501-06.
- [105] Newell, A.C. (editor) 1974. *Nonlinear Wave Motion*, Providence, R.I.: American Mathematical Society.
- [106] Scott, A.C. 1999. *Nonlinear Science: Emergence and Dynamics of Coherent Structures*, Oxford and New York: Oxford University Press.
- [107] L Pitaevskii and S Stringari, *BoseEinstein condensation* (Oxford University Press, Oxford, 2003).
- [108] S Burger et al, *Phys. Rev.Lett.* 83, 5198 (1999).
- [109] L Khaykovich et al, *Science* 292, 1290 (2002).
- [110] E Kolomeisky, T J Newman, J Straley and X Qi, *Phys. Rev.Lett.* 85, 1146 (2000).
- [111] B B Baizakov et al, *J. Phys. B: At. Mol. Opt. Phys.* 42, 175302 (2009).
- [112] Matveev V B and Salle M A 1991 *Darboux Transformations and Solitons* (Springer Series in Nonlinear Dynamics) (Berlin: Springer).
- [113] Usama Al Khawaja *J. Phys. A: Math. Gen.* 39 (2006) 96799691.
- [114] Gross E P 1961 *Nuovo Cimento* 20 454.
- [115] Gross E P 1963 *J. Math. Phys.* 4 195.
- [116] Carr L D, Clark C W and Reinhardt W P 2000 *Phys. Rev. A* 62 063610.
- [117] Carr L D, Clark C W and Reinhardt W P 2000 *Phys. Rev. A* 62 063611.
- [118] Liang Z X, Zhang Z D and Liu W M 2005 *Phys. Rev. Lett.* 94 050402.
- [119] C. Rogers and W. K. Schief, *Bäcklund and Darboux Transformations, Geometry and Modern Applications in Soliton Theory*, Cambridge University Press (2002).
- [120] A. I. Bobenko, *Surfaces in terms of 2 by 2 matrices: Old and New integrable cases, Harmonic maps and integrable systems*, Vieweg (1994), 83.

- [121] M.H. Anderson et al., *Science*, 269 (1995) 198.
- [122] K.B. Davis et al., *Phys. Rev. Lett.*, 75 (1995) 3969.
- [123] C.C. Bradley, C.A. Sackett, and R.G. Hulet, *Phys. Rev. Lett.*, 78 (1997) 985.
- [124] K. Huang, *Statistical Mechanics* (Wiley, New York) 1987.
- [125] M.R. Andrews et al., *J. Low Temp. Phys.*, 110 (1998) 153.
- [126] J. Stenger et al., *J. Low Temp. Phys.*, 113 (1998) 167.
- [127] P. Ehrenfest and J.R. Oppenheimer, *Phys. Rev.*, 37 (1931) 333.
- [128] J.H. Freed, *Journal of Chemical Physics*, 72 (1980) 1414.
- [129] W.D. Phillips, J.V. Prodan, and H.J. Metcalf, *J. Opt. Soc. Am. B*, 2 (1985) 1751.
- [130] W.D. Phillips, in *Laser Manipulation of Atoms and Ions*, Proceedings of the International School of Physics Enrico Fermi, Course CXVIII, edited by E. Arimondo, W.D. Phillips, and F. Strumia (North-Holland, Amsterdam) 1992, p. 289.
- [131] J.V. Prodan, W.D. Phillips, and H. Metcalf, *Phys. Rev. Lett.*, 49 (1982) 1149.
- [132] S. Chu et al., *Phys. Rev. Lett.*, 55 (1985) 48.
- [133] S. Chu, in *Laser Manipulation of Atoms and Ions*, Proceedings of the International School of Physics Enrico Fermi, Course CXVIII, edited by E. Arimondo, W.D. Phillips, and F. Strumia (North-Holland, Amsterdam) 1992, p. 239.
- [134] E.L. Raab et al., *Phys. Rev. Lett.*, 59 (1987) 2631.
- [135] K.B. Davis, M.O. Mewes, M.A. Joffe, and W. Ketterle, in *Fourteenth International Conference on Atomic Physics*, Boulder, Colorado, 1994, Book of Abstracts, 1-M3 (University of Colorado, Boulder, Colorado) 1994.
- [136] W. Petrich, M.H. Anderson, J.R. Ensher, and E.A. Cornell, in *Fourteenth International Conference on Atomic Physics*, Boulder, Colorado, 1994, Book of Abstracts, 1M-7 (University of Colorado, Boulder, Colorado) 1994.
- [137] Strecker, Partridge, Truscott, and Hulet, 2002 and 2003; Khaykovich et al, 2002.
- [138] Pitaevskii and Stringari, book (2003).
- [139] Carretero, Gonzalez, Frantzeskakis and Kevrekidis, 2008.
- [140] Einstein, A., 1924, *Sitzber. Kgl. Preuss. Acad. Wiss.*, 261.
- [141] Anderson et al., 269 (5221), *science journal* (1995).
- [142] K. B. Davis, et al. *Phys. Rev. Lett.* 75, 3969 (1995).
- [143] C. C. Bradley, C. A. Sackett, J. J. Tollett, and R. G. Hulet, *Phys. Rev. Lett.* 75, 1687 (1995).
- [144] IF Silvera, JTM Walraven *Physical Review Letters* 44 (3), 164(1980).

- [145] S. Chu, *Rev. Mod. Phys.* 70, 686 (1998); C. Cohen-Tannoudji, *ibid.* 70, 707 (1998); W.D. Phillips, *ibid.* 70, 721 (1998) 30.
- [146] Ketterle and van Druten *Advance in Atomic, Molecular and Optical Physics* . 37 (1996).
- [147] Einstein, A., 1925, *Sitzber. Kgl. Preuss. Acad. Wiss.*, 3.
- [148] Kapitza, P., 1938, *Nature* 141, 74.
- [149] Allen, J. F. and A. D. Misener, 1938, *Nature* 141, 75.
- [150] London, F., 1938, *Phys. Rev.* 54, 947.
- [151] Bogoliubov, N., 1947, *J. Phys. (USSR)* 11, 23.
- [152] Penrose, O. and L. Onsager, 1956, *Phys. Rev.* 104, 576.
- [153] Yang, C. N., 1962, *Rev. Mod. Phys.* 34, 694.
- [154] Cornell, E. A. and C. E. Wieman, 2002, *Int. J. Mod. Phys B*16, 4503.
- [155] Ketterle, W., D. S., Durfee, D. M., Stamper-Kurn, 1999, in *Bose-Einstein condensation in atomic gases*, Proceedings of the International School of Physics Enrico Fermi Course CXL, edited by M. Inguscio, S. Stringari, and C. E. Wieman, (IOS Press, Amsterdam), p. 67.
- [156] Fedichev, P. O. and U. R. Fischer, 2003, *Phys. Rev. Lett.* 91, 240407.
- [157] Recati, A., P. O. Fedichev, W. Zwerger, J. von Delft, P. Zoller, 2005, *Phys. Rev. Lett.* 94, 040404.
- [158] Indekeu, J. O. and B. Van Schaeybroeck, 2004, *Phys. Rev. Lett.* 93, 210402.
- [159] *Lett. B* , 837. Dalfovo, F., S. Giorgini, L.P. Pitaevskii, and S. Stringari, 1999, *Rev. Mod. Phys.* 71, 463.
- [160] A. L. Fetter and J. D. Walecka, *Quantum Theory of Many-Particle Systems*, McGraw-Hill, New York, 1971.
- [161] S. T. Beliaev, *Soviet. Phys. JETP* 7 (1958), 289.
- [162] A. Griffin and H. Shi, *Phys. Rep.* 304 (1998), 1 and references therein.
- [163] A. Griffin, *Phys. Rev. B*53, (1996), 9341; V. M. Perez-Garcia, H. Michinel, J. I. Cirac, M. Lewenstein and P. Zoller, *Phys. Rev. A*56, (1997), 1424.
- [164] A. K. Kerman and P. Tommasini, *Phys. Rev. B*56, (1997), 14733.
- [165] F. Dalfovo, S. Giorgini, L. P. Pitaevskii and S. Stringari, *Rev. Mod. Phys.* 71, (1999), 463.
- [166] M.H.Anderson,J.R.Ensher,M.R.Matthews, C.E.Wieman,E.A.Cornell,*Science* 269(1995)198.

- [167] A.Einstein,Sitzungsber.Kgl.Preuss.Akad.Wiss 3(1925).
- [168] K.Huang.Statistical Mechanics,2nd ed.,Wiley,new York,1987.
- [169] F.London, Nature 141 (1938)643.
- [170] L.D.Landau,J.Phys.U.S.S.R.5(1941)71.
- [171] J. Bardeen, L.N. Cooper, and J.R. Schrieffer. Phys. Rev. 108 1175 (1957).
- [172] T.D. Lee and CN. Yang, Phys.Rev. 105 1119 (1957); T.D. Lee, K.Huang and CN. Yang, Phys.Rev. 106, 1135 (1957).
- [173] S.T. Beliaev, Sov. Phys.-JETP 7 299 (1958).
- [174] N.M. Hugenholtz, D. Pines, Phys.Rev. 116 489 (1959).
- [175] N.M. Hugenholtz, Physica 26 170 (1960).
- [176] J. Gavoret, Thse, Univ. de Paris, juin 1963; J. Gavoret, Ann. Phys. (Paris) 8 441(1963).
- [177] J. Gavoret, Ph. Nozires, Ann.Phys. (N. Y.) 28 349 (1964).
- [178] E. Talbot, A. Griffin, Ann. Phys. (N. Y.) 151 71 (1983).
- [179] A. Griffin, Excitations in a Bose-Condensated Liquid, Cambridge Univ. Press, Cambridge, 1993.
- [180] E.P. Gross, Nuovo Cimento 20 454 (1961).
- [181] L.P. Pitaevskii, Sov. Phys. JETP 13 451 (1961).
- [182] V.L. Ginzburg and L.D Landau., Zh. Eksp. Teor. Fiz. 20 1064 (1950).
- [183] N.N. Bogoliubov, Lectures on Quantum Statistics: Quasi-Averages, Vol. 2, Gordon and Breach-Science Publishers, New York, London, Paris, 1970.
- [184] N.N. Bogoliubov, Quasi-averages in problems of statistical mechanics, in: collection of Papers, Vol. 3, Naukova Dumka, Kiev, 1971, pp. 174-243.
- [185] V.N. Popov and L.D. Faddeev, J.Exp. Theo.Phys.20, 890 (1965).
- [186] V.N. Popov, Functional Integrals and Collective Excitations, Univ. Press, Cambridge, 1987.
- [187] M. Girardeau, J. Math Phys. 6, 516 (1960).
- [188] E. H. L. and W. Liniger, Phys. Rev. 130, 1605 (1963); E. H.Lieb, ibid. 1605 (1963).
- [189] C. N. Y. and C. P. Y., J. Math. Phys. 10, 1115 (1969).
- [190] H. B. G. Casimir, On Bose-Einstein condensation, Fundamental Problems in
- [191] Kivshar and Malomed, 1989.

- [192] Torruellas et al. (1995).
- [193] Duree et al., (1993).
- [194] Kanashov and Rubenchik, (1981).
- [195] Anderson et al. (1995).
- [196] Bradley, Sackett, Tollett, and Hulet (1995)
- [197] Davis et al. (1995).
- [198] Burger et al., (1999).
- [199] Strecker, Partridge, Truscott, and Hulet (2002).
- [200] Khaykovich et al.(2002).
- [201] Eiermann et al., (2004).
- [202] Statistical Mechanics III, ed E.G.D.Cohen, p. 188-196, (1968). W.C. Stwalley and L.H. Nosanow, Phys. Rev. Lett.,36(15):910 (1976).
- [203] I. F. Silvera and J. T. M. Walraven, Phys. Rev. Lett. 44, 164 (1980).
- [204] R. W. Cline, D. A. Smith, T. J. Greytak, and D. Kleppner, Phys. Rev. Lett. 45, 2117 (1980).
- [205] S. Chu, Rev. Mod. Phys. 70, 685 (1998).
- [206] C. N. Cohen-Tannoudji, Rev. Mod. Phys. 70, 707 (1998).
- [207] W. D. Phillips, Rev. Mod. Phys. 70, 707 (1998).
- [208] J. Dalibard and C. Cohen-Tannoudji, J. Opt. Soc. Am.B 6, 2023 (1989).
- [209] M.H. Anderson, J.R. Ensher, M.R. Matthews, C.E. Wieman, and E.A. Cornell, Science 269, 198 (1995).
- [210] K.B. Davis, M.-O. Mewes, M.R. Andrews, N.J. van Druten, D.S. Durfee, D.M. Kurn, and W. Ketterle, Phys. Rev. Lett. 75, 3969 (1995).
- [211] Kleppner, D., T. J. Greytak, T. C. Killian, D. G. Fried, L. Willmann, D.Landhuis, and S. C. Moss, 1999, in Bose-Einstein Condensation in Atomic Gases, Proceedings of the International School of Physics Enrico Fermi, Course CXL, edited by M. Inguscio, S. Stringari, and C. E. Wieman (IOS Press, Amsterdam), pp. 177 (1999).
- [212] Pereira Dos santos, J. Lonard, Junmin Wang, C. J. Barrelet, F. Perales, E. Rasel, C. S. Unnikrishnan, M. Leduc, C. Cohen- Tannoudji, Phys. Rev. Lett. 86, 3459 (2001).
- [213] W. Pauli, Phys. Rev. 58, 716 (1940) .
- [214] D. S. Jin, Physics World 15, 27 (2002).
- [215] Jochim, S., M. Bartenstein, A. Altmeyer, G. Hendl, C. Chin, J. H. Denschlag, and R. Grimm, Science 302, 2101 (2003).

- [216] S. Gupta, Z. Hadzibabic, M.W. Zwierlein, C.A. Stan, K. Dieckmann, C.H. Schunck, E.G.M. van Kempen, B.J. Verhaar, and W. Ketterle, *Science* 300, 1723 (2003).
- [217] M. Greiner, C. A. Regal, and D. S. Jin, *Nature* 426, 537 (2003).
- [218] A .Boudjemaa, doctor thesis in physical sciences April 2013.
- [219] L. I. Schiff, *Quantum Mechanics* (McGraw-Hill Inc., 1969).
- [220] A. L. Fetter and J. D. Walecka, *Quantum theory of many-particle systems* (McGraw Hill, New York, 1971).
- [221] A. L. Fetter, *Ann. Phys.* 70 67(1972).
- [222] N.N. Bogoliubov, *J. Phys. USSR* 11, 2332 (1947).
- [223] A. L. Fetter, *Ann. Phys.* 70 67(1972).
- [224] E.P. Gross, *Nuovo Cimento* 20 454 (1961).
- [225] L.P. Pitaevskii, *Sov. Phys. JETP* 13 451 (1961).
- [226] V.L. Ginzburg and L.D Landau., *Zh. Eksp. Teor. Fiz.* 20 1064 (1950).
- [227] M. Edwards and K. Burnett, *Phys. Rev. A* 51 1382 (1995).
- [228] R. A. Ruprecht, M. J. Holland, K. Burnett and M. Edwards, *Phys. Rev. A* 51 4704 (1995).
- [229] M. Edwards M, R. J. Dodd, C.W. Clark and K. Burnett, *J. Res. Natl. Inst. Stand. Technol.*101 553 (1996); Edwards M, Ruprecht P A, Burnett K, Dodd R J and Clark C W, *Phys. Rev. Lett.* 77 1671(1996).
- [230] F. J. Dyson, *J. Math. Phys.* 8, 1538 (1967).
- [231] E. H. Lieb and J. Yngvason, *Phys. Rev. Lett.* 80, 2504 (1998).
- [232] M. Edwards M, R. J. Dodd, C.W. Clark and K. Burnett, *J. Res. Natl. Inst. Stand. Technol.*101 553 (1996); Edwards M, Ruprecht P A, Burnett K, Dodd R J and Clark C W, *Phys. Rev. Lett.* 77 1671(1996).
- [233] G. Baym, C. Pethick, *Phys. Rev. Lett.* 76, 6 (1996).
- [234] V.V. Goldman, I.F. Silvera and A.G. Legget, *Phys. Rev. B* 24, 2870 (1981).
- [235] J. Oliva, *Phys. Rev.* B39, 4177 (1989).
- [236] T.T. Chou, C. N. Yang, and L. W. Yu, *Stonybrook preprints* (1996).
- [237] E. Timmermans, P. Tommasini and K. Huang. *Phys. Rev. A*55 3645 (1997).
- [238] P. Schuck, X. Vinas, *Phys. Rev. A*61, 43603 (2000).
- [239] A. L. Fetter, *Ann. Phys.* 70 67(1972).

- [240] de Gennes. P G Superconductivity of Metals and Alloys (Perseus Books Advanced Book Classics, 1999).
- [241] A. Griffin. Phys. Rev. B 53, 9341 (1996).
- [242] A. Griffin and H. Shi, Phys. Rep. 304, 1 (1998).
- [243] M. Benarous, H. Chachou-Samet, Eur. Phys. J. D 50,125 (2008).
- [244] A. Boudjema and M. Benarous, Nature and Technology 4 15 (2011).
- [245] N.N. Bogoliubov, J. Phys. USSR 11, 2332 (1947).
- [246] N.N. Bogoliubov, Izv. Akad. Nauk USSR. 11, 7790 (1947).
- [247] A. Griffin. Phys. Rev. B 53, 9341 (1996).
- [248] D. A. W. Hutchinson, K. Burnett, R. J. Dodd, S. A. Morgan, M. Rusch, E. Zaremba, N. P. Proukakis, M. Edwards, and C. W. Clark. J. Phys. B 33, 3825 (2000).
- [249] J. Goldstone. Nuovo Cimento 19, 154 (1961).
- [250] E. Zaremba, T. Nikuni, and A. Griffin, J. Low Temp. Phys. 116, 277 (1999).
- [251] A. Griffin, T. Nikuni, and E. Zaremba, Bose-Condensed Gases at Finite Temperatures (Cambridge University Press, Cambridge, 2009).
- [252] T. Nikuni, E. Zaremba, and A. Griffin, Phys. Rev. Lett. 83, 10 (1999).
- [253] T. Nikuni and A. Griffin, Phys. Rev. A 63, 033608 (2001).
- [254] B. Jackson and E. Zaremba, Phys. Rev. Lett. 87, 100404 (2001).
- [255] B. Jackson and E. Zaremba, Phys. Rev. Lett. 88, 180402 (2002).
- [256] B. Jackson and E. Zaremba, Phys. Rev. Lett. 89, 150402 (2002).
- [257] B. Jackson, N. P. Proukakis, and C. F. Barenghi, Phys.Rev. A 75, 051601 (2007).
- [258] B. Jackson, N. P. Proukakis, C. F. Barenghi, and E. Zaremba, Phys. Rev. A 79, 053615 (2009).
- [259] N.M. Hugenholtz, D. Pines, Phys.Rev. 116 489 (1959).
- [260] B. Svistunov, J. Moscow Phys. Soc. 1, 373 (1991).
- [261] K. Goral, M. Gajda, and K. Rzazwski, Phys. Rev. A 66, 051602(R) (2002).
- [262] H. T. C. Stoof, J. Low Temp. Phys. 114, 11 (1999).
- [263] M. J. Davis, S. A. Morgan, and K. Burnett, Phys. Rev. Lett. 87, 160402 (2001).
- [264] P. B. Blakie and M. J. Davis, Phys. Rev. A 72, 063608 (2005).
- [265] M. J. Steel, M. K. Olsen, L. I. Plimak, P. D. Drummond, S. M. Tan, M. J. Collett, D. F.Walls, and R. Graham, Phys. Rev. A 58, 4824 (1998).

- [266] A. Sinatra, Y. Castin, and C. Lobo, *J. Mod. Opt.* 47, 2629 (2000).
- [267] C. W. Gardiner and P. Zoller, *Phys. Rev. A* 61, 033601 (2000).
- [268] C. W. Gardiner, J. R. Anglin, and T. I. A. Fudge, *J. Phys. B* 35, 1555 (2002).
- [269] C.W. Gardiner and M. J. Davis, *J. Phys. B* 36, 4731 (2003).
- [270] P. B. Blakie, A. S. Bradley, M. J. Davis, R. J. Ballagh, and C. W. Gardiner, *Adv. Phys.* 57, 363 (2008).
- [271] S. E. Hoffmann, J. F. Corney, and P. D. Drummond, *Phys. Rev. A* 78, 013622 (2008).
- [272] M. Brewczyk, M. Gajda, and K. Rzazewski, *J. Phys. B* 40, R1 (2007).
- [273] A. Polkovnikov, *Ann. Phys. (N. Y.)* 325, 1790 (2010).
- [274] M. J. Davis and P. B. Blakie, *Phys. Rev. Lett.* 96, 060404 (2006).
- [275] C. N. Weiler, T. W. Neely, D. R. Scherer, A. S. Bradley, M. J. Davis, and B. P. Anderson, *Nature* 455, 948 (2008).
- [276] N. P. Proukakis, J. Schmiedmayer, and H. T. C. Stoof, *Phys. Rev. A* 73, 053603 (2006).
- [277] R. A. Duine, B.W. A. Leurs, and H. T. C. Stoof, *Phys. Rev. A* 69, 053623 (2004).
- [278] S. P. Cockburn, H. E. Nistazakis, T. P. Horikis, P. G. Kevrekidis, N. P. Proukakis, and D. J. Frantzeskakis, *Phys. Rev. Lett.* 104, 174101 (2010).
- [279] S. J. Rooney, A. S. Bradley, and P. B. Blakie, *Phys. Rev. A* 81, 023630 (2010).
- [280] V. V. Kocharovskiy, V. V. Kocharovskiy, M. Holthaus, C. R. Ooi, A. Svidzinsky, W. Ketterle, and M. O. Scully, *Adv. At. Mol. Opt. Phys.* 53, 291 (2006).
- [281] Z. Idziaszek, L. Zawitkowski, M. Gajda, and K. Rzazewski, *Europhys. Lett.* 86, 10002 (2009).
- [282] M. Sargent III and M. O. Scully, *Theory of Laser Operation* (North-Holland, Amsterdam, 1972), vol. 1 of *Laser Handbook*, chap. A2, pp. 45.
- [283] V.I. Yukalov, *Ann. of Phys.* 323, 461, (2008).
- [284] V. I. Yukalov, *Laser. Phys* 19, 1 (2009).
- [285] N. Bogoliubov, *J. Phys. USSR* 11 (1947), 23; A. L. Fetter and J. D. Walecka, *Quantum Theory of Many-Particle Systems*, McGraw-Hill, New York, 1971.
- [286] S. T. Beliaev, *Soviet. Phys. JETP* 7 (1958), 289.
- [287] A. Griffin and H. Shi, *Phys. Rep.* 304 (1998), 1 and references therein.
- [288] A. Griffin, *Phys. Rev. B* 53, (1996), 9341; V. M. Perez-Garcia, H. Michinel, J. I. Cirac, M. Lewenstein and P. Zoller, *Phys. Rev. A* 56, (1997), 1424.

- [289] A. K. Kerman and P. Tommasini, Phys. Rev. B56, (1997), 14733.
- [290] F. Dalfovo, S. Giorgini, L. P. Pitaevskii and S. Stringari, Rev. Mod. Phys. 71, (1999), 463.
- [291] W. Krauth, Phys. Rev. Lett. 77, (1996), 3695; A. B. Kuklov N. Chencinski, A. M. Levine, W. M. Schreiber and J. L. Birman, Phys. Rev. A55, (1997), 488; M. Holzmann, W. Krauth and M. Naraschewski, e-print cond-mat/9806201.
- [292] R. Balian and M. Vnéroni, Ann. of Phys. (N.Y.) 187 (1988), 29; Ann. of Phys. (N.Y.) 195 (1989), 324.
- [293] M. Benarous and H. Flocard, Ann. of Phys. (N.Y.) 273 (1999), 242.
- [294] R. Balian and M. Vénéroni, Nucl. Phys. B408 (1993), 445 and references therein.
- [295] M. Benarous, Ann. of Phys. (N.Y.) 269 (1998), 107.
- [296] E. P. Gross, Nuovo Cimento 20 (1961), 454; L. Pitaevskii, Soviet Phys. JETP 13 (1961), 451.
- [297] A. Griffin and H. Shi, Phys. Rep. 304 (1998), 1 and references therein.
- [298] V. N. Popov, Sov. Phys. JETP 20 (1965), 1185; Functional Integrals and Collective Excitations, Cambridge Univ. Press, Cambridge, 1987; D. A. W. Hutchinson and E. Zaremba, Phys. Rev. A57 (1997), 1280; D. A. W. Hutchinson E. Zaremba and A. Griffin, Phys. Rev. Lett. 78 (1997), 1843.
- [299] J. Javanainen, Phys. Rev. A54 (1996), 3722.
- [300] A. Minguzzi and M. P. Tosi, J. Phys.: Condens. Matter 9 (1997), 10211.
- [301] S. Giorgini, Phys. Rev. A57 (1998), 2949.
- [302] A. K. Kerman and P. Tommasini, Ann. of Phys. (N.Y.) 260 (1997), 250.
- [303] Goldman V V, Silvera I F and Leggett A J 1981 Phys. Rev.B
- [304] Gies C, Van Zyl P, Morgan S A and Hutchinson D A W 2004 Phys. Rev. A
- [305] Dodd R J, Edwards M, Clark C W and Burnett K 1998 Phys. Rev. A 57
- [306] Hutchinson D A W, Dodd R J, Burnett K, Morgan S A, Rusch M, Zaremba E, Proukakis N P, Edwards M and Clark C W 2000 J. Phys. B: At. Mol. Opt. Phys.
- [307] Gerbier F, Thywissen J H, Richard S, Hugbart M, Bouyer P and Aspect A 2004 Phys. Rev. A 70
- [308] Zawada M, Abdoul R, Chwedenczuk J, Gartman R, Szczepkowski J, Tracewski L, Witkowski M and Gawlik W 2008 J. Phys. B: At. Mol. Opt. Phys.
- [309] Caracanhas M A, Seman J A, Ramos E R, Henn E A L, Magalhaes K M F, Helmer-son K and Bagnato V S 2009 J. Phys. B: At. Mol. Opt. Phys.

- [310] Castin Y and Dum R 1996 Phys. Rev. Lett. Ketterle W, Durfee D S and Stamper-Kurn D M 1999 Proc. Int. School of Physics Enrico Fermi, Course CXL ed M Inguscio, S Stringari and C E Wieman (Amsterdam: IOS) pp 67176
- [311] Gawryluk K, Brewczyk M, Gajda M and Rzazewski K 2010 J. Phys. B: At. Mol. Opt. Phys.
- [312] Hutchinson D A W, Dodd R J, Burnett K, Morgan S A, Rusch M, Zaremba E, Proukakis N P, Edwards M and Clark C W 2000 J. Phys. B: At. Mol. Opt. Phys.
- [313] S Kouidri and M Benarous, J. Phys. B: At. Mol. Opt. Phys. 44 (2011) 205301 (6pp)
- [314] M Benarous, arXiv:1303.5639 [cond-mat.quant-gas](2013).
- [315] Boudjemaa A and Benarous M 2010 Eur. Phys. J. D 59 427.